ISSN 0031-0204

日本古生物学會報告・紀事

Transactions and Proceedings of the Palaeontological Society of Japan

New Series No. 175

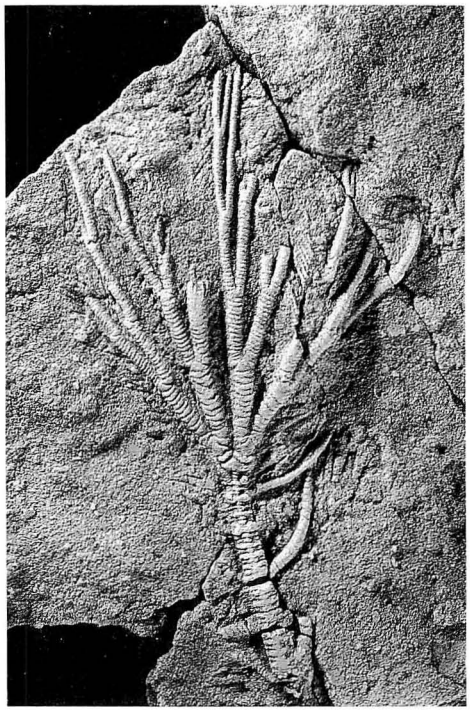

日 本 古 生 物 学 会

Palaeontological Society of Japan

September 30, 1994

The fossil on the cover is *Isocrinus* (*Chladocrinus*) *hanaii* Oji, an Early Cretaceous (Aptian) crinoid, which was described from the Hiraiga Formation exposed at Haipe, Tanohata-mura, Shimo-Hei County, Iwate Prefecture, Northeast Japan. (University Museum of the University of Tokyo coll. cat. no. ME6950, paratype specimen, length about 11 cm)

All communication relating to this journal should be addressed to the

PALAEONTOLOGICAL SOCIETY OF JAPAN

c/o Business Center for Academic Societies,
Honkomagome 5-16-9, Bunkyo-ku, Tokyo 113, Japan

Trans. Proc. Palaeont. Soc. Japan, N.S., No. 175, pp. 497-520, 11 Figs., September 30, 1994

973. BATHYAL BENTHIC FORAMINIFERAL CHANGES DURING THE PAST 210,000 YEARS: EVIDENCE FROM PISTON CORES TAKEN FROM SEAS SOUTH OF ISHIGAKI ISLAND, SOUTHERN RYUKYU ISLAND ARC*

XUEDONG XU

Department of Earth Sciences, Faculty of Science,
Kumamoto University, Kumamoto, 860

and

HIROSHI UJIIÉ

Department of Marine Sciences, University of the
Ryukyus, Okinawa, 903-01

Abstract. Benthic foraminiferal assemblages are studied using two piston cores, RN87-PC4 and RN87-PC5, which were respectively raised from the central site (water depth : 2,488 m) and the outher edge (3,136 m) of the Sakishima Deep-Sea Terrace that is located between the southern Ryukyu Island Arc and Ryukyu Trench. Planktonic foraminiferal $\delta^{18}O$ stratigraphy reveals that RN87-PC4 reaches ~110 Ka and RN87-PC5 encompasses the period from ~115 to ~210 Ka. *Bolivina decussata, Abditodendrix pseudothalmanni, Takayanagia delicata* and *Astrononion novozealandicum* are characteristically dominant throughout RN87-PC4, whereas *Fursenkoina cedrosensis, Epistominella exigua, Epistominella levicula* and *Evolvocassidulina brevis* are clearly richer in RN87-PC5. At present, however, it cannot be decided as to whether these contrasting occurrences are due to differences in age or in habitat reflecting different water depth. *Alabamina* ? rugosa and *Pulleniella asymmetrica* predominate in the oxygen isotope Stages 5 and 7 (interglacial episodes) in RN87-PC5. It is also suggested that a dominant occurrence of *Bulimina aculeata* characterizes the Stage 2 (last glacial episode) ; this phenomenon has been recognized in other cores (*e.g.,* KT84-14PI ; Ujiié, 1990) from this region.

Key words. Bathyal benthic foraminifera, oxygen isotope stratigraphy, Ryukyu Trench slope.

Introduction

Bathyal benthic foraminifera are currently regarded as an important indicator of bottom water behavior. Particularly in the Atlantic Ocean, the late Quaternary changes of the Antarctic Bottom Water, North Atlantic Deep Water and Antarctic Intermediate Water have been argued by many authors (*e.g.,* Schnitker, 1979 ; Streeter and Lavery, 1982 ; Balsam, 1981) based on benthic foraminiferal assemblages contained in sediment cores. Yasuda *et al.* (1993) reported the past ~34 kyrs. changes of benthic foraminifera somewhat analogous to the Atlantic Ocean

*Received March 4, 1994 ; revised manuscript accepted August 8, 1994

cases in a 784 cm long piston core (KT89-18/P4) from the western Pacific off Shikoku (lat. 32°08.7′N ; long. 133°53.6′E ; water depth : 2,700 m). Meanwhile, Ujiié *et al.* (1991) indicated unique faunal changes in a 416 cm long core (KT84-14/P1 ; lat. 23°50.2′N ; long. 124°24.1′E ; water depth : 2,488 m) taken from ca. 300 km northeast of the core sites dealt in this paper, the same area as the Ryukyu Trench slope region ; this core reaches ~170 Ka, although KT89-18/P4 and KT84-14/P1 are located along the northern margin of the West Philippine Basin and at a similar water depth.

Therefore, we would like to obtain more information on late Quaternary changes of bathyal benthic foraminiferal fauna prior to inferring the time-space changes of deep water masses in the northwestern Pacific ; such information and oceanographic observation are scarce in the western Pacific Ocean compared with the Atlantic.

Location and lithology

The Ryukyu Island Arc extends for a distance of about 1,200 km along the northwestern margin of the Pacific Ocean and is separated from the East China Sea shelf by the >2,000 m deep Okinawa Trough. The southern arc faces the Ryukyu Trench beyond the rugged topography of the Sakishima Deep-Sea Terrace, which deepens from ~2,000 m to ~4,000 m southwestward.

A slow sedimentation rate on the terrace is expected as exemplified by Ujiié *et al.* (1991). Two piston cores studied here were collected from the central site (RN87-PC4 ; lat. 23°50′ N ; long. 124°24′E ; water depth : 2,488 m) and the outer edge (RN87-PC5 ; lat. 23°36′ N ; long. 124°22′E ; water depth : 3,136 m) of the terrace (Figure 1).

Core RN87-PC4 is 355 cm long and consists of a rather homogeneous silty clay sequence, except for an ash layer at 321-324 cm (Figure 2). Bioturbation is scanty. The

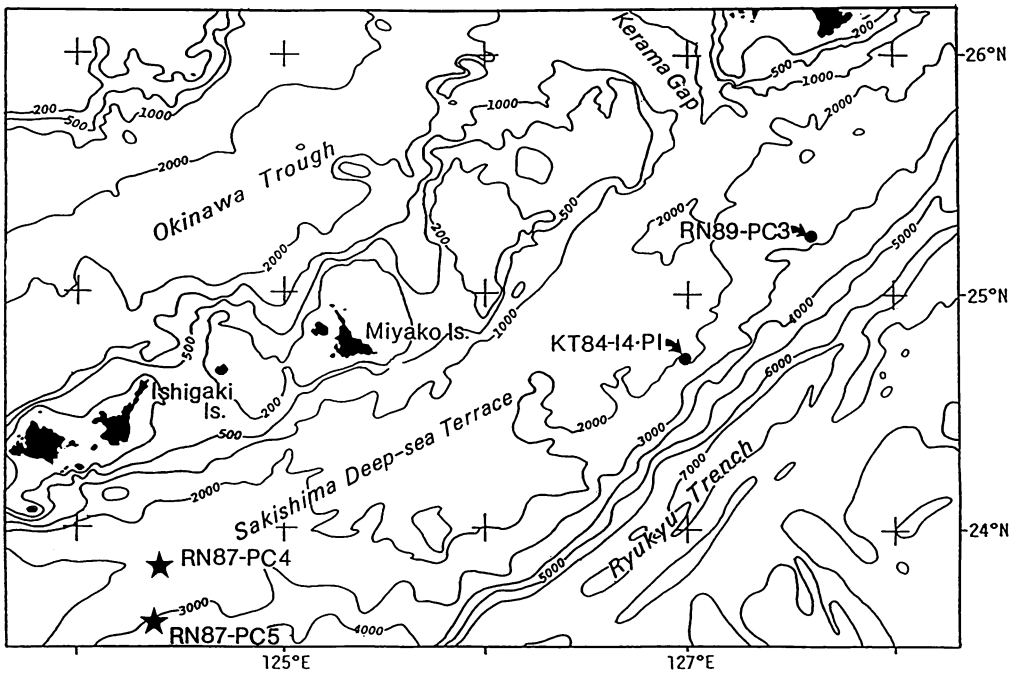

Figure 1. Location map of studied cores (solid stars) and two reference cores (solid circles).

top ~30 cm is brownish in color suggesting oxidized condition, while the rest of the core is olive-grayish suggesting reduced condition. The ash layer was identified as the Ata ash bed from tephrachronologic procedure (Ahagon *et al.*, 1993).

Core RN87-PC5 is 362 cm long and consists of a relatively homogeneous silty clay, excluding a laminated portion around 121-130 cm (Figure 2). The top 44 cm is an oxidized zone, although its base shows gradual change downward.

Oxygen isotope stratigraphy

More than 30 specimens of *Globigerinoides sacculifer* (Brady), a planktonic foraminifera, are collected from a 2 cm thick sample at every 10 cm interval for stable oxygen and carbon isotope analyses. Measurement procedures using a Finnigan MAT delta E mass-spectrometer at Ujiié's Laboratory fol-

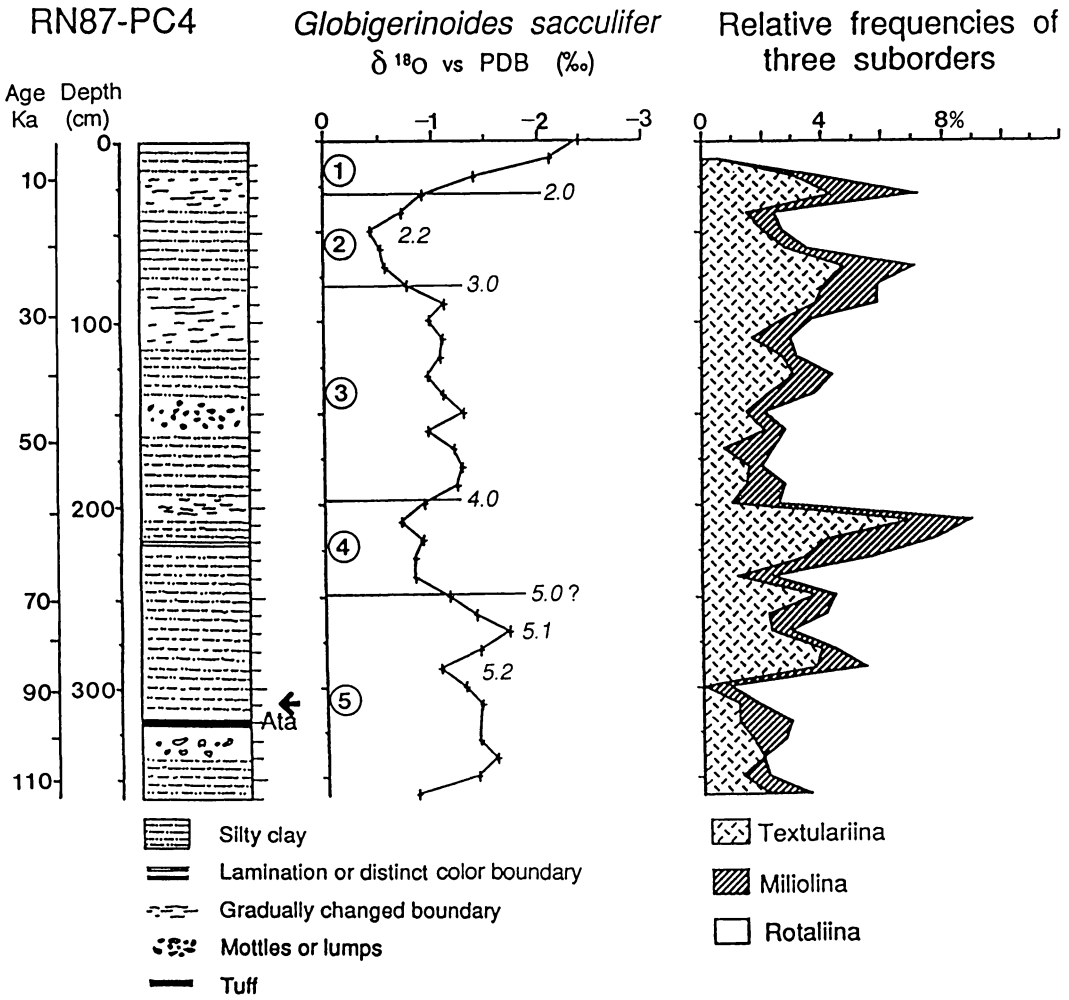

Figure 2. Lithology, planktonic foraminiferal $\delta^{18}O$ stratigraphy, and abundance changes of three foraminiferal suborders in cores RN87-PC4 and -PC5, respectively. Arrow: the abundance change level between *Gephyrocapsa ericsonii* and *Emiliania huxleyi*; ①~⑦: oxygen isotope stages; italic figures: control points.

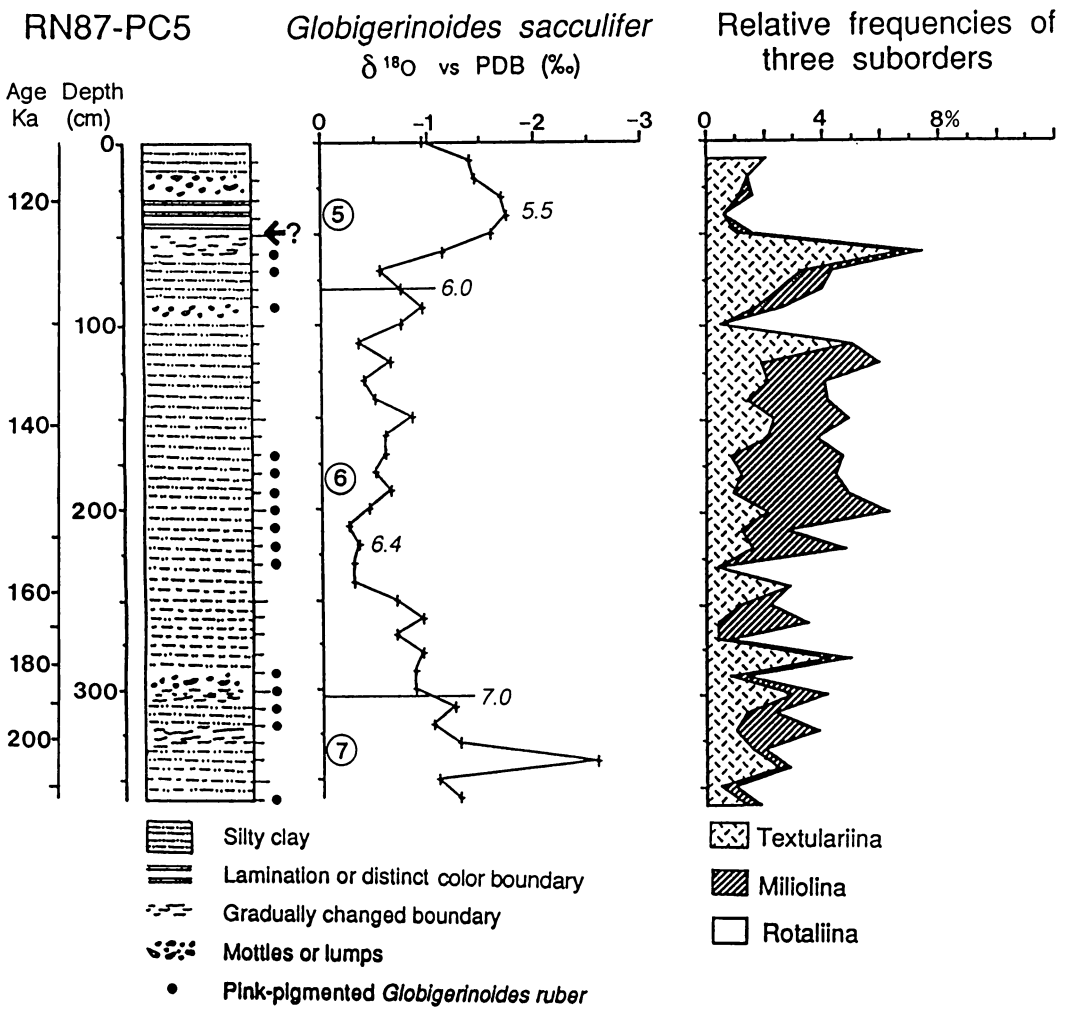

Figure 2. (continued)

low Ahagon *et al.* (1993). Reproducibility of this system was better than ± 0.05 ‰ for $\delta^{18}O$ and ± 0.03 ‰ for $\delta^{13}C$, respectively.

In the oxygen isotope fluctuation pattern of core RN87-PC4, six control points of Imbrie *et al.* (1984) were recognized and the five Isotope Stages from 1 to 5 can be distinguished (Figure 2). At ~30 cm below the event *5.2*, the Ata ash bed is intercalated. This ash bed was dated as ~95 Ka by Ahagon *et al.* (1993). Slightly above the Ata ash bed, we observed a level of abundance change between two calcareous nannoplankton species, *Gephyrocapsa ericsonii* (McIntyre) and *Emiliania huxleyi* (Lohman). According to Thierstein *et al.* (1977), *G. ericsonii* (=their *G. caribbeanica*) quickly increases and *E. huxleyi* decreases above the level within the oxygen isotope stage 5 in their tropical cores. Core RN87-PC4 also shows coincident occurrence between the Isotope Stage and this nannoplankton event, although the precise dating of the event leaves a problem as pointed out by Ujiié *et al.* (1991) and Ahagon *et al.* (1993).

Core RN87-PC5 indicates a quite different

pattern in the fluctuation of planktonic $\delta^{18}O$ values from that in RN87-PC4, suggesting the truncation of the upper portion (Figure 3). We recognized the last appearance datum of pink-pigmented *Globigerinoides ruber* (d' Orbigny) between 50 and 60 cm. This datum was dated as ~120 Ka by a correlation with the oxygen isotope stratigraphy (Thompson *et al.*, 1981). Placing an emphasis on this datum, we concluded that the oxygen isotope fluctuation recognized in core RN87-PC5 represents the change from the early 5 to 7 Isotope Stages and then decided the position of four control points; *i.e. 5.5, 6.0, 6.4* and *7.0*. For RN87-PC5, the abundance change level between *G. ericsonii* and *E.*

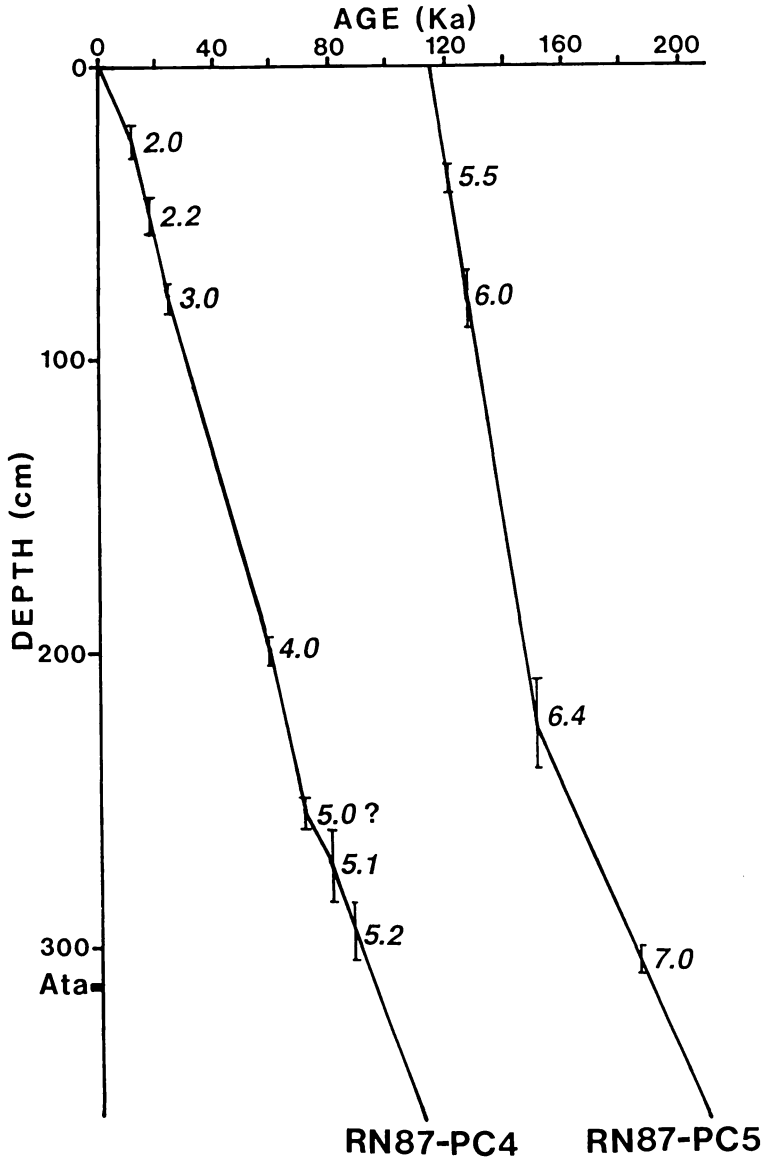

Figure 3. Relationship between core-depth and the ages estimated by isotopic control points and by the Ata ash bed in cores RN87-PC4 and -PC5.

huxleyi is unclear.

Sedimentation rates of two cores are calculated by using these eight time-control points (including Ata ash bed) for RN87-PC4 and four for RN87-PC5 (Figure 3). The sedimentation rate of ~3.60 cm/kyrs. is estimated for the portion above the control point *5.0* and ~1.50 cm/kyrs. for the portion below *5.0* in RN87-PC4, while the value of ~6.28 cm/kyrs. is calculated for the portion above the control point *6.4* and ~2.23 cm/kyrs. for the portion below *6.4* in RN87-PC5. Based on Figure 3, therefore, we determined time scales of both cores and decided that core RN87-PC4 represents the past ~110 Ka, while core RN80-PC5 encompasses the period from ~115 to ~210 Ka.

We also noticed that core RN87-PC5 lacks sediments younger than ~115 Ka. Such a missing section cannot be explained by a failure in sediment recovery during the coring operation, because the core top sediments are of sufficiently oxidized nature. A plausible explanation is the presence of an active undercurrent which sweeps sediments off the edge of the Sakishima Deep-Sea Terrace, the area where the core was collected. Such an undercurrent was observed beneath the western boundary current in the Atlantic Ocean (*e.g.*, Tucholke and Eittreim, 1974; Schnitker, 1979), but has as yet to be documented in the Pacific.

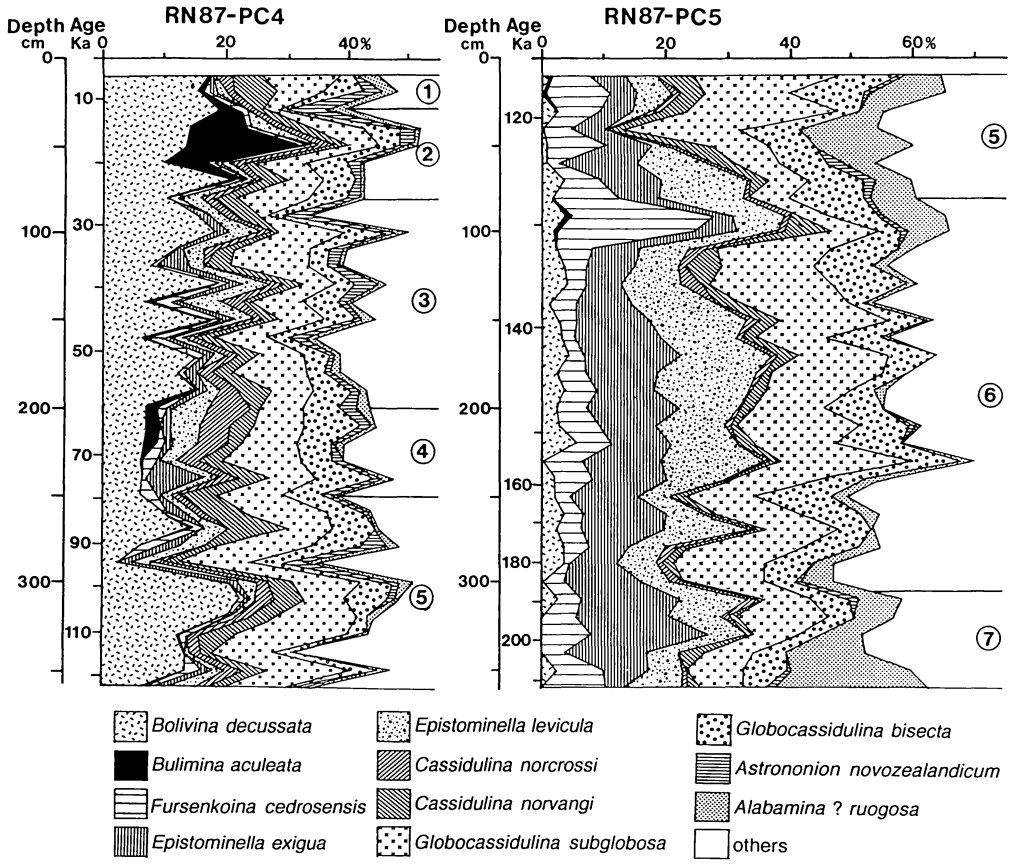

Figure 4. Relative frequency changes of 11 dominant benthic foraminiferal species in cores RN87-PC4 and -PC5.

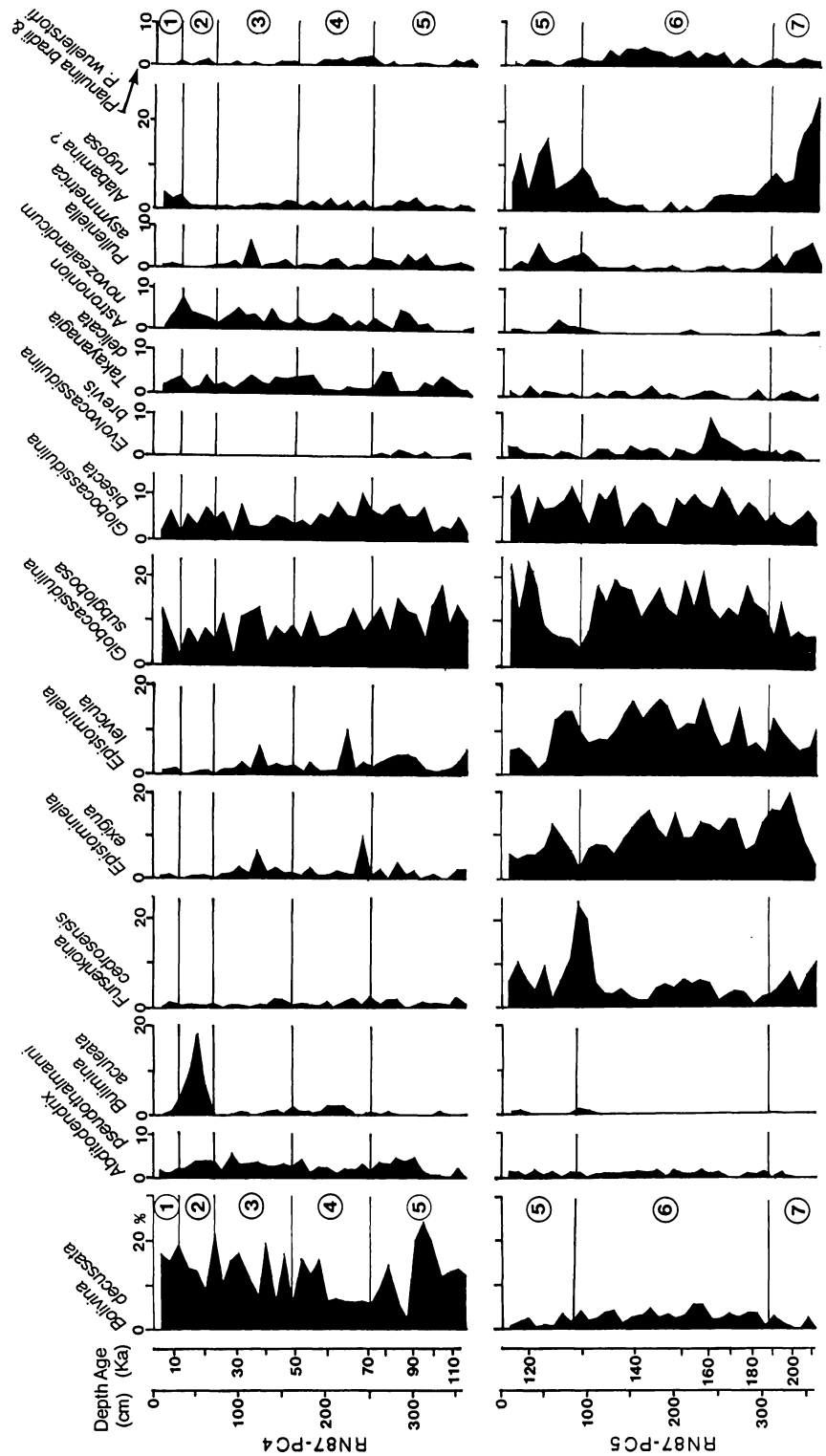

Figure 5. Down-core changes in the relative abundance of 14 selected benthic foraminiferal taxa in cores RN87-PC4 and -PC5.

Table 1. Occurrence chart of "dominant species" in core RN87-PC4.

	RN87-PC4	10-12	20-22	30-32	40-42	50-52	60-62	70-72	80-82	90-92	100-102	110-112	120-122	130-132
1	*Karreriella hanzawai* (Takayanagi)	0	2	1	5	3	6	7	4	2	1	0	3	4
2	*Bolivina decussata* Brady	40	55	65	36	54	30	80	28	56	52	35	19	74
3	*Bolivina pusilla* Schwager	2	4	11	0	1	1	2	0	0	0	1	2	2
4	*Bolivina* sp.	1	1	1	0	7	3	0	1	4	0	0	0	4
5	*Abditodentrix pseudothalmanni* (Boltovskoy & Giussani de Khan)	4	3	6	5	14	12	12	5	20	8	8	9	10
6	*Bulimina aculeata* d'Orbigny	0	2	12	23	72	20	1	0	0	2	0	0	3
7	*Uvigerina proboscidea vadescens* Cushman	3	5	2	0	2	3	0	1	1	3	2	1	0
8	*Siphouvigerina porrecta* (Brady)	1	3	4	1	7	3	5	3	7	5	5	4	5
9	*Trifarina angulosa* (Williamson)	4	6	19	2	16	6	14	5	18	4	6	4	13
10	*Epistominella exigua* (Brady)	1	3	0	0	1	1	0	3	4	7	3	15	5
11	*Epistominella levicula* Resig	1	5	0	11	12	10	5	11	9	16	12	5	18
12	*Eponides tenerus* (Brady)	1	0	2	0	1	3	3	8	1	2	2	1	4
13	*Eponides lamarkianus* (d'Orbigy)	0	4	0	1	0	5	3	4	2	1	0	2	1
14	*Eponides tumidulus* (Brady)	2	0	1	0	1	0	1	1	1	0	2	0	2
15	*Cibicides* cf. *refulgens* Montfort	5	1	1	0	0	3	3	1	0	1	1	5	4
16	*Planulina bradii* Tolmachoff & *P. wuellerstorfi* (Schwager)	0	0	3	0	4	3	0	0	1	0	1	0	0
17	*Fursenkoina cedroensis* (McCulloch)	0	4	2	1	2	1	3	0	2	1	0	1	2
18	*Cassidulina* cf. *neocarinata* Thalmann	6	12	6	6	7	8	6	4	2	9	10	9	14
19	*Cassidulina norcrossi* Cushman	6	6	4	6	7	8	4	6	5	4	6	0	10
20	*Cassidulina norvangi* Thalmann	11	24	4	10	11	5	16	10	12	3	9	11	10
21	*Globocassidulina subglobosa* (Brady)	30	26	8	21	20	26	23	32	6	33	37	32	19
22	*Globocassidulina bisecta* Nomura	5	24	5	15	15	23	19	17	6	24	10	8	13
23	*Favocassidulina favus* (Brady)	0	0	0	0	0	1	0	0	8	1	0	0	0
24	*Evolvocassidulina brevis* (Aoki)	0	0	0	0	0	0	0	0	0	0	0	0	0
25	*Takayanagia delicata* (Cushman)	4	8	11	2	4	12	5	5	7	3	6	9	9
26	*Astrononion novozealandicum* Cushman & Edwards	1	11	23	7	9	7	4	7	15	8	8	4	16
27	*Pullenia* sp. B of Ujiié(1990)	0	6	0	0	0	1	4	6	9	4	3	6	4
28	*Pulleniella asymmetrica* Ujiié	1	2	0	0	0	0	2	1	5	0	2	0	2
29	*Gyroidina* sp. A of Ujiié(1990)	0	1	0	3	0	4	0	1	3	4	0	2	0
30	*Oridorsalis umbonatus* (Reuss)	1	2	2	2	4	5	1	1	4	1	0	4	2
31	*Alabamina* (?) *rugosa* (Phleger & Parker)	8	9	11	2	1	1	1	1	0	1	1	2	3
32	*Melonis sphaeroides* Voloshinova	0	0	2	0	0	0	6	0	10	3	14	3	4
33	*Melonis barleeanum* (Williamson)	0	0	1	0	0	0	0	0	0	1	5	0	0
T	Total Specimens	232	350	340	254	398	312	368	270	359	301	305	249	375

	140-142	150-152	160-162	170-172	180-182	190-192	200-202	210-212	220-222	230-232	240-242	250-252	260-262	270-272	280-282	290-292	300-302	310-312	319-321	330-332	340-342	350-352	360-362
1	3	0	3	2	0	3	1	15	5	3	0	0	0	1	2	5	0	0	1	1	0	0	4
2	18	56	18	47	30	51	18	18	20	18	17	20	26	49	18	7	53	71	53	34	31	41	19
3	0	2	0	1	3	1	0	0	2	3	2	1	0	0	1	0	0	0	0	0	0	0	0
4	1	2	3	3	2	2	2	2	1	3	1	5	2	6	12	11	12	11	1	10	5	9	0
5	7	10	8	9	3	7	6	3	6	4	8	5	9	9	12	10	11	4	9	2	0	7	0
6	3	2	4	2	0	1	6	6	7	1	0	1	0	1	0	0	0	0	0	1	0	0	1
7	0	0	3	1	2	4	0	1	2	2	0	8	0	2	1	2	1	7	1	3	2	11	1
8	3	6	9	7	2	3	3	1	1	7	4	3	3	8	5	7	2	9	1	5	3	7	2
9	1	7	9	3	1	3	4	4	7	6	6	6	2	3	2	3	1	1	1	3	0	4	4
10	5	5	4	1	5	1	1	4	3	1	26	3	6	0	10	3	4	0	1	0	0	6	5
11	19	10	8	6	0	7	16	12	12	9	7	5	6	11	11	11	9	3	1	1	2	7	14
12	4	2	3	1	5	1	5	3	2	4	1	5	1	0	1	4	2	0	0	1	1	0	3
13	2	0	5	1	1	1	0	0	0	0	3	0	2	0	3	0	0	0	0	0	2	2	3
14	1	1	0	0	1	0	0	1	1	1	3	4	2	4	3	2	1	2	2	1	1	1	2
15	2	3	3	6	4	6	3	1	0	4	3	1	4	4	2	2	3	1	5	2	8	0	7
16	1	2	1	0	0	3	3	4	2	4	0	7	0	3	0	0	1	1	0	0	3	1	3
17	5	6	2	3	1	1	4	0	4	6	1	8	2	5	6	0	0	4	2	1	0	7	1
18	7	8	7	17	8	16	10	0	3	3	5	7	10	15	3	9	8	15	11	15	10	6	6
19	11	5	5	5	6	9	18	13	15	11	7	5	4	1	0	4	4	10	6	6	5	9	5
20	3	9	7	11	9	18	4	10	7	11	14	21	18	31	7	6	11	16	11	17	5	12	7
21	24	24	25	21	29	22	19	21	27	38	21	35	36	25	43	33	30	21	36	52	23	43	28
22	15	17	11	13	8	20	15	23	17	15	28	22	16	25	23	14	14	24	5	9	6	16	5
23	1	1	3	3	0	1	2	1	1	6	2	6	1	4	0	0	1	2	0	0	0	3	1
24	0	0	0	0	0	0	0	0	0	0	0	0	1	0	3	2	1	0	3	0	0	1	1
25	5	10	9	11	10	4	3	1	3	3	3	5	14	16	1	1	2	9	5	11	7	4	3
26	4	3	7	3	2	5	9	6	2	5	1	9	2	0	12	9	3	4	0	0	0	0	1
27	8	4	7	3	4	4	7	6	10	6	16	17	1	4	5	9	5	2	0	1	1	4	3
28	3	6	0	2	2	1	4	5	0	2	2	9	4	4	2	9	4	10	2	1	0	5	2
29	0	1	0	1	2	1	1	2	0	0	0	4	0	1	4	2	1	2	3	3	1	3	1
30	14	7	7	2	4	4	3	8	3	12	1	1	1	5	1	7	2	5	2	0	0	4	0
31	2	6	4	2	4	3	6	2	5	0	5	0	1	1	5	4	6	1	3	1	0	4	2
32	7	5	1	0	1	3	1	4	7	5	3	6	2	4	3	10	2	4	0	1	0	0	0
33	0	0	3	0	2	0	0	0	0	0	0	0	0	0	0	0	0	0	0	0	0	1	0
T	271	325	281	296	244	322	266	257	303	296	268	341	269	331	279	270	264	319	267	281	241	308	267

Table 2. Occurrence chart of "dominant species" in core RN87-PC5.

	RN87-PC5	10-12	20-22	30-32	40-42	50-52	60-62	70-72	80-82	90-92	100-102	110-112	120-122	130-132
1	*Karreriella hanzawai* (Takayanagi)	0	0	0	0	0	11	2	4	1	1	6	2	4
2	*Bolivina decussata* Brady	4	0	6	0	2	2	8	5	9	4	5	11	13
3	*Bolivina pusilla* Schwager	1	2	2	0	1	4	4	2	5	2	0	0	1
4	*Bolivina* sp.	1	0	0	2	0	1	2	1	0	0	0	0	4
5	*Abditodentrix pseudothalmanni* (Boltovskoy & Giussani de Khan)	3	4	1	3	0	3	9	3	2	0	2	3	3
6	*Bulimina aculeata* d'Orbigny	1	1	0	0	0	0	0	0	2	1	0	0	0
7	*Uvigerina proboscidea vadescens* Cushman	0	0	2	0	1	0	2	0	0	1	0	3	0
8	*Siphouvigerina porrecta* (Brady)	0	0	3	1	0	0	0	0	0	1	0	1	0
9	*Trifarina angulosa* (Williamson)	2	2	3	3	1	0	3	3	0	2	5	4	2
10	*Epistominella exigua* (Brady)	20	10	14	12	15	30	21	17	6	15	17	22	18
11	*Epistominella levicula* Resig	18	13	9	2	6	28	31	38	20	15	17	22	31
12	*Eponides tenerus* (Brady)	8	12	7	2	1	12	13	13	7	6	5	17	8
13	*Eponides lamarkianus* (d'Orbigy)	5	3	0	3	2	0	2	3	0	5	0	0	0
14	*Eponides tumidulus* (Brady)	12	4	6	4	9	7	1	1	0	1	0	1	0
15	*Planulina bradii* Tolmachoff & *P. wuellerstorfi* (Schwager)	1	0	4	2	1	0	2	0	4	2	2	11	6
16	*Fursenkoina cedroensis* (McCulloch)	21	24	18	9	19	5	14	30	51	47	13	11	11
17	*Cassidulina* cf. *neocarinata* Thalmann	1	0	4	2	2	0	0	2	3	9	5	4	3
18	*Cassidulina norcrossi* Cushman	0	3	2	0	1	1	1	1	1	1	6	2	10
19	*Cassidulina norvangi* Thalmann	22	9	12	4	13	8	7	1	3	17	4	18	4
20	*Globocassidulina subglobosa* (Brady)	81	30	63	40	19	18	15	18	11	17	41	44	64
21	*Globocassidulina bisecta* Nomura	35	29	9	21	15	18	20	34	18	7	24	28	41
22	*Favocassidulina favus* (Brady)	7	1	3	2	4	8	3	0	2	0	8	7	3
23	*Evolvocassidulina brevis* (Aoki)	7	4	1	1	1	0	2	1	0	0	3	4	1
24	*Takayanagia delicata* (Cushman)	3	0	4	0	2	1	3	1	0	0	1	0	3
25	*Astrononion novozealandicum* Cushman & Edwards	1	1	0	0	0	7	4	3	2	2	0	0	0
26	*Pullenia* sp. B of Ujiié(1990)	7	5	5	2	9	1	0	2	0	5	7	10	17
27	*Pulleniella asymmetrica* Ujiié	2	4	4	13	6	4	5	8	9	5	1	2	2
28	*Gyroidina* sp. A of Ujiié(1990)	6	4	7	4	0	1	1	3	1	0	3	6	0
29	*Oridorsalis umbonatus* (Reuss)	6	0	0	2	0	1	4	4	0	4	3	4	5
30	*Alabamina* (?) *rugosa* (Phleger & Parker)	21	29	11	27	33	11	13	20	22	15	5	7	4
31	*Melonis sphaeroides* Voloshinova	2	0	1	0	0	0	0	2	0	0	0	0	0
32	*Melonis barleeanum* (Williamson)	0	0	0	0	0	0	1	0	1	0	0	3	0
T	Total Specimens	349	229	261	213	205	240	225	278	223	214	221	297	325

	140-142	150-152	160-162	170-172	180-182	190-192	200-202	210-212	220-222	230-232	240-242	250-252	260-262	270-272	280-282	290-292	300-302	310-312	320-322	330-332	340-342	350-352	360-362
1	1	4	4	1	2	0	3	0	3	1	3	0	0	0	6	0	3	0	0	0	1	0	0
2	3	8	7	10	6	8	8	7	14	0	5	5	8	6	9	8	1	7	1	0	0	5	0
3	1	0	1	0	0	1	0	0	1	1	0	3	0	1	0	0	1	3	1	4	0	0	3
4	0	0	0	0	0	0	2	1	3	0	0	1	0	0	0	0	0	0	0	0	1	2	0
5	1	3	2	1	2	0	4	0	1	4	1	2	0	0	2	1	3	0	2	0	0	0	0
6	0	0	0	0	0	0	0	0	0	0	0	0	0	0	0	0	0	0	0	0	0	0	0
7	1	1	0	0	0	0	0	1	0	0	0	0	0	0	1	3	1	0	0	0	0	0	0
8	0	0	0	0	0	0	0	0	0	0	0	0	0	0	0	1	0	0	0	0	0	0	0
9	1	1	1	1	1	1	0	4	0	2	8	2	3	2	3	3	2	1	2	0	2	0	2
10	19	35	32	35	27	21	49	23	25	36	29	25	30	32	16	16	28	38	44	48	32	15	7
11	28	48	28	33	40	34	31	27	28	47	24	13	15	35	14	14	10	29	26	16	12	12	20
12	5	9	11	12	6	7	6	8	10	6	10	9	5	8	15	8	10	2	11	4	4	3	8
13	0	1	0	0	2	0	0	0	0	0	0	0	0	0	0	0	0	0	4	5	0	0	8
14	4	5	4	5	5	3	0	2	4	2	1	2	2	4	2	1	5	7	4	3	15	5	3
15	9	9	9	7	7	4	8	8	2	8	5	6	0	0	4	1	2	3	1	2	4	2	1
16	9	9	5	5	12	12	16	15	15	18	14	5	7	10	9	2	7	9	15	20	9	16	23
17	1	4	2	3	3	2	0	1	4	0	2	2	1	3	4	3	2	0	0	3	1	2	0
18	1	5	2	2	3	1	0	1	0	3	0	0	2	3	5	2	4	2	1	0	1	1	2
19	8	11	5	8	3	6	8	3	6	3	3	5	1	1	4	4	1	4	4	2	10	0	4
20	38	52	26	32	44	31	38	48	34	61	33	25	31	29	45	32	29	18	44	18	19	19	15
21	6	20	20	17	10	8	31	20	28	23	19	28	22	14	22	17	11	15	13	9	12	15	9
22	5	7	13	6	13	5	10	8	10	9	3	5	4	4	11	9	7	4	10	9	6	0	1
23	0	7	3	4	4	0	6	3	0	2	5	21	10	9	7	4	5	4	4	3	3	0	0
24	2	0	1	5	1	1	0	0	1	3	3	1	0	0	0	3	0	0	2	3	1	0	1
25	0	0	0	0	0	0	0	2	0	0	0	0	0	0	0	0	1	3	0	0	0	1	2
26	11	3	10	6	4	9	8	4	8	6	8	8	6	5	4	5	3	12	2	0	3	10	0
27	1	3	0	1	1	2	0	0	0	2	2	3	0	1	0	1	4	8	2	10	12	14	3
28	0	0	0	0	2	7	7	0	0	3	0	3	6	10	2	2	7	4	3	8	19	7	14
29	0	1	1	0	11	3	1	2	0	3	2	2	1	0	5	3	0	0	4	9	0	0	0
30	1	3	2	0	0	4	0	2	0	2	6	7	7	0	8	7	13	18	18	17	31	41	55
31	3	4	1	0	3	6	5	8	4	1	3	3	2	6	6	4	4	0	8	4	2	1	0
32	0	0	3	0	0	0	5	0	3	3	0	0	1	4	0	5	7	6	3	7	1	0	0
T	214	302	229	224	245	226	329	243	258	278	241	228	226	243	241	217	223	246	292	251	242	209	218

Benthic foraminiferal faunas

The same samples used for isotope analysis were subjected to benthic foraminiferal analyses. More than 200 (sometimes 300) specimens were picked out at random from fractions coarser than 75 μm.

Planktonic ratios (percentage of planktonic forms versus all foraminiferal tests) are very high throughout the cores; it ranges from 83.5 to 95.5% (94% in average) in core RN87-PC4 and from 87.8 to 98.4% (95% in average) in RN87-PC5. These high ratios suggest that a hemipelagic environment prevailed over the period represented by the two cores.

Down-core abundance changes of the three foraminiferal suborders defined by Loeblich and Tappan (1964; not 1988) indicate the following trends (Figure 2): 1) Rotaliina always predominates, showing more than 92% in relative frequency, implying hemipelagic environment. 2) In core RN87-PC4, a relative proportion of Textulariina seems to increase during the glacial episodes (Isotope Stages 2 and 4). 3) In core RN87-PC5, however, Textulariina does not exhibit such a trend but Miliolina is relatively rich in the upper two-thirds of Stage 6.

In Tables 1 and 2, we document the occurrence of 32 species, whose relative abundances exceed three percent in any one of the treated samples, with the total number of examined specimens given at the bottom. Scanning electron micrographs of the 32 species are shown in Figures 6-10.

Down-core changes in relative abundance of 11 species that represent more than 6.8% in any sample are shown in Figure 4, where *Gyroidina* sp. A of Ujiié (1990) is excluded because of the uncertainty of its taxonomic status. The general patterns of faunal changes shown in this figure indicate a contrasting difference between two cores. In core RN87-PC4, faunal changes related to the glaciation and deglaciation are rather indistinct, except for the fact that *Bulimina aculeata* (d'Orbigny) predominates exclusively in Stage 2 (last glacial episode). On the other hand, *Alabamina* ? rugosa (Phleger and Parker) is more abundant in Stages 5 and 7 (interglacial episodes) in core RN87-PC5. The blank area in Figure 4, representing the "others" category, donotes combined percentages of those taxa occurring as a minor component of the fauna. Therefore, the area width depicts the degree of specific diversity of the respective fauna. This "others" category in core RN87-PC4 nearly always occupies more than 60%, whereas it is less than about 40% in RN87-PC5. This difference is considered to reflect the degree of habitability of the two core sites, with the shallower depth of RN87-PC4 being better suited for a greater number of species to thrive.

Figure 5 graphically portrays the stratigraphic occurrences of 14 taxa inclusive of 11 species shown in Figure 4. All these species attain more than 3% of the fauna in any given sample with the exception of a taxon group consisting of *Planulina wuellerstorfi* (Schwager) and *Planulina bradii* Tolmachoff. *Bolivina decussata* Brady occurs much more abundantly throughout RN87-PC4 than in

→ **Figure 6.** Scanning electron micrographs of some representative species. **1**: *Karreriella hanzawai* (Takayanagi) (lateral view), from RN87-PC5, 300-302 cm, ×250. **2, 3**: *Bolivina decussata* Brady. 2: Broad-test type (lateral view); 3: slender test type (a: lateral, b: apertural views); both from RN87-PC4, 70-72 cm, ×300. **4**: *Bolivina pusilla* Schwager (a: lateral, b: apertural views), from RN87-PC4, 30-32 cm, ×250. **5**: *Bolivina* sp. (lateral view), from RN87-PC4, 310-312 cm, ×300. **6-8**: *Abditodendrix pseudothalmanni* (Boltovskoy and Guissani de Khan) (lateral views, except for apertural view of 6b). 8: A variety with not-quadrangled periphery, from RN87-PC4, 90-92 cm; 6 and 7: from RN84-PC4, 280-282 cm; all ×300. **9**: *Bulimina aculeata* d'Orbigny (side view), from RN87-PC4, 40-42 cm, ×250. **10**: *Uvigerina proboscidea vadescens* Cushman (side view), from RN87-PC4, 350-352 cm. **11**: *Siphouvigerina porrecta* (Brady) (side view), from RN87-PC4, 310-312 cm, ×300. **12**: *Trifarina angulosa* (Williamson) (side view), from RN87-PC4, 30-32 cm, ×300.

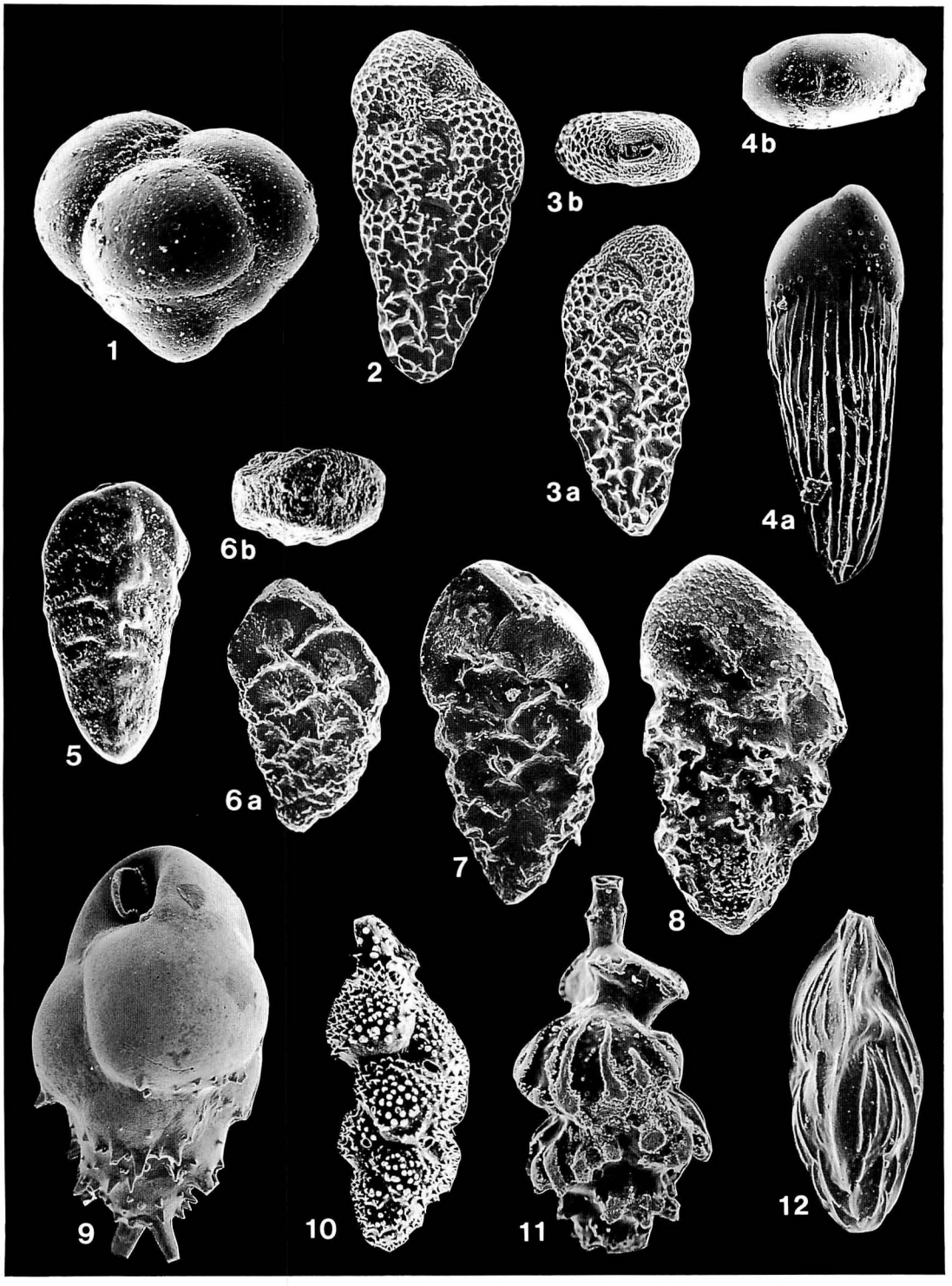
1
2
3b
4b
3a
4a
5
6b
6a
7
8
9
10
11
12

RN87-PC5. A similar but less distinct trend can be observed for *Abditodendrix pseudothalmanni* (Boltovskoy and Guissani de Khan), *Takayanagia delicata* (Cushman), or *Astrononion novozealandicum* Cushman and Edwards. Contrastingly, *Fursenkoina cedrosensis* (McCulloch), *Epistominella exigua* (Brady) and *Epistominella levicula* Resig are distinctly richer in RN87-PC5. *Evolvocassidulina brevis* (Aoki) disappeared at the Stage 4/5 boundary, and *Alabamina* ? *rugosa* is also somewhat more abundant in RN87-PC5. The interglacial Stages 5 and 7 are characterized by the increases of *A.* ? *rugosa*, as mentioned above, and of *Pulleniella asymmetrica* Ujiié. The former species slightly increases in the postglacial period (Stage 1).

Discussion

Planktonic foraminiferal $\delta^{18}O$ stratigraphy revealed that core RN87-PC4 reaches ~110 Ka (middle Stage 5), whereas core RN87-PC5 represents the period from ~115 Ka to ~210 Ka (middle Stage 5 to upper Stage 7). By taking the two cores as a composite section, therefore, a continuous stratigraphic occurrence of benthic foraminifera for the past ~210 kyrs. can be monitored in the trench slope region off Ishigaki Island. Before discussing of this, however, we must emphasize the 648 m difference in water depth between the cores (RN87-PC4 : 2,488 m, RN87-PC5 : 3,136 m), even though the coring sites are only 25 km apart.

Different habitats related to water depth can be expected for *Bolivina decussata, Takayanagia delicata* and *Astrononion novozealandicum*, all of which are clearly more predominant in the shallower core, RN87-PC4, than in RN87-PC5, as well as for *Fursenkoina cedrosensis, Epistominella exigua, Epistominella levicula* and *Evolvocassidulina brevis*, all of which are characteristically richer in RN87-PC5, as explained above.

Nevertheless, abundant occurrences of both *E. exigua* and *A. novozealandicum* in Stage 6 were observed in core KT84-14/P1 (lat. 23°50.2′N ; long. 124°24.1′E ; water depth, 2,488 m) raised from the margin of the Sakishima Deep-Sea Terrace about 275 km east-northeast of RN87-PC4 (Ujiié *et al.*, 1991). This 416 cm long core covers that past ~170 kyrs. Other dominant species, however, show large discrepancies in their stratigraphic occurrences, probably because of different test sizes treated. For core KT84-14/P1, fractions coarser than 105 μm were treated, and for both RN87-PC4 and -PC5 fractions coarser than 75 μm.

More significant differences are recognized between our cores and a core KT89-18/p4 collected from seas off the coast of Shikoku, Southwest Japan (lat. 32°8.7′N ; long. 133°53.6′E ; water-depth, 2,700 m) (Yasuda *et al.*, 1993). In a preliminary report, Yasuda *et al.* showed down-core changes in the occurrence of major benthic foraminiferal components that are somewhat analogous to the North Atlantic studies reported by Streeter an Lavery (1982) who treated the >149 μlm fraction, Schnitker (1979) who treated the >125 μm fraction, and Balsam (1981) who did not indicate what fraction was used. The purpose of these studies was to estimate bottom water-mass changes during

→ **Figure 7.** **1, 2** : *Epstominella exigua* (Bardy). 1 : Adult (a : spiral side, b : apertural edge views) ; 2 : young form (spiral side view) ; both from RN83-PC5, 230-232 cm, ×300. **3** : *Epistominella levicula* Resig (a : spiral side, b : apertural edge views), from RN87-PC5, 230-232 cm, ×300. **4** : *Eponides tenerus* (Bardy) (spiral side view), from RN87-PC5, 210-212 cm, ×300. **5** : *Eponides lamarckianus* (d'Orbigny) (spiral view), from RN87-PC4, 160-162 cm, ×300. **6** : *Cibicides* cf. *C. refulgens* Montfort, Juvenile form (a : spiral side, b : umbilical side, c : apertural edge views), from RN87-PC4, 190-192 cm, ×400. **7, 8** : *Planulina bradii* Tolmachoff (a : spiral side, b : apertural edge views). 7 : Adult from RN87-PC5, 160-162 cm, 8 : Juvenile form from RN87-PC5, 140-142 cm ; both ×200. **9, 10** : *Planulina wuellerstorfi* (Schwager) (a : spiral, b : apertural edge views). 9 : Adult from RN87-PC5, 290-292 cm, ×100 ; 10 : young form from RN87-PC5, 250-252 cm, ×150.

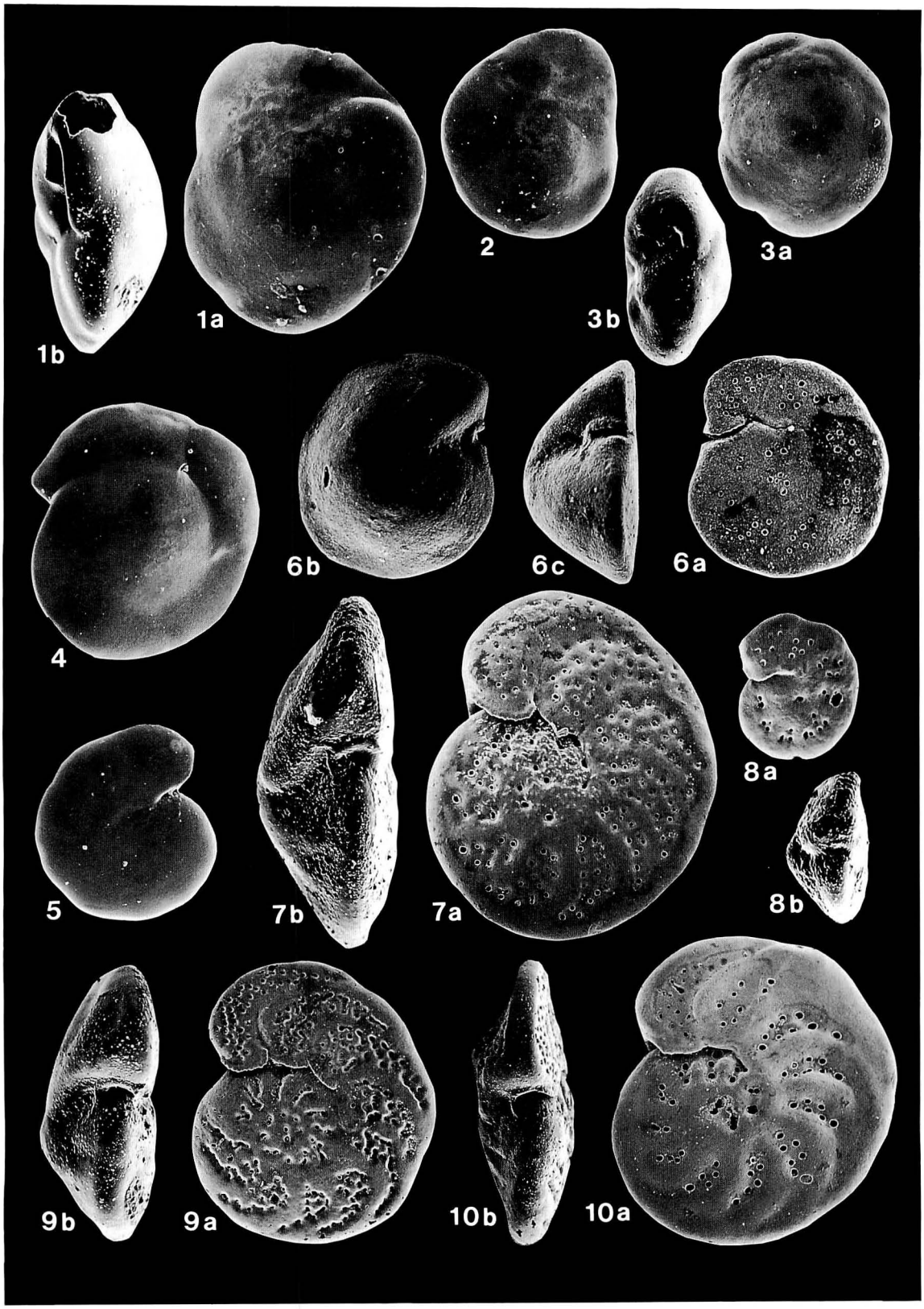
1b
1a
2
3b
3a
4
6b
6c
6a
5
7b
7a
8a
8b
9b
9a
10b
10a

the period from the last glacial to Recent based on analyses of benthic foraminiferal assemblages. In particular, Yasuda *et al.* (1993) emphasized that *Uvigerina peregrina* disappeared around ~10 Ka after its abundant occurrence in the last glacial episode, which is marked by similar occurrences of *Melonis barleeanum* and *Melonis sphaeroides*. They supposed that the Circumpolar Deep Water or Antarctic Intermediate Water characterized by the three species was displaced by the North Atlantic Deep Water (NADW) after the last glacial episode as well as in the North Atlantic Ocean. In core KT84-14/P1 from the Ryukyu Trench slope region (Ujiié *et al.*, 1991), however, no similar mode of species occurrence can be recognized, even though the test size treated is similar to that of Yasuda *et al.* (1993). Besides, no oceanographer recognized the water corresponding to the NADW in the northern Pacific.

For further comparative study of benthic foraminifera from core to core, we would like to point out the need of the same or similar-sized fractions. Particulary, test sizes between 75 μm and 103~148 μm should be examined because a considerable number of benthic species occur as small-size adults. For examples, such minute- but dominant species as *Bolivina decussata, Epistominella levicula*, and *Fursenkoina cedrosensis*, all characteristic of cores RN87-PC4 and -PC5, were hardly observed in the fraction coarser than 103 μm of core KT84-14/P1 as dominant taxa.

The next problem concerns the taxonomy, which seems to differ from author to author. Every foraminiferalogist has his or her own opinions regarding the taxonomic status of many species and this is to be expected. However, every author should strive to illustrate (and if possible, describe) major species, at least those of critical importance to the subject of the paper, in order to give other authors every convenience for comparisons. Judging from a drawing of umbilical side, *Osangularia umbonifera* (Cushman) of Schnitker (1979) (=? *Nuttallides umbonifera* of Yasuda *et al.*, 1993) may be identical to *Alabamina*? *rugosa* in our study. *As* pointed out by Ujiié (1990), *A.*? *rugosa* has erroneously been reported under various specific names, sometimes under the genus *Nuttallides*. Recently, Loeblich and Tappan (1994) assigned this species as *Nuttallides rugosus* without any notice on the generic heterogeneity of its type species, *Eponides truempyi* Nuttal, 1930. Ujiié (1990) also distinguished *Oridorsalis umbonatus* (Reuss) and *Eponides tenerus* (Brady) by a detailed anatomic analysis, though some authors made isotope measurements by treating the two species as a single taxon. In our study, we found that *Planulina bradii* may have been grouped with *Planulina wuellerstorfi* in many previous works. *A.*? *rugosa, O. umbonatus* and *P. wuellerstorfi* have been recognized as important indices of bottom water (*e.g.*, Schnitker, 1979; Streeter and Lavery, 1982).

The last problem to be proposed here is how to accumulate information regarding the

→ **Figure 8.** **1**: *Fursenkoina cedrosensis* (McCulloch) (lateral view), from RN87-PC4, 90-92 cm, ×300. **2, 3**: *Cassidulina* cf. *C. neocarinata* Thalmann (apertural lateral views). 2: Young form, ×250; 3: adult, ×200; both from RN87-PC4, 190-192 cm. **4**: *Cassidulina norcrossi* Cushman (apertural lateral view), from RN87-PC5, 130-132 cm, ×300. **5**: *Cassidulina norvangi* Thalmann (a: apertural lateral, b: apertural edge views), from RN87-PC4, 270-272 cm, ×400. **6**: *Globocassidulina subglobosa* (Brady) (apertural lateral view), from RN87-PC4, 250-252 cm, ×300. **7, 8**: *Takayanagia delicata* (Cushman) (a: apertural lateral, b: apertural edge views). 7: Specimen with grooves radiating from the apertural face like in *Takayanagia quasisulcata* (Belford) (= *Cassidulina quasisulcata* Belford, 1966), although the other characters are identical to *T. delicata*; 8: normal type, both from RN87-PC4, 270-272 cm, ×400. **9**: *Globocassidulina bisecta* Nomura (apertural lateral view), from RN87-PC4, 360-362 cm, ×400. **10**: *Favocassidulina favus* (Brady) (lateral view opposite to apertural side), from RN87-PC5, 280-282 cm, ×100.

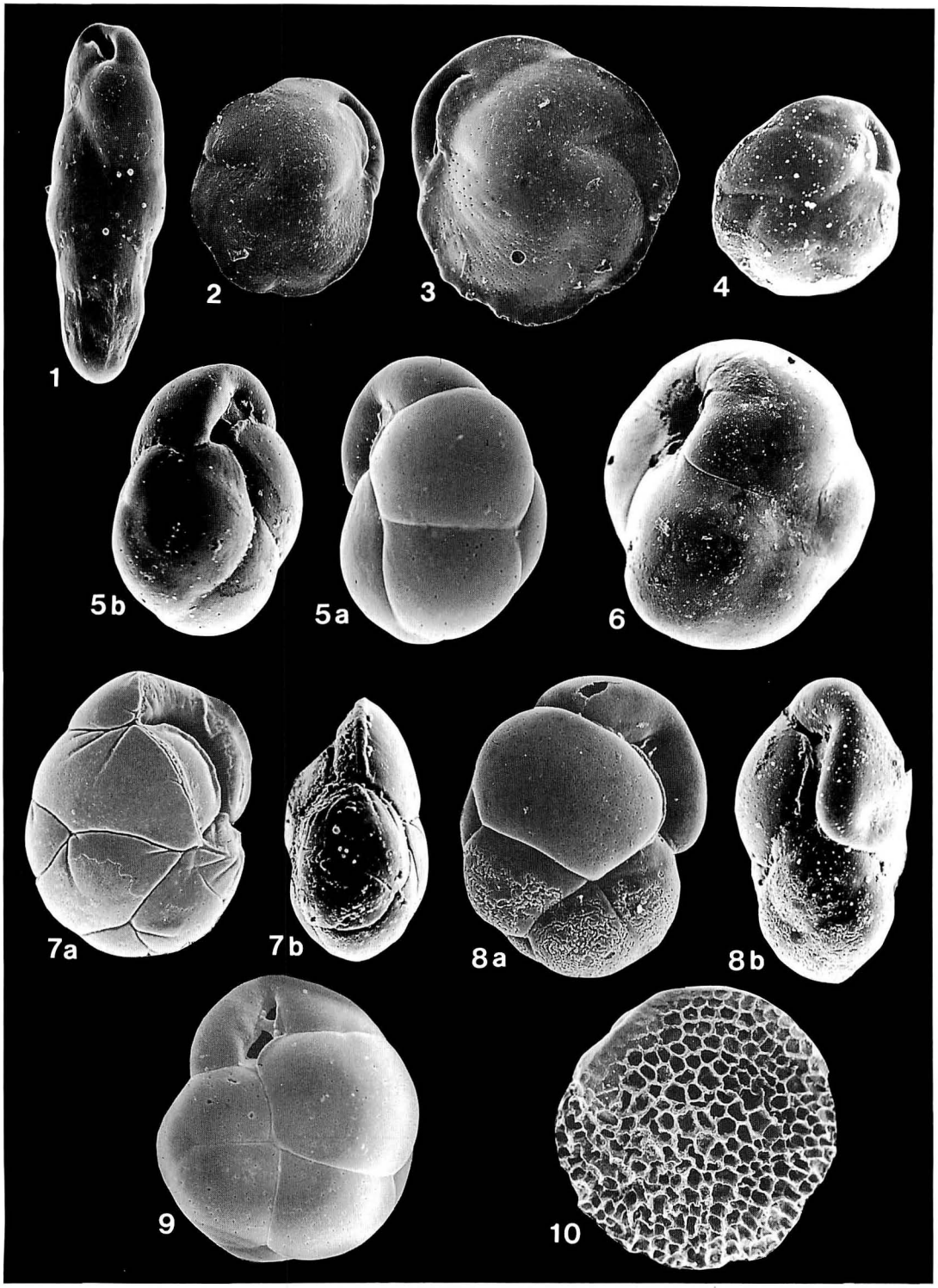
1
2
3
4
5b
5a
6
7a
7b
8a
8b
9
10

distribution of Recent benthic foraminifera in the Northwest Pacific Ocean, where such information is scanty. Inoue (1989) compiled the benthic foraminiferal distribution in seas adjacent to Japan using numerous sediment dredgings along with a few piston cores. However, dredged samples and the top of piston cores do not represent real surface sediments in many cases, because the former are frequently contaminated with older sediments and the latter lose the top few cm in the core pushing-out process owing to their soupy nature. Therefore, the assemblages contained in those samples can't be strictly correlated to oceanographic observation on bottom waters. Instead, we are collecting many top samples of pilot corers and of multiple corers in order to clarify real Recent distribution of benthic foraminifera around the Ryukyu Island Arc region. At present, we should document in detail down-core changes of benthic foraminiferal assemblages as much as possible, before we speculate on the relationship between the assemblages and bottom water conditions so far as the Northwest Pacific Ocean cases are concerned.

Conclusions

A planktonic foraminiferal oxygen isotope stratigraphy provides a kind of analog time-scale for two piston cores, RN87-PC4 and -PC5. The former was collected from 2,488 m in water depth in the middle part of the Sakishima Deep-Sea Terrace south of Ishigaki Island, Okinawa, and the latter from a 3,136 m-depth and the terrace edge. The time scale was substantiated by recognizing a tephrachronology based on the Ata ash bed and by two micropaleontologic events, namely the abundance change between two calcareous nannoplankton species, *Gephyrocapsa ericsonii* and *Emiliania huxleyi*, and the last appearance datum of pink-pigmented *Globigerinoides ruber*.

Core RN87-PC4 contains an oceanographic record spanning the past ~110 kyrs. and RN87-PC5 covers the period from ~115 Ka to ~210 ka. The missing sequence younger than ~115 Ka in the latter core may be ascribed to scouring by an unknown bottom current along the outer edge of the Sakishima Deep-Sea Terrace.

Based on the time scale thus established, we showed down-core changes in a relative abundance of 32 dominant benthic foraminiferal taxa. *Bulimina aculeata* predominates characteristically in the last glacial episode (Isotope Stage 2). *Epistominella exigua* becomes dominant in the period older than Stage 5, while *Astrononion novozealandicum* increases its abundance upward after the middle of Stage 5. These trends were recognized in core KT84-14/P1 that was raised from the same Sakishima Deep-Sea Terrace, some 275 km north-northeast of RN87-PC4. We also observed biased occurrences in RN87-PC4 of *Bolivina decussata, Abditodendrix pseudothalmanni* and *Takayanagia*, in contrast to *Fursenkoina cedrosensis* and *Epistominella levicula* which are more abundant in RN87-PC5. At present, however, we are uncertain as to whether these biased modes of occurrence were due to different geologic times or to different water-depths; there is a 648 m depth difference between the two cores. Additionally, we pointed out that

→ **Figure 9. 1, 2**: *Evolvocassidulina brevis* (Aoki) (lateral views except for 1b, apertural view), both from RN87-PC5, 270-272 cm, ×400. **3**: *Astrononion novozealandicum* Cushman and Edwards (a: lateral, b: apertural edge views), from RN87-PC5, 60-62 cm, ×300. **4, 5**: *Pullenia* sp. of Ujiié (1990). 4: involute type (a: lateral, b: apertural edge views), from RN87-PC4, 250-252 cm; 5: lateral view of weakly evolute type, from RN87-PC5, 130-132 cm; both ×300. **6-8**. *Pulleniella aymmetrica* Ujiié (b: apertural edge view). 6a, 8a: incompletely coiled side views of adult and juvenile form, respectively; 7a: completely coiled side view of young specimen; all from RN87-PC5, 350-352 cm, ×250. **9**: *Gyroidina* sp. A of Ujiié (1990) (a: spiral side, b: apertural edge views), from RN87-PC5, 50-52 cm, ×300.

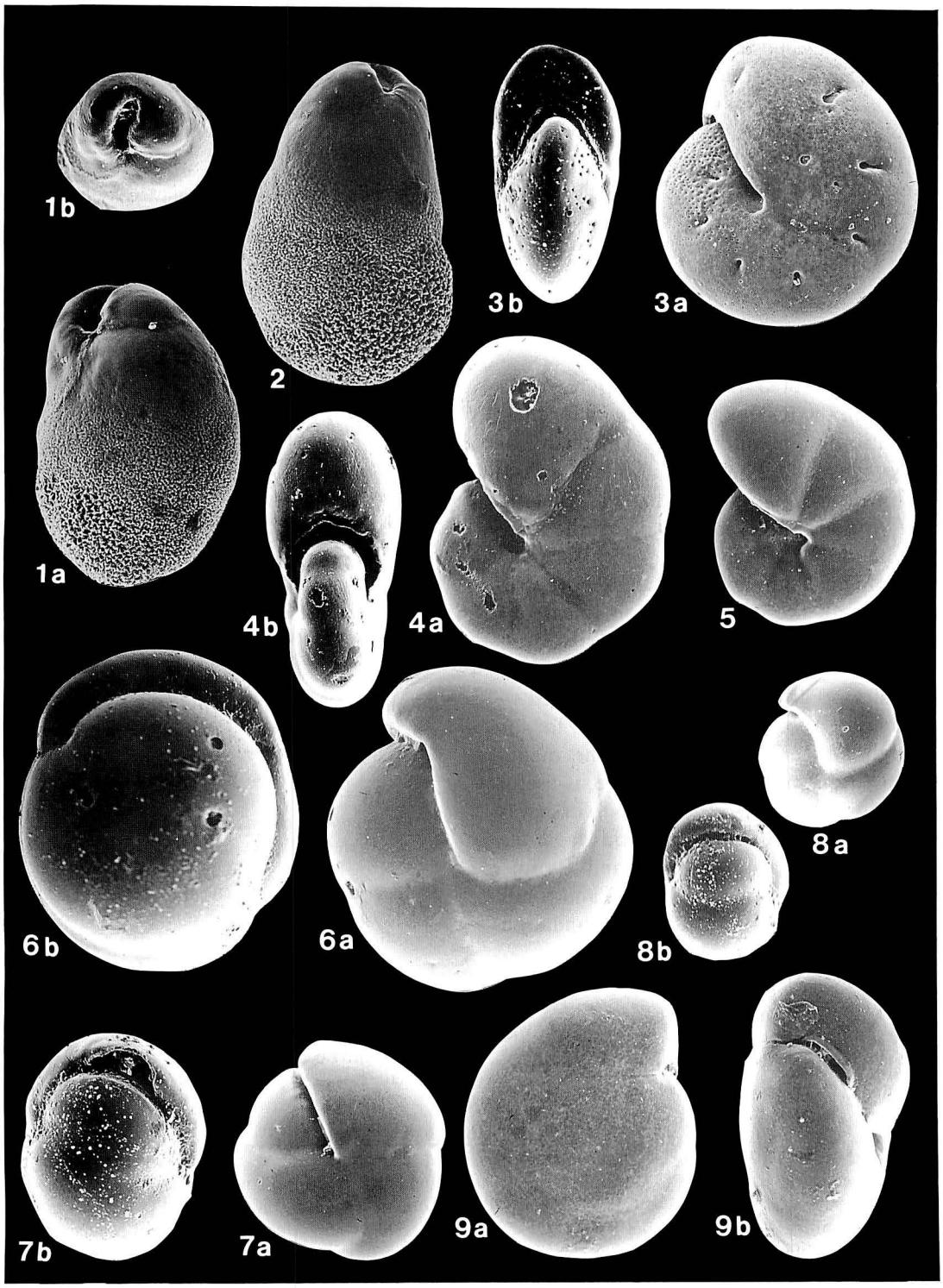
1b
2
3b
3a
1a
4b
4a
5
6b
6a
8a
8b
7b
7a
9a
9b

Alabamina? *rugosa* and, though subordinately, *Pulleniella asymmetrica* predominated Stages 5 and 7 assemblages.

In this paper, we have refrained from discussing the relationship between the mode of occurrence of benthic foraminifera and oceanographic conditions of bottom waters, since our knowledge on the distribution of Recent benthic foraminifera in the Northwest Pacific is insufficient.

Acknowledgments

We are indebted to Captain Uero Yada and crew of the R/V *Nagasaki-maru* for their cooperation. Tomonori Ono, University of the Ryukyus, and Tohru Nakasone, Kawasaki Chishitsu Co., and Naokazu Ahagon, University of Tokyo, assisted us in the shipboard and laboratory work. Yuichiro Tanaka, Geological Survey of Japan, kindly provided us with the information on calcareous nannoplankton stratigraphy. The first draft was reviewed by Motoyoshi Oda, Kumamoto University. Particularly, we are indebted to Tsunemasa Saito, Tohoku University, for his thorough and critical review of the manuscript. Anonymous reviewers gave us useful advice on the manuscript. This work was supported in part by Grand-in-Aids from the Ministry of Education, Science and Culture of Japan given to H.U. (02640603) and funds from the Nippon Life Insurance Foundation given to H.U.

Faunal references

The following list of taxonomic references concerns 31 species listed as "dominant species" in Tables 1 and 2. Publication names are not given when they are cited in the references section of this paper. Asterisk denotes those species for which Ujiié (1990) gave a description, cited more detailed taxonomic references, or both.

Karreriella hanzawai (Takayanagi)* (Figure 6-1)
Tosaia hanzawai Takayanagi, 1953, Short Papers, Inst. Geol. Paleont. Sendai, no. 5, p. 30, pl. 4, figs. 7a, b.
Karreriella hanzawai (Takayanagi), Ujiié, 1990, p. 13, pl. 2, figs. 6a-8b).

Bolivina decussata Brady (Figure 6-2, 3)
Bolivina decussata Brady, 1881, Quart. Jour. Micro. Sci., New Ser., vol. 21, p. 28;—Brady, 1884, Rep. Voy. *Challenger*, Zoology, vol. 9, p. 423, pl. 53, figs. 12, 13.

Bolivina pusilla Schwager* (Figure 6-4)
Bolivina pusilla Schwager, 1866, *Novara*-Exped., Geol. Theil, vol. 2, p. 254, pl. 7. fig. 101.

Abditodendrix pseudothalmanni (Boltovskoy and Guissani de Khan)* (Figure 6-6—8)
Bolivina pseudothalmanni Boltovskoy and Guissani de Khan, 1981 (*fide* Loeblich and Tappan, 1988, p. 503, pl. 554, figs. 1-5).
Abditodendrix pseudothalmanni (Boltovskoy and Guissani de Khan), Ujiié, 1990, p. 29, pl. 12, figs. 2a, b.

Bulimina aculeata d'Orbigny* (Figure 6-9)
Bulimina aculeata d'Orbigny, 1826, Annales Sci. Nat., vol. 7, p. 269, no. 7.

Uvigerina proboscidea vadescens Cushman* (Figure 6-10
Uvigerina proboscidea Schwager, var. *vadescens* Cushman, 1933, U.S. Nat. Mus. Bull., no. 104, p. 85, pl. 8, figs. 14, 15.

Siphouvigerina porrecta (Brady)* (Figure 6-11)
Uvigerina porrecta Brady, 1879, Quart. Jour. Micro. Sci., New ser., vol. 19, p. 31;—Brady, 1884, Rep. Voy. *Challenger,* Zoology, vol. 9, p. 577, pl. 74, figs. 21-23.

Trifarina angulosa (Williamson) (Figure 6-12)
Uvigerina angulosa Williamson, 1858, On the Recent Foraminifera of Great Britain, Ray Society, London, p. 67, fig. 140.
Trifarina angulosa (Williamson), Loeblich and Tappan, 1964, p. C571, figs. 450-1a—3.

→ **Figure 10.** **1, 2**: *Oridorsalis umbonatus* (Reuss). 1: Adult (a: spiral side, b: umbilical side, c: apertural edge views), ×150; 2: juvenile form already provided with a supplementary aperture (spiral side view), ×300; both from RN87-PC5, 10-12 cm. **3**: *Alabamina*? *rugosa* (Phleger and Parker) (a: spiral side, b: umbilical side views), from RN87-PC5, 50-52 cm, ×300. **4, 5**: *Melonis sphaeroides* Voloshinova. 4: adult (a: lateral, b: apertural edge views), ×200; 5: lateral view of juvenile form, ×400; both from RN87-PC5, 50-52 cm. **6**: *Melonis barleeanum* (Williamson) (lateral view), from RN87-PC5, 290-292 cm, ×200. **7**: *Eponides tumidulus* (Brady) (a: spiral, b: umbilical side views), from RN87-PC5, 10-12 cm, ×300.

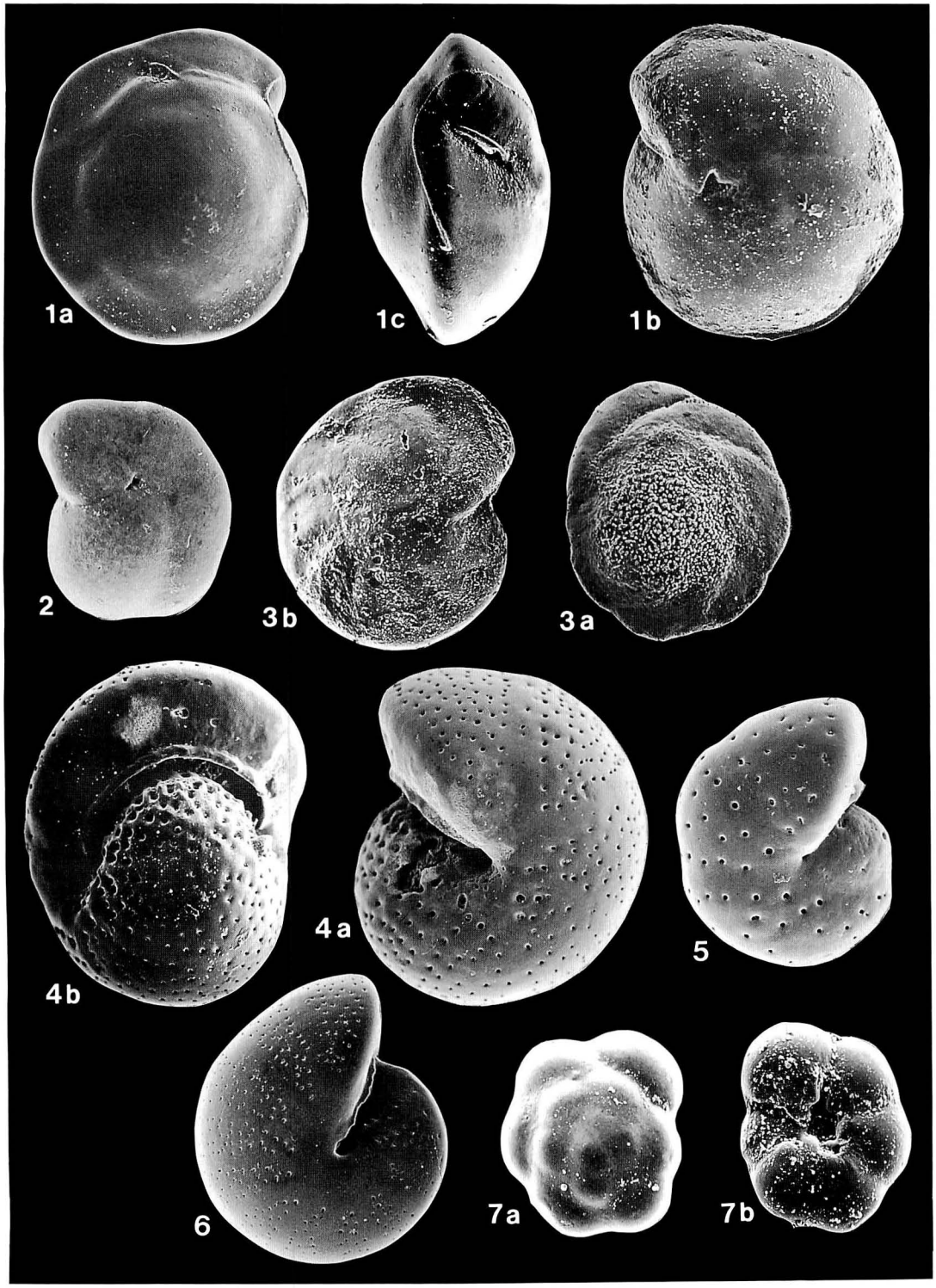
1a
1c
1b
2
3b
3a
4b
4a
5
6
7a
7b

Epistominella exigua (Brady)* (Figure 7-1, 2)
Pulvinulina exigua Brady, 1884, Rep. Voy. *Challenger,* Zoology, vol. 9, p. 696, pl. 103, figs. 13a-14c.
Epistominella exigua (Brady), Parker, 1954, Bull. Mus. Comparative Zool., vol. 111, no. 10, p. 533, pl. 10, figs. 22, 23.

Epistominella levicula Resig* (Figure 7-3)
Epistominella levicula Resig, 1958, Micropaleontology., vol. 4, no. 3, p. 304, text-fig. 16 (see Ujiié, Ichikura and Kurihara, 1983, for further references).

Eponides tenerus (Brady)* (Figure 7-4)
Truncatulina tenera Brady, 1884, Rep. Voy. *Challenger*, Zoology, vol. 9, p. 665, pl. 95, figs. 11a-c.
Eponides tenerus (Brady), Cushman, 1927, Bull. Scripps Inst. Oceanogr., Tech. ser., vol. 1, p. 163, pl. 5, figs. 6, 7 ;—Ujiié, 1990, p. 34, pl. 16, figs. 5a-6 ; text-fig. 1).

Eponides lamarckianus (d'Orbigny)* (Figure 7-5)
Rotalina lamarckiana d'Orbigny, 1839, *in* Barker-Webb, P., and Berthelot, S., Histoire naturelle des iles Canaries, Béthune, Paris, vol. 2, p. 131, pl. 2, figs. 13-15.

Eponides tumidulus (Brady)* (Figure 10-7)
Truncatulina tumidulus Brady, 1884, Rep. Voy. *Challenger*, Zoology, vol. 9, p. 666, pl. 95, figs. 8a-c.
Eponides tumidulus (Brady), Cushman, 1931, U.S. Nat. Mus. Bull., no. 104, p. 55, pl. 11, figs. 6a, b.

Planulina bradii Tolmachoff (Figure 7-7, 8)
Truncatulina wuellerstorfi (Schwager), Brady, 1884, Rep. Voy. *Challenger,* Zoology, vol. 9, pl. 93, figs. 8a-c, not figs. 9a-c (not *Anomalina wuellerstorfi* Schwager, 1866).
Planulina bradii Tolmachoff, 1984, Ann. Carnegie Mus., p. 333.

Planulina wuellerstorfi (Schwager)* (Figure 7-9, 10)
Anomalina wuellerstorfi Schwager, 1866, *Novara* —Exped., Geol. Theil, vol. 2, p. 258, pl. 7, fig. 107.
Planulina wuellerstorfi (Schwager), Cushman, 1929, Contr. Cushman Lab. Foram. Res., vol. 5, p. 102, pl. 15, figs. 1, 2.

Fursenkoina cedrosensis (McCulloch) (Figure 8-1)
Neobuliminoides cedrosensis McCulloch, 1977, Qualitative Observations on Recent Foraminiferal Tests with Emphasis on the Eastern Pacific, Univ. Southern Calif., L.A., p. 247, pl. 104, figs. 27, 28 ; pl. 578, figs. 24-25.

Cassidulina cf. *Cassidulina neocarinata* Thalmann* (Figure 8-2, 3)
Cassidulina cf. *neocarinata* Thalmann, Ujiié, 1990, p. 38, pl. 18, figs. 6a, b.

Cassidulina norcrossi Cushman (Figure 8-4)
Cassidulina norcrossi Cushman, 1933, Smithsonian Misc. Coll., vol. 89, no. 9, p. 7, pl. 2, figs. 7a-c.

Cassidulina norvangi Thalmann* (Figure 8-5)
Cassidulina norvangi Thalmann, 1950 (*in* Phleger, 1952, Contr. Cushman Found. Foram. Res., vol. 3, no. 2, p. 83.

Globocassidulina subglobosa (Brady)* (Figure 8-6)
Cassidulina subglobosa Brady, 1881, Quart. Jour. Micro. Sci., New ser., vol. 21, p. 60 ;—Brady, 1884, Rep. Voy. *Challenger*, Zoology, vol. 9, p. 430, pl. 54, figs. 17a-c.
Globocassidulina subglobosa (Brady), Belford, 1966, Bur. Mineral Res. Geol. Geophysics, Australia, Bull., no. 79, p. 149, pl. 25, figs. 11-16.

Globocassidulina bisecta Nomura (Figure 8-9)
Globocassidulina bisecta Nomura, 1983, Sci. Rep. Tohoku Univ., 2nd ser., vol. 53, no. 1, p. 73.

Favocassidulina favus (Brady)* (Figure 8-10)
Pulvinulina favus Brady, 1877, Geol. Magazine, New ser., vol. 4, p. 535 ; Brady, 1884, Rep. Voy. *Challenger*, Zoology, vol. 9, p. 701, pl. 104, figs. 12a-16.
Favocassidulina favus (Brady), Loeblich and Tappan, 1957, U.S. Nat. Mus. Bull., vol. 215, p. 230, pl. 73, figs. 7-11.

Evolvocassidulina brevis (Aoki) (Figure 9-1, 2)
"Cassidulina" brevis Aoki, 1968, Trans. Proc. Palaeont. Soc. Japan, N.S., no. 70, p. 261, pl. 27, fig. 4.
Evolvocassidulina brevis (Aoki), Nomura, 1983, Sci. Rep. Tohoku Univ., 2nd ser., vol. 54, no. 1, p. 49, pl. 4, figs. 4a-7 ; pl. 20, fig. 11 ; pl. 21, figs. 1-5 ; text-figs. 41-43.

Takayanagia delicata (Cushman) (Figure 8-7, 8)
Cassidulina delicata Cushman, 1927, Bull. Scripps Inst. Oceanogr., Tech. ser., vol. 1, no. 10, p. 168, pl. 6, fig. 5.
Takayanagia delicata (Cushman), Nomura, 1983, Sci. Rep. Tohoku Univ., 2nd ser., vol. 53, p. 53, pl. 1, figs. 3 ; pl. 7, figs. 1-5.

Astrononion novozealandicum Cushman and Edwards* (Figure 9-3)
Astrononion novozealandicum Cushman and Edwards 1937, Cushman Lab. Foram. Res., vol. 13, pt. 1, p. 35, pl. 3, figs. 18a, b.

Pullenia sp. B* (Figure 9-4, 5)
Pullenia sp. B, Ujiié, 1990, p. 44, pl. 22, figs. 12a-13b ; pl. 24, figs. 10a, b.

Pulleniella asymmetrica Ujiié* (Figure 9-6~8)
Pulleniella asymmetrica Ujiié, 1990, p. 45, pl. 23, figs. 3a-b.

Gyroidina sp. A (Figure 9-9)
Gyroidina sp. A, Ujiié, 1990, p. 47, pl. 27, figs. 2a-c.

Oridorsalis umbonatus (Reuss)* (Figure 10-1, 2)
Rotalina umbonata Reuss, 1851 (*fide* Ellis and

Messina, 1940 *et seq.*).
Oridorsalis umbonatus (Reuss), Parker, 1964, Jour. Paleont., vol. 38, no. 4, p. 626, pl. 99, figs. 4-6 ;—Ujiié, 1990, p. 48, pl. 28, figs. 1-6 ; text-fig. 4.

Alabamina ? *rugosa* (Phleger and Parker)* (Figure 10-3)
Pseudoparrella ? *rugosa* Phleger and Parker, 1951, Geol. Soc. America, Mem., no. 46, pt. 2, p. 28, pl. 15, figs. 8a-9b.
Alabamina ? *rugosa* (Phleger and Parker), Ujiié, 1990, p. 49, pl. 29, figs. 1a-2c.
Nuttallides rugosa (Phleger and Parker), Loeblich and Tappan, 1994, Cushman Found. Foram. Res., Spec. Pub., no. 31, p. 156, pl. 350, figs. 11-13.

Melonis sphaeroides Voloshinova* (Figure 10-4, 5)
Melonis sphaeroides Voloshinova, 1958, Mikrofauna SSSR, Sbornik 9, Trudy, no. 115, p. 153, pl. 3, figs. 8a, b.

Melonis barleeanum (Williamson)* (Figure 10-6)
Nonionina barleeanum Williamson, 1858, On the Recent Foraminifera of Great Britain, Ray, Soc., London, p. 31, pl. 3, figs. 68, 69.
Melonis barleeanum (Williamson), Pflum and Frerichs, 1976, Cushman Found. Foram. Res., Spec. Pub., no. 14, pl. 7, figs. 5, 6.

References

Ahagon, N., Tanaka, Y. and Ujiié, H., 1993 ; *Florisphaera profunda*, a possible nannoplankton indicator of late Quaternary changes in sea-water turbidity at the northwestern margin of the Pacific. *Marine Micropaleont.*, vol. 22, p. 255-273.

Balsam, W.L., 1981 : Late Quaternary sedimentation in the western North Atlantic : Stratigraphy and paleoceanography. *Palaeogeogr., Palaeoclimat., Palaeoecol.*, vol. 35, p. 215-240.

Imbrie, J., Hays, I.D., Martinson, D.G., McIntyre, A., Mix, A.C., Morley, J.J., Pisias, N.G., Prell, W.L., and Shackleton, N.J., 1984 : The orbital theory of Pleistocene climate : Support from a revised chronology of the marine $\delta^{18}O$ record. *In*, Berger, A., Imbrie, J., Hays, J., Kukla, G., and Salzman, B. *eds. Milankovitch and Climate*, p. 269-305. Riedel, Dordrecht.

Inoue, Y., 1989 : Northwest Pacific foraminifera as paleoenvironmental indicators. *Sci. Rep., Inst. Geosci., Univ. Tsukuda, Sec. B*, vol. 10, p. 57-162, pls. 18-33.

Loeblich, A.R., Jr., and Tappan, H., 1964 : Part C. Protista 2. Sarcodina, chiefly "thecamoebians" and Foraminiferida. *In*, Moore, R.C. *ed., Treatise on invertebrate paleontology*, 900 p. Geol. Soc. America, Boulder.

—— and ——, 1988 : Foraminiferal genera and their classification. x+970 p., 837 pls. Van Nostrand Reinhold Co., N.Y.

—— and ——, 1994 : Feraminifera of the Sahul Shelf and Timor Sea. *Cushman Found. Foram. Res., Spec. Pub.*, no. 31, p. 1-661, pls. 1-393.

Schnitker, D., 1979 : The deep waters of the western North Atlantic during the past 24,000 years, and re-initiation of the Western Boundary Undercurrent. *Marine Micropaleont.*, vol. 4, p. 265-280.

Streeter, S.S., and Lavery, S.A., 1982 : Holocene and latest glacial benthic foraminifera from the slope and rise off eastern North America. *Geol. Soc. America, Bull.*, vol. 93, p. 190-199.

Thierstein, H.R., Geitzenauer, K.R., Molfino, B., and Schackleton, N.G., 1977 : Global synchroneity of late Quaternary coccolith datum levels : Validation by oxygen isotopes. *Geology*, vol. 5, p. 440-404.

Thompson, P.R., 1981 : Planktonic foraminifera in the western North Pacific during the past 150,000 years : Comparison of modern fossil assemblages. *Palaeogeogr., Palaeoclimat., Palaeoecol.*, vol. 35, p. 241-279.

——, Bé, W.H.A., Duplessy, J.C., and Shackleton, N.J., 1979 : Disappearance of pink-pigmented *Globigerinoides ruber* at 120,000 yr. BP in the Indian and Pacific Oceans. *Nature*, vol. 280, p. 554-558.

Tucholke, B.E., and Eittreim, S., 1974 : The western boundary under-current as a turbidity maximum over the Puerto Rico Trench. *J. Geophys. Res.*, vol. 79, p. 4115-4118.

Ujiié, H., 1990 : Bathyal benthic foraminifera in a piston core from east off the Miyako Islands, Ryukyu Island Arc. *Bull. Coll. Sci., Univ. Ryukyus*, no. 49, p. 1-60, 32 pls.

——, Ichikura, M., and Kurihara, K., 1983. Quaternary benthonic foraminiferal changes observed in the Sea of Japan piston cores. *Bull. Natn. Sci. Mus., Tokyo, ser. C.*, vol. 9, p. 41-78, 10 pls.

——, Tanaka, Y., and Ono, T., 1991 : Late Quaternary paleoceanographic record from the middle Ryukyu Trench slope, northwest Pacific. *Marine Micropaleont.*, vol. 18, p. 115-128.

Yasuda, H., Murayama, M., Oba, T., and Schnitker, D., 1993 : Deep-sea circulation changes after the last glacial episode in the northwestern Pacific. *Kaiyo Monthly*, vol. 25, p. 344-349. (*in Japanese*)

Sakishima 先島，Ishigaki 石垣，Miyako 宮古，Kerama 慶良間．

過去 210,000 年間における半深海性有孔虫群集変化：南琉球弧・石垣島南方沖ピストンコアからの情報：石垣島南方の琉球海溝に望む先島深海平坦面上の水深 2,488 m と同外縁部の水深 3,136 m からピストン・コア RN87-PC4 と RN87-PC5 を採取した．浮遊性有孔虫 *Globigerinoides sacculifer* の殻を用いた酸素同位体年代区分は，阿多火山灰層の年代や二つの微古生物層序イヴェントに対しても調和的であり，RN87-PC4 は酸素同位体ステージ①から⑤まで，RN87-PC5 は⑤から⑦までをカバーしている点を明らかにした．RN87-PC5 において⑤上部以上が欠けていることは，先島深海平坦面外縁部に沿って大西洋と同様に Western Boundary Undercurrent が存在している可能性を示唆するものである．こうして得られた過去 210,000 年間の時系列について，底生有孔虫の優勢種（いずれかのサンプルで 3% を越える種）32 の産出量変化を求めた．特に強調すべき点は，*Alabamina*? *rugosa* と傾向がより顕著ではないが *Pulleniella asymmetrica* の産出量が，表層水温の変化に対応していることと，*Bulimina aculeata* が最終氷期（酸素同位体ステージ②）に特徴的に産出することである．　　徐　学東・氏家　宏

Trans. Proc. Palaeont. Soc. Japan, N.S., No. 175, pp. 521-552, 8 Figs., September 30, 1994

974. PLANKTONIC FORAMINIFERAL BIOSTRATIGRAPHY OF UPPER PALEOCENE TO MIDDLE EOCENE SEQUENCES IN THE EASTERN DESERT AREA, EGYPT*

HIROSHI NISHI

Institute of Geoenvironmental Science, Faculty of Science,
Tohoku University, Sendai, 980 Japan

ASHRAF M.T. ELEWA

Geology Department, Faculty of Science,
El Minia University, Egypt

and

KUNIHIRO ISHIZAKI

Institute of Geoenvironmental Science, Faculty of Science,
Tohoku University, Sendai, 980 Japan

Abstract. The studied sections are located in the Eastern Desert area, along the El Sheikh Fadl road running from Ras Gharib on the west bank of the Gulf of Suez to El-Sheikh Fadl village on the east side of the Nile River. Rocks exposed in this area comprise five lithological units, the Esna (shale), Thebes (limestone and chert), Maghagha (marl and limestone), Qarara (shale and sandstone) and El Fashn (limestone) Formations, and can be divided into the following five planktonic foraminiferal biozones; the *Planorotalites pseudomenardii* Zone, *Acarinina aspensis* Zone, *Globigerinatheka subconglobata* Zone, *Morozovella lehneri* Zone and *Truncorotaloides rohri* Zone in ascending order. Although some zonal marker species have not been found in the investigated area, these zones are considered to correspond, respectively, to Zone P4, Zones P9-10, lower Zone P11, upper Zone P11, Zones P12-14 of the standard zonation established in low latitude areas. Therefore, the Esna Formation is assigned to the late Paleocene, the Thebes Formation to the late Paleocene to latest early Eocene, and the Maghagha and Qarara Formations to the middle Eocene. The limestone-marl Maghagha Formation was deposited in the west, simultaneously with the sandstone-shale Qarara Formation in the east.

Key words. Planktonic foraminifera, biostratigraphy, Paleocene, Eocene, Eastern Desert, Egypt.

Introduction

Egypt is divided geomorphologically into the following four major provinces from west to east; the Western Desert, the Nile Valley and the Delta, the Eastern Desert, and the Sinai Peninsula. Biostratigraphical investigations of planktonic foraminifera have been made mostly in the Nile Valley (e.g. Said,

*Received March 28, 1994; revised manuscript accepted July 5, 1994

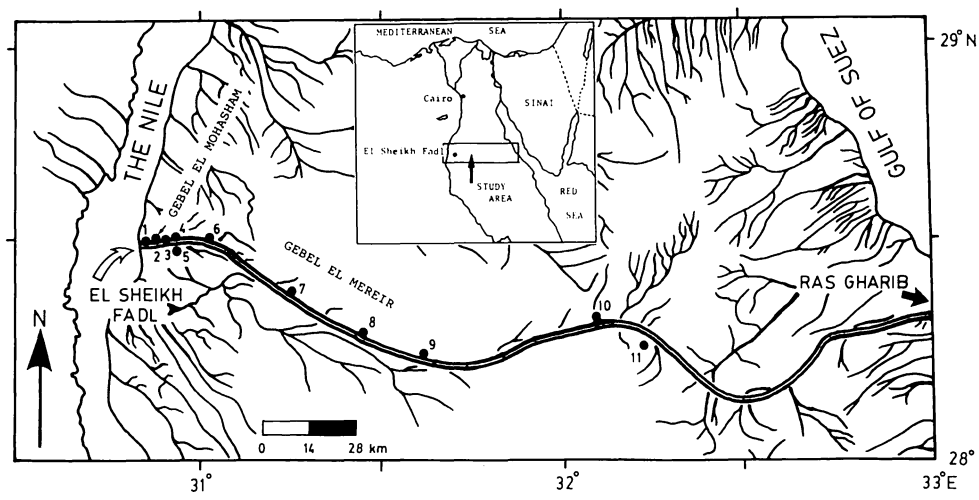

Figure 1. Map showing locations of the sections measured along the El Sheikh Fadl-Ras Gharib stretch, the Eastern Desert. 1. Gebel El Sheikh Fadl section, 2. Gebel El Mohasham section, 3. section at km 8, 4. section A at km 10, 5. section B at km 10, 6. Gebel El Mereir section at km 18, 7. Gebel El Mereir section at km 40, 8. Gebel El Mereir section at km 68, 9. Gebel El Mereir section at km 92, 10. section at km 127, 11. section at km 140. km refers to the distance (km) from the village of El Sheikh Fadl.

1960; Said and Sabby, 1961; Abdel-Kireem, 1985; Haggag, 1989a, 1989b), Sinai (e.g. Said and Kenawy, 1956; Haggag and Luterbacher, 1991; Shahin, 1992), and in small oases in the Western Desert such as the Farafra (Said and Kerdany, 1961) and the Kharga (Nakkady, 1959; Abdel-Kireem *et al.*, 1985). The Eastern Desert was studied with a biostratigraphical emphasis on the Esna Formation (Shales) (e.g. Nakkady, 1950), while a few workers dealt with middle Eocene planktonic foraminifera in this area (Khalifa and El-Sayed, 1984). Along the El Sheikh Fadl road traversing the Eastern Egyptian Desert, Paleogene sequences are distributed. This road extends for a distance of approximately 245 km from Ras Gharib on the western coast of the Gulf of Suez to El-Sheikh Fadl village on the eastern bank of the Nile River near Beni Mazar. Older, pre-Tertiary rocks are exposed widely in the eastern region close to the Gulf of Suez. The Paleogene sections occupy the western region. A total of 11 sections were measured in this area (Figure 1). We were successful in obtaining abundant foraminifer and ostracode specimens from these sections, thus enabling the establishment of biostratigraphic divisions based on these microfossils for the late Paleocene to middle Eocene interval. This paper focuses on a planktonic foraminiferal biostratigraphy of the Eastern Egyptian Desert, giving descriptions of the recognized zones and discussing a correlation with other zones and their geological ages. Biostratigraphical and paleontological conclusions for the ostracodes were summarized by Elewa and Ishizaki (1994).

Lithostratigraphy

The Paleogene rocks exposed along the El Sheikh Fadl road can be divided lithologically into the follwing rock units in ascending order:

1. The Esna Formation

The Esna Formation was originally described by Beadnell (1905) as the Esna Shale consisting of think green and gray shale

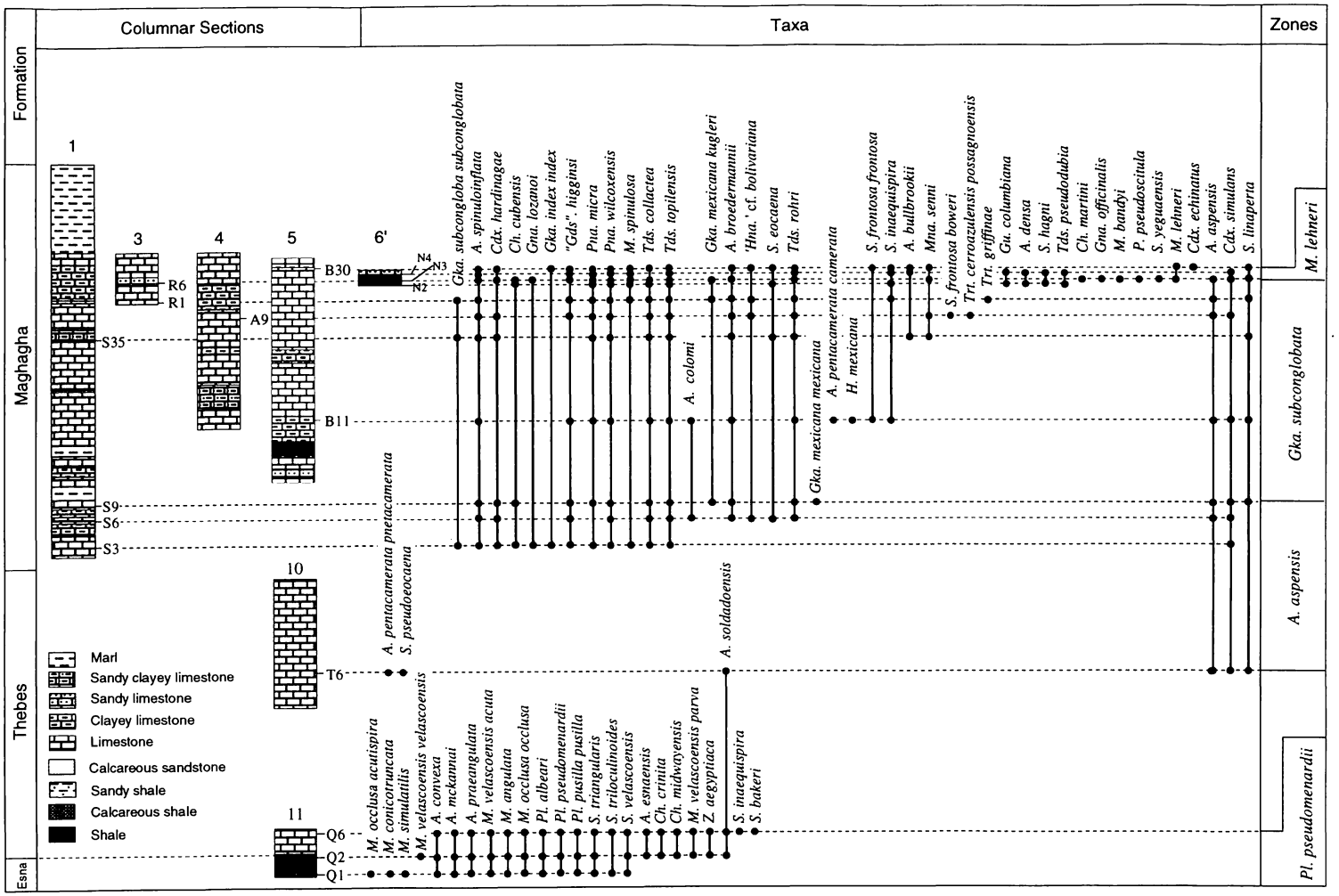

Figure 2. Generalized lithostratigraphic sequence of the Esna, Thebes, and Maghagha Formations and biostratigraphic distribution of planktonic foraminifera. The top and right numbers of columnar sections denote localities of sections in Figure 1 and sample numbers, respectively.

A.: *Acarinina*; *Cdx.*: *Catapsydrax*; *Ch.*: *Chiloguembelina*; *Gna.*: *Globigerina*; *Gka.*: *Globigerinatheka*; "*Gds.*": "*Globigerinoides*"; *Gu.*: *Guembelitria*; *H.*: *Hantkenina*; *Hna.*: *Hastigerina*; *M.*: *Morozovella*; *Mna.*: *Muricoglobigerina*; *P.*: *Planorotalites*; *Pna.*: *Pseudohastigerina*; *S.*: *Subbotina*; *Tds.*: *Truncorotaloides*; *Trt.*: *Turborotalia*; *Z.*: *Zeauvigerina*.

exposed at Gebel Aweina, south of Luxor.

The Esna Formation is distributed at the eastern margin of the study area, 140 km east of El Sheikh Fadl village (Section 11). At this locality, it is composed of gray to dark gray, soft to moderately hard, gypsiferous shale. The thickness is approximately 5 m (Figure 2).

2. The Thebes Formation

The Thebes Formation was originally introduced by Said (1960) from the Gebel Gurnah locality, opposite Luxor. The name is applied to a 290 m-thick limestone section, with intercalations of many chert bands, which overlies the Esna Shale at Thebes.

In the investigated area, the Thebes Formation is observed at two outcrops, 127 and 140 km east of El Sheikh Fadl village (sections 10 and 11). At section 10, it spans the whole thickness of the section and is about 25 m in thickness, while at section 11 it occupies the uppermost 5 m and overlies a shale unit (Figure 2). The rocks are yellowish white, hard limestone, showing a papery structure on weathered surfaces. This limestone is accompanied characteristically by dark brown chert nodules arranged horizontally in parallel bands.

3. The Maghagha Formation

The uniit was first proposed by Bishay (1966) to designate a chalk-marl complex exposed in Maghagha district in the Nile Valley. The Maghagha Formation is considered to be coeval with the Samalut Formation which represents the lowermost lithostratigraphic unit of the Mokattam Subgroup in Egypt (Said, 1990).

In the study area, the Maghagha Formation is exposed at sections 1 (the type section as designated by Azab (1984)), 3, 4, and 5 (Figure 2). It consists of alternating beds of white, moderately hard, chalky limestone, and grayish white to yellowish white, soft to moderately hard marl. The Maghagha Formation attains its maximum thickness (approximately 81.30 m) in the study area in section 1.

4. The Qarara Formation

The name of the Qarara Formation was introduced by Bishay (1966) to designate the sequence exposed at Gebel Qarara opposite Maghagha. This sequence is composed of quartzose calcareous sandstone and clay with abundant nummulites and macrofossils (Azab, 1984).

In the study area, it is represented by yellowish white, very hard calcareous sandstones and greenish white to gray, moderately hard shales. Macrofossils and nummulites are abundant. This sequence occurs in sections 2, 6, 7, 8, and 9, and attains its maximum thickness of about 91.30 m in section 6 (Figure 3).

5. The El Fashn Formation

The name of this rock unit, typically exposed at El Fashn, was also introduced by Bishay (1966) for a sequence of limestone beds rich in nummulites and bryozoans, which intercalate with chert bands near the base. This sequence overlies disconformably the Qarara Formation (Said, 1990).

In the study area, the El Fashn Formation consists of white limestone with chert bands and is rich in nummulites and bryozoans. Planktonic foraminifers and ostracodes are rare in this formation. The El Fashn Formation crops out at the top of exposures in sections 6, 7, 8 and 9, attaining a maximum thickness of about 20 m in section 6 (Figures 2, 3).

Methods and Materials

Bulk samples were washed through a 115 μm-opening mesh screen, using water for shale and sandstone, and hydrogen peroxide (H_2O_2) and water for calcareous rocks. Specimens studied in this paper were obtained from splits (using microsplitter) which contain approximately 200-300 indi-

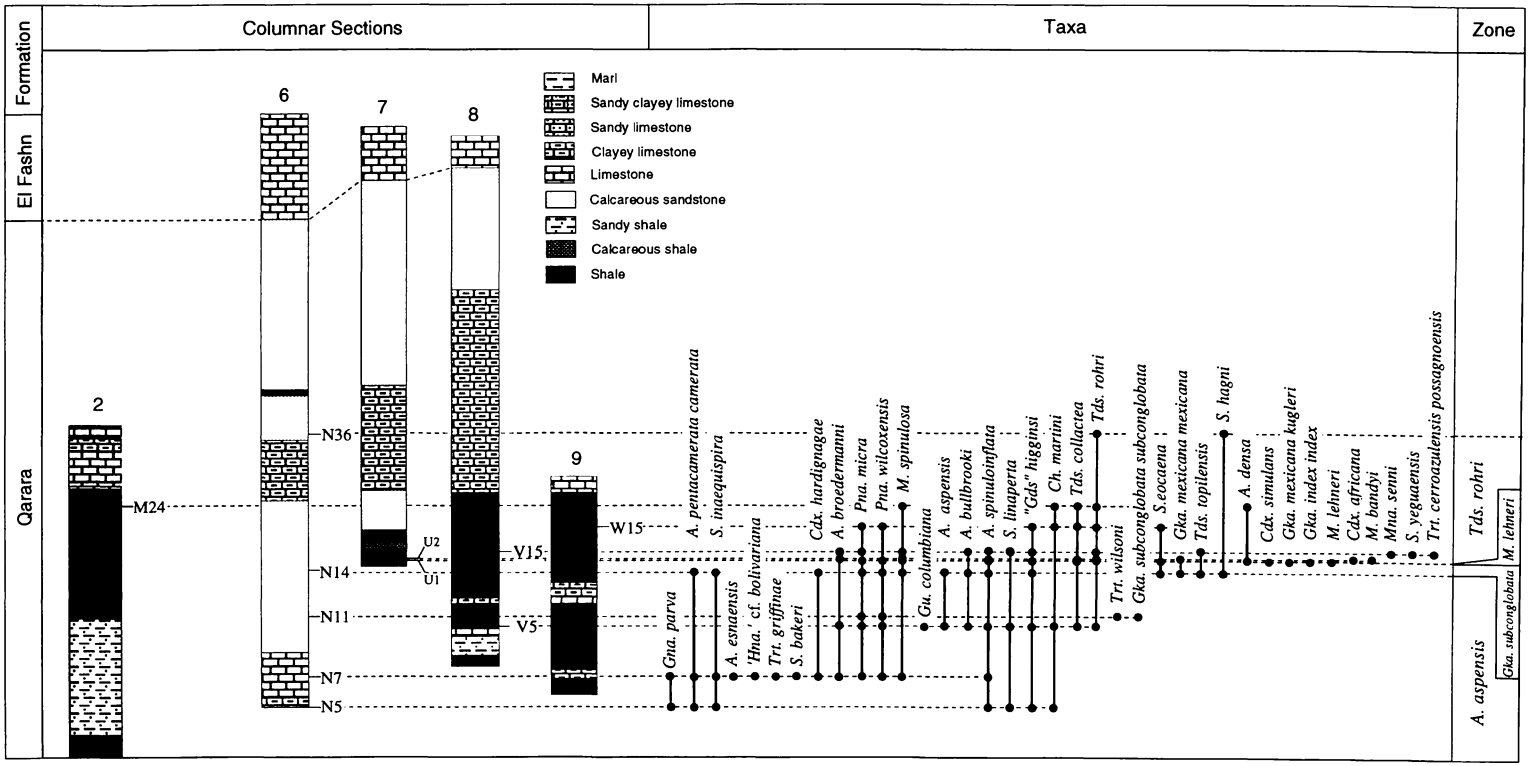

Figure 3. Generalized lithostratigraphic sequence of the Qarara and El Fashn Formations and biostratigraphic distribution of planktonic foraminifera.

Table 1. List of planktonic foraminiferal species in the study area.

Sample Number	*Acarinina aspensis*	*Acarinina broedermanni*	*Acarinina bullbrooki*	*Acarinina colomi*	*Acarinina convexa*	*Acarinina densa*	*Acarinina esnaensis*	*Acarinina mckannai*	*Acarinina pentacamerata camerara*	*Acarinina pentacamerata pentacamerata*	*Acarinina praeangulata*	*Acarinina soldadoensis*	*Acarinina spinuloinflata*	*Catapsydrax africana*	*Catapsydrax echinatus*	*Catapsydrax hardingae*	*Catapsydrax simulans*	*Chiloguembelina crinita*	*Chiloguembelina cubensis*	*Chiloguembelina martini*	*Chiloguembelina midwayensis midwayensis*	*Globigerina lozanoi*	*Globigerina officinalis*	*Globigerina parva*	*Globigerinatheka index index*	*Globigerinatheka mexicana kugleri*	*Globigerinatheka mexicana mexicana*	*Globigerinatheka subconglobata subconglobata*	*Globigerinoides higginsi*	*Guembelitria columbiana*	*Hantkenina mexicana*	*Hastigerina' cf. bolivariana*	*Morozovella angulata*	*Morozovella bandyi*	*Morozovella conicotruncata*
N36																																		
M24						X														X														
W15																				X									X					
V15		X	X										X																X					
U2		X											X	X													X						X	
U1						X							X				X								X	X			X					
N14	X		X						X				X			X											X		X					
N11																												X						
V5	X	X	X										X							X									X	X				
N7		X					X		X				X			X								X								X		
N5									X				X							X				X					X					
B30		X	X										X		X	X									X				X			X		
N4			X			X							X				X												X	X				
N3																							X											
R6	X	X											X			X	X		X	X		X				X			X				X	
N2						X													X											X				
R1	X	X											X													X		X	X			X		
A9	X	X											X			X	X												X			X		
S35		X	X										X			X												X						
B11	X	X		X					X				X				X												X		X			
S9	X	X											X			X	X		X							X	X		X					
S6	X	X		X									X			X	X												X			X		
S3													X				X		X			X			X			X	X					
T6	X									X		X					X								X									
Q6					X		X	X			X	X						X			X											X		
Q2					X		X	X			X	X						X			X											X		
Q1					X			X			X																					X		X

viduals. All foraminiferal specimens were picked and identified. Of 297 samples washed, 27 were used in this biostratigraphical study.

Biostratigraphy and planktonic foraminiferal zonation

The Paleogene rocks in the studied area yielded rich and diverse planktonic and benthic foraminifera. Concerning the planktonics, although quantitative analyses of these faunas remain to be done, some 70 species and subspecies belongng to 17 genera were identified (Table 1). Their stratigraphic distributions are shown in Figures 2 and 3. The sequence of the Esna, Thebes, Maghagha, and Qarara Formations distributed in this area can be divided biostratigraphically into the following five biozones in ascending order which range in age from the late Paleocene to middle Eocene (Figures 4, 5): the *Planorotalites pseudomenardii* Zone, *Acarinina aspensis* Zone, *Globigerinatheka subconglobata* Zone, *Morozovella lehneri* Zone, and *Truncorotaloides rohri* Zone. The zonal marker species are selected and they are shown in Figures 6, 7 and 8.

Table 1. (continued)

Sample Number	*Morozovella lehneri*	*Morozovella occlusa acutispira*	*Morozovella occlusa occlusa*	*Morozovella simulatilis*	*Morozovella spinulosa*	*Morozovella velascoensis acuta*	*Morozovella velascoensis parva*	*Morozovella velascoensis velascoensis*	*Muricoglobigerina senni*	*Planorotalites albeari*	*Planorotalites pseudomenardii*	*Planorotalites pseudoscitula*	*Planorotalites pusilla pusilla*	*Pseudohastigerina micra*	*Pseudohastigerina wilcoxensis*	*Subbotina bakeri*	*Subbotina eocaena*	*Subbotina frontosa boweri*	*Subbotina frontosa frontosa*	*Subbotina hagni*	*Subbotina inaequispira*	*Subbotina linaperta*	*Subbotina pseudoeocaena*	*Subbotina triangularis*	*Subbotina triloculinoides*	*Subbotina velascoensis*	*Subbotina yeguaensis*	*Truncorotaloides collactea*	*Truncorotaloides pseudodubia*	*Truncorotaloides rohri*	*Truncorotaloides topilensis*	*Turborotalia cerroazulensis possagnoensis*	*Turborotalia griffinae*	*Turborotalia wilsoni*	*Zeauvigerina aegyptiaca*
N36																				X										X					
M24					X																							X		X					
W15														X	X		X											X		X					
V15					X				X					X								X					X			X	X	X			
U2					X																							X		X					
U1	X				X									X	X		X											X		X					
N14					X									X	X		X			X	X										X				
N11														X	X																			X	
V5														X	X							X						X		X					
N7					X									X	X	X					X												X		
N5																					X	X													
B30	X				X				X					X	X		X		X		X	X						X		X	X				
N4					X									X	X					X	X								X	X	X				
N3	X													X	X															X					
R6	X				X				X			X		X	X							X					X	X		X	X				
N2					X									X	X		X			X	X							X	X		X				
R1					X									X	X						X	X						X		X	X		X		
A9									X					X	X			X										X		X	X	X			
S35									X					X	X		X					X						X		X	X				
B11														X	X				X		X	X						X		X	X				
S9														X	X							X						X		X	X				
S6															X		X											X		X	X				
S3					X									X	X													X			X				
T6														X	X							X	X												
Q6			X			X	X			X	X		X			X					X			X	X	X									X
Q2			X			X	X	X		X	X		X											X		X									X
Q1		X	X	X		X				X	X		X											X	X	X									

Two representative Paleogene zonations have been proposed in low-latitude regions. One is the zonal scheme proposed by Bolli (1957a, b), and subsequently modified by Bolli (1966) and Toumarkine and Luterbacher (1985). The other is the P-zone system and its revised versions (Blow, 1969, 1979; Berggren, 1969b, 1969c ; Berggren and Miller, 1988) (Figure 5). Because the Paleocene fauna obtained from the studied area abundantly contains zonal marker species characteristic of tropical and subtropical waters, the Paleocene zonation recognized here can easily be correlated with internationally recognized zonal scheme. The middle Eocene faunas, however, lack index species such as *Hantkenina nuttalli, Morozovella aragonensis*, and *Orbulinoides beckmanni*, whose datum levels are used to define the top and base of the zones in these two standard low-latitude zonations. The absence of important index species has also been reported in other Egyptian sequences (Haggag 1985, 1989a, 1989b ; Haggag and Luterbacher, 1991), and has led to a difficulty in correlating the Egyptian Eocene zones with the international zonal schemes. In this paper, we describe five regional zones applicable to the

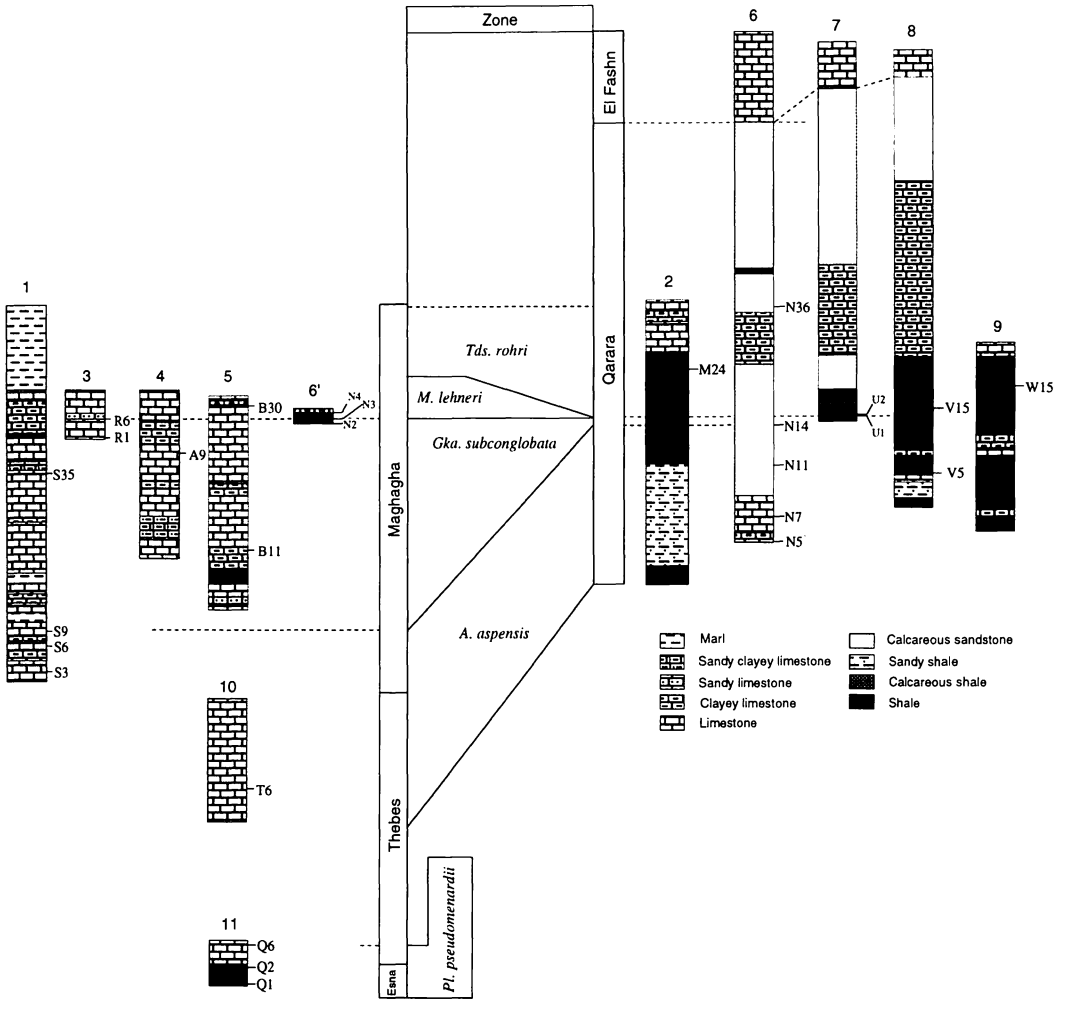

Figure 4. Biostratigraphic correlation of the Paleogene sequence distributed in the studied area based on planktonic foraminiferal zones.

studied sections, and discuss their characteristics and regional and international correlations.

1. *Planorotalites pseudomenardii* Assemblage-Zone

Definition : This zone is defined by the occurrence of *Planorotalites pseudomenardii* (Bolli). The top and base are not firmly defined in the studied area because of the lack of adequate section.

Characteristic species : In addition to the zone nominal species, this zone is characterized by the common occurrences of *Morozovella velascoensis* as three subspecies (*M. velascoensis acuta, M. velascoensis velascoensis*, and *M. velascoensis parva*). Other diagnostic species in the middle and late Paleocene interval are *Planorotalites pusilla pusilla* (Bolli), *P. albeari* (Cushman and Bermúdez), *Chiloguembelina midwayensis midwayensis* (Cushman), *Zeauvigerina aegyptiaca* Said and Kenawy, *Morozovella angulata* (White), *M. conicotruncata* (Subbotina), and *M. occlusa occlusa* (Loeblich and Tappan).

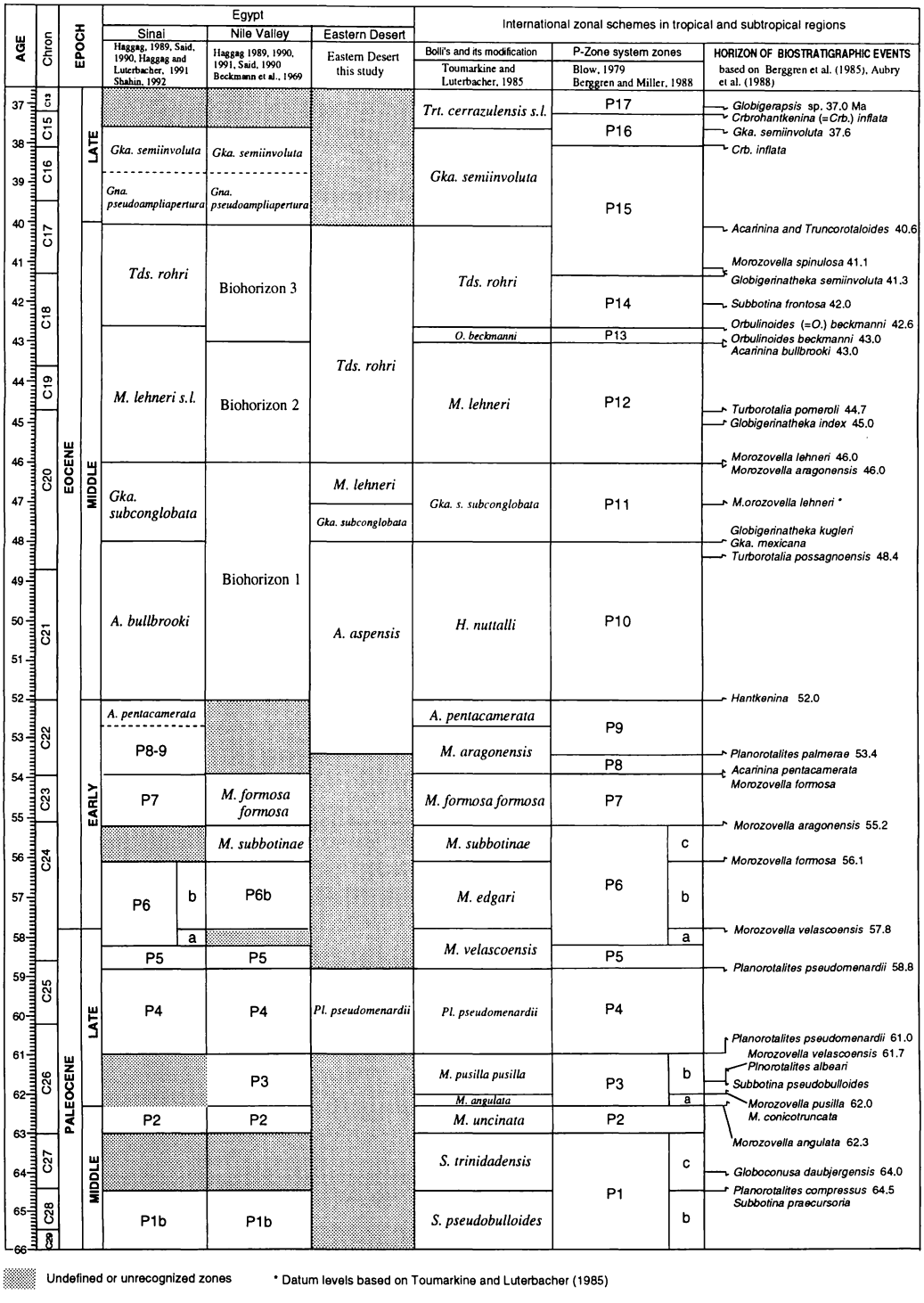

Figure 5. Correlation of planktonic foraminiferal zones of the studied area with the standard low-latitude zonations and other Egyptian zones. Age and epoch boundaries are adopted from Berggren *et al.* (1985) and Aubry *et al.* (1988).

Occurrence: Esna and Thebes Formations in section 11 (Figures 2, 4).

Correlation and age: Many workers considered *Planorotalites* (= *Globorotalia*) *pseudomenardii* to be an easily recognizable species and an excellent marker species of the late Paleocene (Bolli, 1957a; Berggren, 1969b, 1969c; Luterbacher, 1975; Stainforth *et al.* 1975; Toumarkine and Luterbacher, 1985; Berggren and Miller, 1988). However, Blow (1979) reported a longer stratigraphic range of this specis with its occurrence extending upward into the early Eocene Zone P7.

The faunal assemblages occurring in the studied sections abundantly contain acarinid and morozovellid forms indicative of the late Paleocene, and include no such early Eocene zonal markers as *Morozovella marginodentata, M. subbotinae,* or *M. formosa.* Therefore, the *P. pseudomenardii* Zone recognized in the Esna Formation can be correlated exactly with Zone P4. The age of this zone is late Paleocene (Selandian) (Figure 5).

2. *Acarinina aspensis* Partial Range-Zone

Definition: Partial range of the nominate taxon, but the base is not clearly defined in the studied sections. The top is marked by the initial appearance of both *Globigerinatheka mexicana kugleri* and *G. mexicana mexicana.*

Characteristic species: This zone is characterized by common to abundant occurrences of *Acarinina pentacamerata pentacamerata* and its related forms (*Acarinina aspensis, A. pentacamerate camerata,* and *A. colomi*). The zonal marker species is accompanied by *Acarinina soldadoensis, A. bullbrooki* (Bolli), *A. spinuloinflata* (Bandy), *Globigerina lozanoi* Colom, "*Globigerinoides*" *higginsi* Bolli, *Morozovella spinulosa* (Cushman), *Pseudohastigerina* spp. and *Subbotina inaequispira* (Subbotina).

Occurrence: The Thebes Formation and the lower part of the Maghagha Formation, and the lower part of the Qarara Formation (Figures 2, 3, 4).

Correlation and age: As mentioned above, such early to middle Eocene zonal markers as *Planorotalites palmerae, Morozovella aragonensis, M. caucasica, Hantkenina* spp., and *Subbotina frontosa* are extremely rare or absent in the studied sequences. Therefore, the local zones are rather difficult to correlate with the standard tropical to subtropical zonal schemes.

Acarinina pentacamerata appears initially at the base of Zone P8, which can be correlated with the base of the *Morozovella aragonensis* Zone defined by Toumarkine and Luterbacher (1985). The last appearance datum (LAD) of this species has, however, considerable uncertainty; it is placed at the top of Zone P10 by Blow (1979), or at a considerably higher level within the *Morozovella lehneri* Zone by Toumarkine and Luterbacher (1985), which corresponds to Zone P12 of Blow (1979). The occurrence of *A. pentacamerata camerata* ranges from Zones P8b to P10, while *Acarinina aspensis* first occurs at the top of Zone P9 and disappears within Zone P11 (Blow, 1979). The first appearance datums (FADs) of *'Hastigerina'* cf. *bolivariana* and *Turborotalia griffinae*

→ **Figure 6.** **1-3**, "*Globigerinoides*" *higginsi* Bolli, two side and umbilical views, Sample B11 of the Maghagha Formation; **4-6**, *Subbotina frontosa boweri* (Bolli), spiral, side, and umbilical views, Sample B30 of the Maghagha Formation; **7-9**, *Globigerina lozanoi* Colom, spiral, side and umbilical views, Sample B30 of the Maghagha Formation; **10-12**, *Acarinina soldadoensis* (Brönnimann), spiral, side and umbilical views, Sample Q2 of the Esna Formation; **13-15**, *Acarinina mckannai* (White), spiral, side and umbilical views, Sample Q2 of the Esna Formation; **16-18**, *Acarinina bullbrooki* (Bolli), spiral, side and umbilical views, Sample B11 of the Maghagha Formation; **19-21**, *Acarinina spinuloinflata* (Bandy), spiral, side and umbilical views, Sample B11 of the Maghagha Formation; **22-24**, *Truncorotaloides rohri* Brönnimann and Bermúdez, umbilical, side and spiral views, Sample B11 of the Maghagha Formation; **25-27**, *Truncorotaloides topilensis* (Cushman), umbilical, side and spiral views, Sample B11 of the Maghagha Formation. Scale bars = 100 μm.

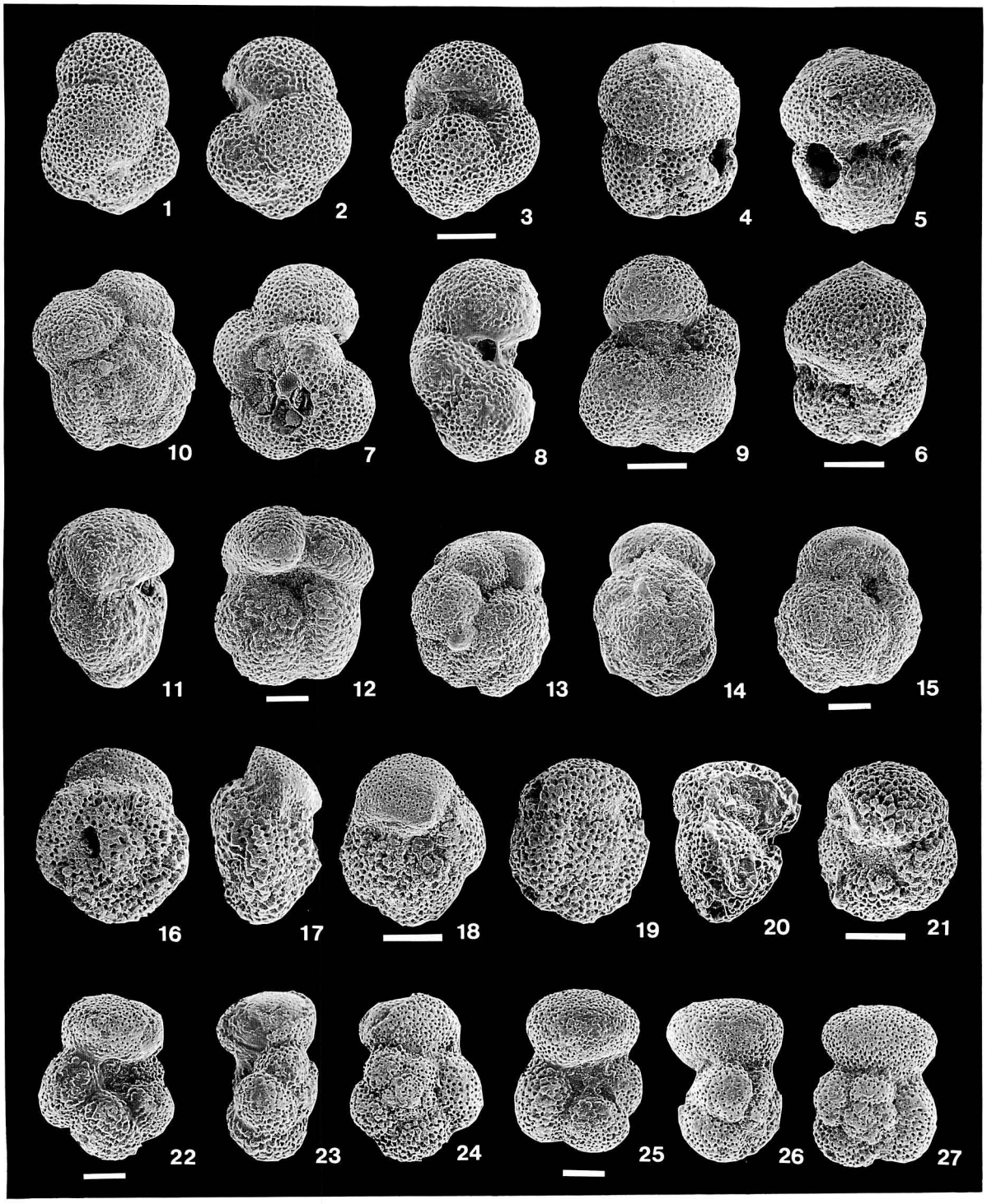
1
2
3
4
5
10
7
8
9
6
11
12
13
14
15
16
17
18
19
20
21
22
23
24
25
26
27

mark the base or just above the base of Zone P9, whereas *Globigerinatheka index index, G. subconglobata subconglobata,* and *Subbotina frontosa boweri* first appear at somewhat higher levels within Zone P10 (Blow, 1979; Toumarkine and Luterbacher, 1985).

Because of the co-occurrence of other species, the *Acarinina aspensis* Zone in this paper can be correlated with the combined interval of both Zones P9 and P10, which correspond to the *Hantkenina nuttalli* Zone and the *A. pentacamerata* Zone of Toumarkine and Luterbacher (1985) (Figure 5). Such typical middle Eocene representatives as *Acarinina bullbrooki, A. spinuloinflata, "Globigerinoides" higginsi, Morozovella spinulosa,* and *Truncorotaloides* spp. are observed frequently in this zone (Figures 2, 3). The abundant occurrence of *A. pentacamerata* suggests that the Thebes Formation was deposited in the latest early Eocene, while the Maghagha and Qarara Formations are assigned to the middle Eocene, because the *G. subconglobata* and *G. index* groups occur. The total geological age of the *A. aspensis* Partial Range-Zone ranges from the latest early Eocene to early middle Eocene (Ypresian to Lutetian) (Figure 5).

3. *Globigerinatheka subconglobata* Interval-Zone

Definition: A zonal interval between the initial appearance of *Globigerinatheka mexicana kugleri*, or *G. mexicana mexicana* (base), and the initial appearance of *Morozovella lehneri* (top).

Characteristic species: This zone shows a faunal affinity with the underlying, *A. aspensis* Zone in the composition and abundance of characteristic species, with the exception of species belonging to the genus *Globigerinatheka*. However, globigerinathekids are rare to few in all the studied sections. In addition, *Acarinina broedermanni* (Cushman and Bermúdez), *Truncorotaloides rohri* Brönnimann and Bermúdez and *Truncorotaloides topilensis* (Cushman) occur commonly in this zone.

Occurrence: The Maghagha and Qarara Formations; the middle part of section 1 and the lower and middle part of sections 3 to 5 (Maghagha Formation), and the middle part of sections 2, 8, 9 and the lower part of sections 6, 7 (the Qarara Formation) (Figures 2, 3, 4).

Correlation and Age: The FADs of *Globigerinatheka mexicana mexicana* and *G. mexicana kugleri* are found at the base or within the *Globigerinatheka subconglobata subconglobata* Zone of Toumarkine and Luterbacher (1985). Bolli (1972) originally defined this zone as being characterized by the rapid evolution of the genus *Globigerinatheka* and by the presence of several subspecies of *G. subconglobata, G. mexicana* and *G. index*. This interval corresponds to Zone P11 (Toumarkine and Luterbacher, 1985; Berggren and Miller, 1988). Therefore, the base of the *Globigerinatheka subconglobata* Zone proposed in this paper is correlatable with the base of Zone P11 or the internationally recognized *G. subconglobata subconglobata* Zone. However, the top of the latter zone is defined by the LAD of *Morozovella aragonensis*, which is not applicable to the

→ **Figure 7.** **1-3**, *Acarinina broedermanni* (Cushman and Bermúdez), umbilical, side and spiral views, Sample B30 of the Maghagha Formation; **4-6**, *Acarinina aspensis* (Colom), spiral, side and umbilical views, Sample B11 of the Maghagha Formation; **7-9**, *Acarinina pentacamerata camerata* Khalilov, umbilical, side and spiral views, Sample B11 of the Maghagha Formation; **10-11**, *Acarinina pentacamerata pentacamerata* (Subbotina), umbilical and spiral views, Sample T6 of the Thebes Formation; **12-14**, *Acarinina praeangulata* (Blow), spiral, side and umbilical views, Sample Q1 of the Esna Formation; **15-17**, *Planorotalites albeari* (Cushman and Bermúdez), spiral, side and umbilical views, Sample Q1 of the Esna Formation; **18-20**, *Morozovella conicotruncata* (Subbotina), spiral, side and umbilical views, Sample Q1 of the Esna Formation; **21-23**, *Morozovella angulata* (White), spiral, side and umbilical views, Sample Q2 of the Esna Formation; **24-26**, *Planorotalites pseudomenardii* (Bolli), spiral, side and umbilical views, Sample Q2 of the Esna Formation. Scale bars = 100 μm.

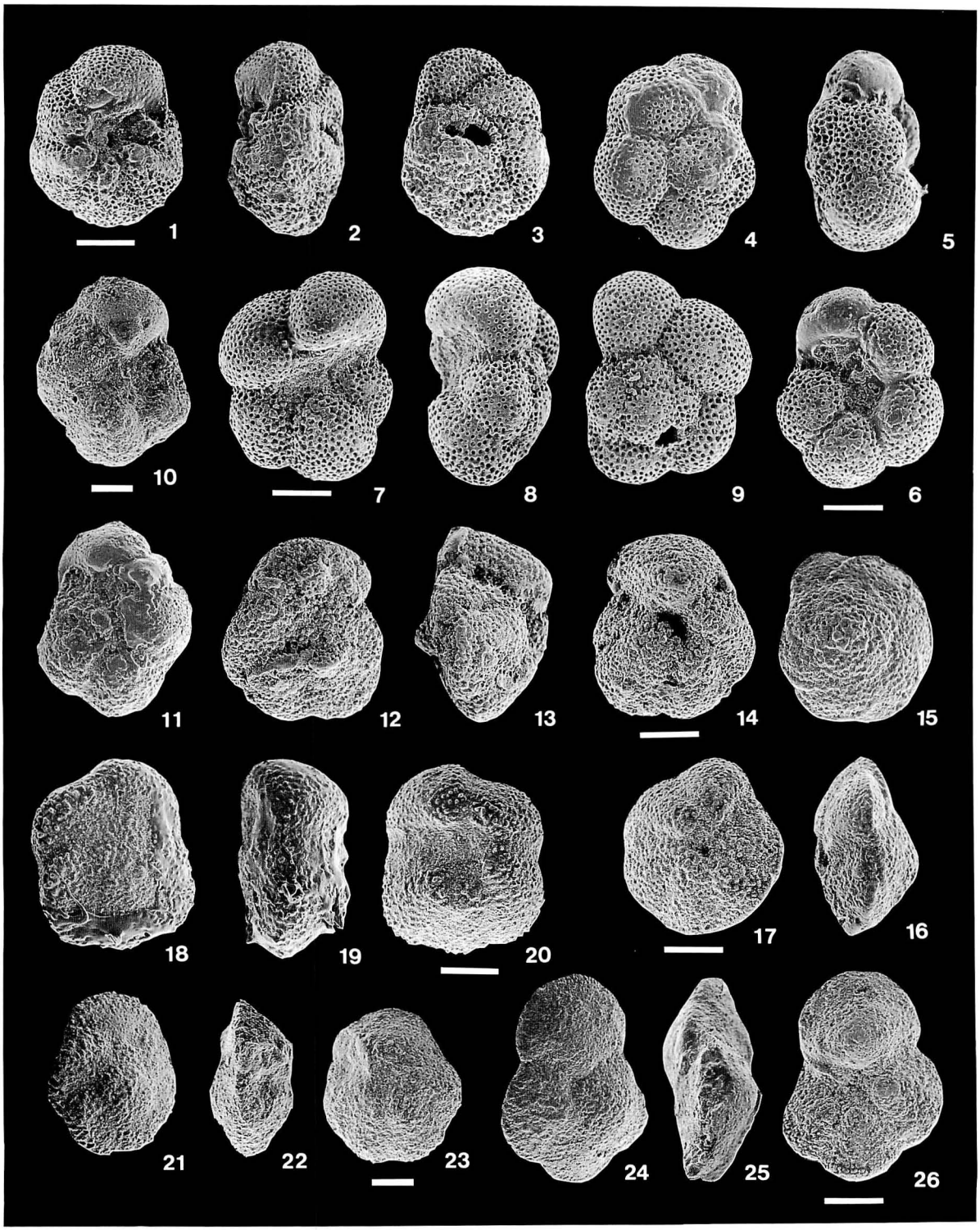
1
2
3
4
5
10
7
8
9
6
11
12
13
14
15
18
19
20
17
16
21
22
23
24
25
26

present study area because this species is absent. We instead used the FAD of *Morozovella lehneri* as a zonal marker because *M. lehneri* is a conspicuous species in the middle Eocene interval. The FAD of *M. lehneri* has been recognized in the upper part of Zone P11 (Blow, 1979) or near the base of the *G. subconglobata subconglobata* Zone (Toumarkine and Luterbacher, 1985).

Therefore, the *G, subconglobata* Zone established in this paper can be correlated with Zone P11 or the *G. subconglobata subconglobata* Zone, and probably corresponds to the lower part of these zones (Figure 5). On the other hand, *Globigerinatheka index index* and *G. subconglobata subconglobata* first appear earlier than *G. mexicana* subspecies within the lower *A. aspensis* Zone (Figures 2, 3). The age of this zone is middle Eocene (Lutetian).

4. *Morozovella lehneri* Total Range-Zone

Definition : Total range of the nominal taxon between the initial appearance of *G. mexicana* (base) and the last appearance of *Morozovella lehneri* (top).

Characteristic species : In addition to the nominate taxon, diagnostic species of this zone include *Pseudohastigerina* spp., *Morozovella spinulosa* (Cushman), *Truncorotaloides collactea* (Finlay), *T. rohri* Brönnimann and Bermúdez, *T. topilensis* (Cushman), "*Globigerinoides*" *higginsi* Bolli, and *Acarinina spinuloinflata* (Bandy).

Occurrence : The *Morozovella lehneri* Zone is thinner than other zones in the studied sections. We recognized this zone in the uppermost parts of sections 3, 5, and 6 (Maghagha Formation), and the lower part of section 7 (Qarara Formation) (Figures 2, 3, 4).

Correlation and Age : Blow (1979) noted that *Morozovella lehneri* initially appeared in the upper part of Zone P11 and disappeared at the top of Zone P13, but Toumarkine and Luterbacher (1985) stated that this species persisted upward to the Middle/Upper Eocene boundary. The nominate taxon is accompanied by such age-diagnostic species as *Acarinina aspensis* and *Morozovella bandyi,* which disappear at the top or in the upper part of Zone P11. The joint occurrence of these species suggests that the *Morozovella lehneri* Zone established herein can be correlated with the upper part of Zone P11 or the *Globigerinatheka subconglobata subconglobata* Zone of Toumarkine and Luterbacher (1985).

Although *Globigerina lozanoi* Colom was previously seen as a Lower to Middle Eocene marker species ranging from Zones P8 to P10 (Blow, 1979 ; Toumarkine and Luterbacher, 1985), this species ranges upwards to Zone P11 in the present study. The age is middle Eocene (Lutetian).

→ **Figure 8.** **1-3**, *Morozovella spinulosa* (Cushman), umbilical, side and spiral views, Sample R6 of the Maghagha Formation ; **4-6**, *Morozovella lehneri* (Cushman and Jarvis), umbilical, side and spiral views, Sample R6 of the Maghagha Formation ; **7-8**, *Morozovella occlusa occlusa* (Loeblich and Tappan), umbilical, side and spiral views, Sample Q2 of the Esna Formation ; **10-12**, *Planorotalites pseudoscitula* (Glaessner), umbilical, side and spiral views, Sample Q2 of the Esna Formation ; **13-15**, *Morozovella occlusa acutispira* (Bolli and Cita), spiral, side and umbilical views, Sample Q1 of the Esna Formation ; **16-18**, *Morozovella velascoensis parva* (Rey), umbilical, side and spiral views, Sample Q2 of the Esna Formation ; **19-21**, *Morozovella velascoensis velascoensis* (Cushman), umbilical, side and spiral views, Sample Q2 of the Esna Formation ; **22-23**, *Pseudohastigerina wilcoxensis* (Cushman and Ponton), lateral view and apertural face, Sample B11 of the Maghagha Formation ; **24-26**, *Globigerinatheka subconglobata subconglobata* (Shutskaya), umbilical and two side views, Sample S35 of the Maghagha Formation ; **27-28**, *Zeauvigerina aegyptiaca* Said and Kenawy, edge and lateral views, Sampe Q2 of the Esna Formation ; **29-30**, *Chiloguembelina crinita* (Glaessner), edge and lateral views, Sample Q2 of the Esna Formation ; **31-32**, *Chiloguembelina midwayensis midwayensis* (Cushman), edge and lateral views, Sample Q2 of the Esna Formation. Scale bars = 100 μm.

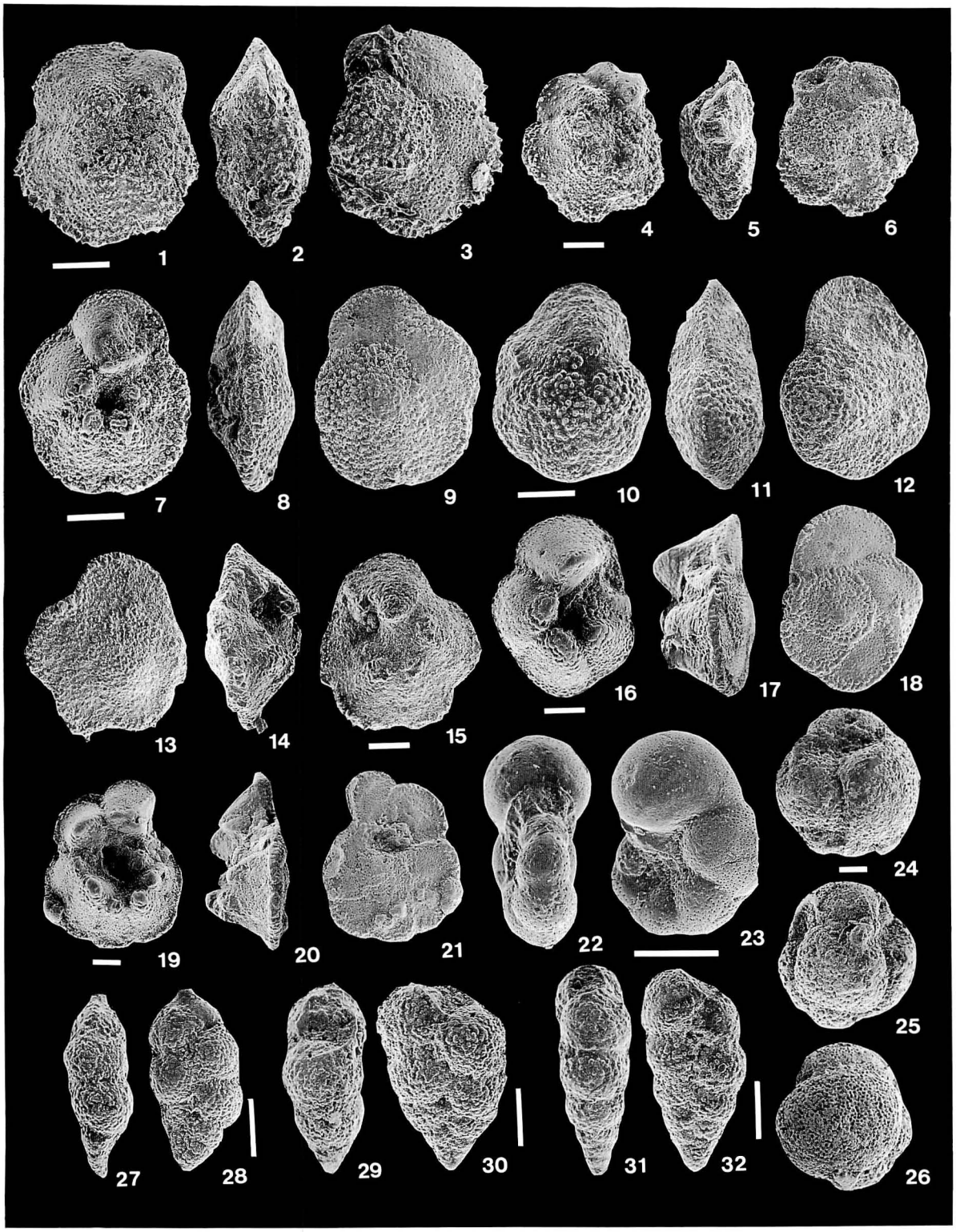
1
2
3
4
5
6
7
8
9
10
11
12
13
14
15
16
17
18
19
20
21
22
23
24
25
26
27
28
29
30
31
32

5. *Truncorotaloides rohri* Assemblage-Zone
Definition : The zonal base is marked by the FAD of *M. lehneri*, but the top is not defined.
Characteristic species : Abundant occurrences of *Truncorotaloides* spp. and *A. spinuloinflata* characterize this zone. Other representative species include *G. higginsi, M. spinulosa*, and *A. broedermanni*. Planktonic foraminifers are generally rare, as compared with benthic species.
Occurrence : The Qarara Formation in all sections (Figures 3, 4).
Correlation and Age : *Orbulinoides beckmanni* has been used to establish the *O. beckmanni* Total Range-Zone in the P-zone system and other zonal schemes (e.g. Stainforth *et al.*, 1975 ; Berggren, 1969a, 1969b ; Blow, 1979 ; Toumarkine and Luterbacher, 1985 ; Berggren and Miller, 1988). The last occurrence of spinose forms (*Acarinina, Morozovella* and *Truncorotaloides*) characterizes the uppermost Middle Eocene zone, Zone P14 or the *Truncorotaloides rohri* Zone.

The absence of *O. beckmanni* in the studied area presents a difficulty in correlating our zones with the international zones as well as other middle Eocene zones. We believe that our *Truncorotaloides rohri* Zone here proposed is correlative with the combined interval of Zones P12 through P14, but further biostratigraphic work is desired in this area. The age of the zone is late middle Eocene (late Lutetian).

Interregional correlation between the study area and other regions in Egypt

1. Paleocene sequence

The Esna Formation (Esna Shale) has been recognized in Egypt to be developed in widely separated areas from the Farafra Oases in the west to the eastern part of the Sinai Peninsula in the east. This formation shows minor variations in its thickness and lithology, consisting mainly of green and gray shales. The Esna Formation is a conspicuous mappable unit in the Egyptian stratigraphic column. It is overlain by the Tarawan Formation (chalk beds) and in turn underlain by the Thebes Formation (hard limestone beds with many chert concretions). In the type locality, Said and Sabry (1964) recognized six biozones of planktonic foraminifers corresponding to the interval from Zones P3 to P6 of Blow (1979).

On the other hand, Said (1960) described and illustrated the following early Eocene planktonic foraminifera from the type locality of the Thebes Formation : *Globorotalia planoconica* Subbotina, *G. conicotruncata* (Subbotina), *G. thebaica* (Said), *G. imitata* Subbotina, *Hastigerina aspera* (Ehrenberg), *H. micra* (Cole) and *Globigerina triloculinoides* Plummer. Said (1990) also demonstrated that the Thebes Formation encompasses planktonic foraminiferal biozones ranging from Zones P6b to P10 (i.e. early Eocene in age).

The approximately 11 m sequence exposed in section 11 consists of gray shale in the lower part and limestone beds in the upper. These two types of rocks, correlated with the lower part of the type Esna Formation, yield abundant planktonic foraminifers which are assignable to Zone P4. Zone P4 (*Planorotalites pseudomenardii* Zone) is a well known unit traceable in Egypt from the Western Desert to Sinai regions (Said and Kenawy, 1956, 1961 ; Said and Sabry, 1964 ; Beckmann *et al.*, 1969 ; Abdel-Kireem *et al.*, 1985 ; Said, 1990 ; Shahin, 1992), and also outside of Egypt in such regions as U.A.E. (Anan and Hamdan, 1993), Saudi Arabia (El-Khayal, 1974), Libya (Berggren, 1969a), Israel (Benjamini, 1980), and Syria (Bolli and Krasheninnikov, 1977). Although the Thebes Formation has been considered to be early Eocene in age by many workers, our biostratigraphic work indicates that the Thebes Formation includes an upper Paleocene sequence and ranges in age from late Paleocene to early Eocene.

2. Eocene sequence

Beckmann *et al.* (1969) discussed the age and geographical distribution of planktonic foraminiferal zones in Egypt, and described eight zones starting from the *Globorotalia subbotinae* Zone upwards to the *Truncorotaloides pseudodubia* Zone, all of early to middle Eocene age. The sections located in the Western Desert region contain successively all these zones, but several zones have not been recognized in the Eastern Desert, Nile Valley, and Sinai areas where regional biostratigraphic zonal schemes have been used (Haggag, 1985, 1986, 1989a, 1989b, 1990; Haggag and Luterbacher, 1991)

Haggag (1989a) summarized a series of her biostratigraphic works, and divided Middle Eocene rocks exposed in the Nile Valley into three biostratigraphic units (Biohorizons 1, 2 and 3) using the FADs of *Morozovella aragonensis, Turborotalia cerroazulensis frontosa,* and *T. cerroazulensis possagnoensis*. These intervals can be correlated approximately with the tropical to subtropical zones of Toumarkine and Luterbacher (1985) as shown in Figure 5. In the Sinai Peninsula, Haggag and Luterbacher (1991) modified the standard low-latitude zonation by using the FAD of *Acarinina bullbrooki* and the FAD of *Globigerinatheka subconglobata rubriformis* to define their zonal boundaries instead of FADs of *Hantkenina* spp. and *Globigerinatheka mexicana mexicana*. They proposed three new zones, the *Acarinina bullbrooki* Zone, the *Globigerinatheka subconglobata subconglobata* Zone, and the *Morozovella lehneri* s.l. Zone, in ascending order, which collectively correspond to an interval from Zones P10 to P13 of Blow (1979). On the other hand, the uppermost middle Eocene zones established in the Nile Valley were well correlated with the standard Paleogene zonal sequence from Zones P14 and P15 or the *Truncorotaloides rohri* Zone of Toumarkine and Luterbacher (1985) (Haggag, 1985; Abdel-Kireem, 1985).

An attempt at interregional correlation between the zones established here and other modified Egyptian zones in the middle Eocene interval from Zones P10 to P13 presents some difficulty because of the different stratigraphical ranges of some marker species. For example, *Morozovella lehneri* became extinct in the study area at a level lower than in Sinai and the Nile Valley. *Morozovella aragonensis* and *Turborotalia cerroazulensis* and its subspecies occur commonly in Sinai and the Nile Valley, but they are rare or absent in the studied sections. In the Eastern Desert sequences, these plankton fossils occur in various lithofacies, each of which was given various formational names by different authors. The complexities of lithology of the middle Eocene sequence may be ascribed to the development of isolated sedimentary basins in shallowing seas. The retreating sea shifted the shoreline northwards, near to the region of Minia during early and middle Eocene times (Said, 1990). Accordingly, some plankton faunas (e.g. *Morozovella aragonensis, M. lehneri* and *Orbulinoides beckmanni,* all considered to be dwellers of deeper waters than acarinid species) are scarce or entirely absent in the Eastern Desert where the studied sections are located, whereas sediments in the Western Desert and the Sinai Peninsula were deposited at greater depths, commonly inhabited by morozovellid forms (Haggag, 1989a; Haggag and Luterbacher, 1991).

Based on our biostratigraphy, the Maghagha and Qarara Formations are isochronous, and range from the *Acarinina aspensis* to *Truncorotaloides rohri* Zones, but the stratigraphic interval from the *A. aspensis* to *M. lehneri* Zones is thicker in the Maghagha Formation than in the Qarara Formation (Figure 5). Such a stratigraphic setting suggests that 1) the limestone-marl facies in the west (the Maghagha Formation) grade laterally into the sandstone-shale facies in the east (the Qarara Formation), 2) the rate of sedimentation was considerably higher in the west than in the east during early middle

Eocene time (*A. aspensis* to *M. lehneri* Zone interval), and 3) the deep depositional center shifted eastward in the late middle Eocene (*T. rohri* Zone).

Species list and taxonomic notes

Paleocene through middle Eocene taxa identified in the studied sections are listed below. Additionally, comments are appended to some taxa to clarify morphological features that are valuable for species identification and to record their stratigraphic occurrences. Because of space limitations, we only illustrate zonal marker species or those taxa characteristic of the established zones. Synonymies are limited to original references plus some additional references effected taxonomic change or provided high-quality illustrations.

Acarinina aspensis (Colom) (Figures 7-4—6)

Globigerina aspensis Colom, 1954, p. 151, pl, 3, figs. 1-35, pl. 4, figs. 1-31.

Globorotalia aspensis (Colom). Postuma, 1971, p. 174-175.

Acarinina aspensis (Colom). Hillebrandt, 1976, p. 340, pl. 5, figs. 8, 12, 13; Blow, 1979, p. 908-911, pl. 148, figs. 7-9, pl. 153, figs. 5-6, pl. 157, figs. 1-6, pl. 165, figs. 5-6, pl. 203, fig. 6.

Forms morphologically related to *Acarinina pentacamerata* are listed by several workers. The following species are identified in our materials; *A. pentacamerata, A. camerata, A. aspensis, A. pentacamerata* (Subbotina) var. *acceleratoria*, and *A. colomi.*

Acarinina aspensis is characterized by having 5 to 7 subglobular chambers in the last whorl and possessing a *Globorotalia*-like, umbilical-extraumbilical aperture. Most of specimens obtained from the studied samples have 5 chambers, rarely 6 in the last whorl. This species is distinguished by possessing an aperture situated in a fairly extraumbilical rather than umbilical position. In the study area, this is one of the representative species of the early middle Eocene faunas.

Acarinina broedermanni (Cushman and Bermúdez) (Figures 7-1—3)

Globorotalia (*Truncorotalia*) *bröedermanni* Cushman and Bermúdez, 1949, p. 40, pl. 7, figs. 22-24.

Globorotalia broedermanni Cushman and Bermúdez. Bolli, 1957b, p. 167, pl. 37, figs. 13a-c.

Globorotalia (*Acarinina*) *broedermanni broedermanni* Cushman and Bermúdez. Blow, 1979, p. 911-914, pl. 148, figs. 1-3, pl. 153, figs. 7-8, pl. 179, figs. 3-5.

This species has a low trochospiral, biconvex test with nearly circular equatorial periphery. Chambers in the last whorl number 6 or more, and increase very gradually in size.

Acarinina bullbrooki Bolli (Figures 6-16—18)

Globorotalia bullbrooki Bolli, 1957b, p. 167, pl. 38, figs. 5a-c; Postuma, 1971, p. 180-181.

Intermediate forms between *Acarinina bullbrooki* and *A. spinuloinflata* are recognized. Such forms produced some confusion as to their taxonomic identity and made it difficult to determine the FAD and LAD levels of these species. Blow (1979) noted that *A. bullbrooki* ranges from Zone P8b to Zone P11, whereas Toumarkine and Luterbacher (1985) extended the LAD of this species upward to the top of P14. *A. bullbrooki* is identified here by such features as its last whorl consistently comprising 4 chambers and the acute periphery of the last chamber, as shown by Bolli (1957b) in his holotype illustrations. The paratype figures (Figures 4a-c of Bolli (1957b)) appear to be referable to *Acarinina spinuloinflata* as judged by their more rounded shoulder in lateral view. In the Sinai Peninsula, *A. bullbrooki* ranges from the *Acarinina bullbrooki* Zone to the *Morozovella lehneri* s.l. Zone. This range corresponds to an interval from the middle part of Zone P10 to the middle part of Zone P13 (Haggag and Luterbacher, 1991).

Acarinina colomi (Bermúdez)

Globigerina colomi Bermúdez, 1961, p. 1167, pl. 2, figs. 6a-c.

Acarinina colomi (Bermúdez). Hillebrandt, 1976, p. 344, pl. 5, figs. 1-3, 5-6.

This species differs from *Acarinina aspensis* in having fewer chambers (4 ½ to 5) in the last whorl and a fairy lobulated equatorial outline. The range of this species is not exactly known in tropical to subtropical regions.

Acarinina convexa (Subbotina)

Globorotalia convexa Subbotina, 1953, p. 209, pl. 17, figs. 2-3; 1971, p. 263, pl. 17, figs. 2-3; Loeblich and Tappan, 1957, p. 188-189, pl. 48, figs. 4a-c, pl. 57, figs. 6-7.

This species has a small, tightly coiled, lenticular, equally biconvex test. The test in lateral view displays a rounded to subacute margin.

Acarinina densa (Cushman)

Pulvinulina crassata Cushman var. *densa* Cushman, 1925d, p. 300; Ciffelli, 1972, p. 157, 159, figs. 1a-c.

Acarinina densa is diagnosed by its nearly flat spiral side and lobulate peripheral margin. The last whorl has 4 ¼ to 5 chambers and an acute periphery in side view. This species differs from *A. bullbrooki* in possessing a greater number of chambers in the last whorl and by the lower height of the umbilical side.

Acarinina esnaensis (LeRoy)

Globigerina esnaensis LeRoy, 1953, p. 31, pl. 6, figs. 8-10.

Globorotalia esnaensis (LeRoy). Loeblich and Tappan, 1957, p. 189-190, pl. 61, figs. 2a-c.

Blow (1979) synonymized this species with *Globorotalia* (=*Acarinina*) *wilcoxensis* Cushman and Ponton. However, this species is distinguished from the latter by its slightly convex spiral side and by having a more rounded peripheral margin in side view. *A. wilcoxensis* ranges from Zone P6a to P8 (Blow, 1979), whereas *A. esnaensis* has been reported to occur upwards to Zone P14 (Boersma *et al.*, 1987; Premoli-Silva and Boersma, 1988).

Acarinina mckannai (White) (Figures 6-13—15)

Globigerina mckannai White, 1928, p. 194, pl. 27, figs. 16a-c; Loeblich and Tappan, 1957, p. 181-182, pl. 47, figs. 7a-c, pl. 53, figs. 1a-2c, pl. 57, figs. 8a-c, pl. 62, figs. 5-7.

Globorotalia mckannai (White). Bolli, 1957a, p. 79, pl. 19, figs. 16-18; Postuma, 1971, p. 200-201.

This species is characterized by: 1) tightly coiled and dorsally convex test, 2) the last whorl having 5 to 6 globular to ovate chambers which increase regularly in size, and 3) an aperture tending to take an extraumbilical position. Blow (1979) assigned this species to the genus *Muricoglobigerina* because of its muricate wall, but other workers placed it under the genus *Acarinina* (Berggren, 1977; Toumarkine and Luterbacher, 1985; Premoli-Silva and Boersma, 1988). Unfortunately, we cannot resolve this taxonomic question because of dissolution of the shell surface of our specimens due to diagenesis. We herein follow conventional taxonomy, leaving the problem of generic assignment to future studies.

Acarinina pentacamerata camerata Khalilov (Figures 7-7—9)

Acarinina pentacamerata (Subbotina) var. *camerata* Khalilov, 1956, p. 252, pl. 5, figs. 6a-c.

Globorotalia (*Acarinina*) *camerata* (Khalilov). Blow, 1979, p. 917, pl. 135, figs. 6, pl. 156, figs. 5-6.

This subspecies is discriminated from *A. pentacamerata pentacamerata* by its broader aperture, situated in a slightly intraumbilical rather than extraumbilical position, and by having a somewhat loosely coiled test. Blow (1979) showed this species to range from Zone P8b to P10, but in the study area its LAD level appears to be higher, probably within Zone P11.

Acarinina pentacamerata pentacamerata (Subbotina) (Figures 7-10—11)

Globorotalia pentacamerata Subbotina, 1947, p. 128-129, pl. 7, figs. 12-17, pl. 9, figs. 24-26.

Acarinina pentacamerata (Subbotina). Subbotina, 1953, p. 233-234, pl. 23, figs. 8a-c; 1971, p. 305, 308, pl. 23, figs. 8a-c.

Subbotina (1947) showed this species to have a rounded, planoconvex test with a slightly flattened dorsal side and strongly convex ventral side. Five to eight chambers in the last whorl increase in size gradually.

The aperture is slitlike and umbilical to extraumbilical in position. *A. pentacamerata pentacamerata* is distinguished from *A. pentacamerata camerata* by having a slitlike extraumbilical aperture with a narrower umbilicus and its tighter mode of coiling.

Acarinina praeangulata (Blow) (Figures 7-12—14)

Globorotalia (*Acarinina*) *praeangulata* Blow, 1979, p. 942, pl. 82, figs. 5-6, pl. 83, figs. 1, 7-8, pl. 85, fig. 1, pl. 87, fig. 2, pl. 212, figs. 1-2.

This species is morphologically close to *A. angulata*, but differs in having a less acute peripheral margin in side view. Blow (1979) reported this species to range from Zone P2 to the earlier part of Zone P4.

Acarinina soldadoensis (Brönnimann) (Figures 6-10—12)

Globigerina soldadoensis Brönnimann, 1952, p. 9, pl. 1, figs. 1-9; Bolli, 1957a, p. 71, pl. 16, figs. 7-12, p. 162, pl. 35, figs. 9a-c; Postuma, 1971, p. 158-159.

Globigerina cf. *soldadoensis* Brönnimann. Loeblich and Tappan, 1957, p. 182, pl. 35, figs. 4a-c.

Diagnoses of this species include its lobulated, low trochospiral test with a nearly flattened spiral side, depressed, subrounded chambers in the last whorl, and the aperture tending to take an umbilical position. The generic position of this species is as yet unsettled. Blow (1979) placed it in the genus *Muricoglobigerina*, whereas other workers maintained the generic assignment to *Acarinina*. This species has been found to range from Zone P5 to P9 in tropical regions (Blow, 1979, Toumarkine and Luterbacher, 1985), but its subspecies *A. soldadoensis angulosa* disappears in Zone P10 (Boersma and Premoli-Silva, 1988).

Acarinina spinuloinflata (Bandy) (Figures 6-19—21)

Globorotalia spinuloinflata Bandy, 1949, p. 122, pl. 23, figs. 1a-c.

Globigerina spinuloinflata (Bandy). Cifelli, 1972, p. 159, pl. 1, figs. 2a-c.

This species, one of the conical acarinids which characterize the middle Eocene fauna in the low latitudes, occurs commonly, often dominantly. The FAD of this species, however, has not been evaluated fully, although it has been placed either within Zone P11 (Boersma and Premoli-Silva, 1988) or within Zone P12 (Blow, 1979). This species is distinguished from *Acarinina bullbrooki* and *Acarinina densa* by its last chamber having a rounded periphery.

Catapsydrax africana (Blow and Banner)

Globigerinita africana Blow and Banner, 1962, p. 105-106, pl. 15, figs. a-c.

Globigerinita echinatus africana Blow and Banner. Blow, 1979, p. 1336-1337, pl. 24, pl. 240, fig. 8.

Blow (1979) used the generic name *Globigerinita* for bullate forms of the Paleogene species and stated that the genus *Catapsydrax* is a synonym of *Globigerinita*. Many subsequent workers, however, separated these two genera phylogenetically on account of differences in their ultrastructure, stratigraphic distribution, and taxonomic relations.

The bullae of this species are slightly inflated, moderate in size, with three accessory apertures. Although Blow (1979) included this species in the genus *Globigerinita*, its wall structure is coarse-pitted and is different from the typical smooth surface characteristic of *Globigerinita glutinata* (Egger). Our specimens of *C. africana* have a low trochospiral test with 3 to 4 chambers in the last whorl, and their wall structure is coarse-pitted, neither cancellate nor hispid. Herein we classify this species in the genus *Catapsydrax*.

Catapsydrax echinatus (Bolli)

Catapsydrax echinatus Bolli, 1957b, p. 165, pl. 37, figs. 2a-c.

Catapsydrax hardingae (Blow)

Globigerinita hardingae Blow, 1979, p. 1338-1340, pl. 178, figs. 1-5.

This species is morphologically similar to *Globigerinita martini* Blow and Banner, but is distinguished by its more slowly enlarging last chamber, more lobulated equatorial margin, and smaller bullae with an infralaminal aperture. Blow (1979) noted the stratigra-

phic range of this species to extend from Zones P10 to P12.

Catapsydrax simulans (Bermúdez)

Catapsydrax cf. *dissimilis* (Cushman and Bermúdez). Bolli, 1957b, p. 166, pl. 37, fig. 6.

Globigerina simulans Bermúdez, 1961, p. 1198, pl. 6, fig. 1a.

Globigerinita simulans (Bermúdez). Blow, 1979, p. 1343-1345, pl. 186, figs. 6-7.

This species resembles *Catapsydrax dissimilis dissimilis* and *C. dissimilis riveroae*, in having a small, tubelike to rectangular bulla. The former possesses a single small infralaminal opening at the posterior margin of the bulla, and the latter has a lower trochospiral test.

Chiloguembelina crinita (Glaessner) (Figures 8-29—30)

Gümbelina crinita Glaessner, 1937b, p. 383, pl. 4, fig. 34.

Chiloguembelina crinita (Glaessner). Beckmann, 1957, p. 98, pl. 21, figs. 4a-b.

This species is distinguished from *Chiloguembelina midwayensis* by having more globular and more rapidly enlarging chambers. This species ranges from the base of the *Globorotalia* (=*Planorotalites*) *pseudomenardii* Zone to the middle part of the *Globorotalia* (=*Morozovella*) *velascoensis* Zone (Beckmann, 1957).

Chiloguembelina cubensis (Palmer)

Gümbelina cubensis Palmer, 1934, p. 74, text-figs. 1-6.

Chiloguembelina cubensis (Palmer). Beckmann, 1957, pl. 21, fig. 21, text-figs. 14-5—8.

This is one of the small biserial species, and has a long stratigraphic range from the *Porticulasphaera* (=*Globigerinatheka*) *mexicana* to *Globorotalia opima opima* Zone of late middle Eocene to early Oligocene age (Beckmann, 1957).

Chiloguembelina martini (Pijpers)

Textularia martini Pijpers, 1933, p. 57, figs. 6-10.

Chiloguembelina martini (Pijpers). Beckmann, 1957, p. 89, pl. 21, fig. 14, text-figs. 4-8—11, 14—18, 20—23.

This characteristic Eocene chiloguembelid occurs abundantly in low-latitude regions in association with *C. cubensis*. Beckmann (1957) reported *C. martini* to range from the *Globorotalia* (=*Morozovella*) *aragonensis* Zone to *Globorotalia cocoaensis* Zone of late early Eocene to late Eocene age.

Chiloguembelina midwayensis midwayensis (Cushman) (Figures 8-31—32)

Gümbelina midwayensis Cushman, 1940, p. 65, pl. 11, fig. 15.

Chiloguembelina midwayensis midwayensis (Cushman). Beckmann, 1957, p. 90, pl. 21, figs. 1a-b.

This biserial species has a fairly elongate test and obliquely running sutures to the axial direction. This species is restricted to the Paleocene (Beckmann, 1957).

Globigerina lozanoi Colom (Figures 6-7—9)

Globigerina lozanoi Colom, 1954, p. 149, pl. 2, figs. 1-48; Blow, 1979, p. 854-855, pl. 145, figs. 2-9.

Globigerina (*Eoglobigerina*) *lozanoi* Colom. Hillebrandt, 1976, p. 336, pl. 3, figs. 8-17.

This species is characterized by having a relatively large number of chambers (up to 6) in the last whorl and by its high, slightly irregular trochospiral coiling. "*Globigerinoides*" *higginsi* Bolli resembles this species, but shows a more loosely coiled and high trochospire. Many workers (Hillebrandt, 1966, Blow, 1979, Toumarkine and Luterbacher, 1985, and Haggag, 1989a) consider *G. lozanoi* to be an ancestral form of "*G.*" *higginsi*. This species is reported to range from Zone P8 to P10 in the literature (e.g. Blow, 1979), but in the studied sections the species ranges to the upper part of Zone P11.

Globigerina officinalis Subbotina

Globigerina officinalis Subbotina, 1953, p. 78, pl. 11, figs. 1-7; 1971, p. 105, p. 108, pl. 11, figs. 1-7; Blow and Banner, 1962, p. 88, pl. 4, A-C, fig. 16.

Although Blow (1969) noted the range of this species as Zone P13 to P22, we believe the FAD of this species occurred earlier, probably in the later part of Zone P11 because of its rare occurrence in the basal part of the *M. lehneri* Zone in the Maghagha Formation.

Globigerina parva Bolli

Globigerina parva Bolli, 1957b, p. 108, pl. 22, figs. 14a-c.

The lobulated last whorl having consistently 4 chambers and fairly high trochospiral coiling are the most important morphological characteristics of this species. This species closely resembles *G. officinalis*, but the latter has a narrow umbilicus.

Globigerinatheka index index (Finlay)

Globigerinoides index Finlay, 1939a, p. 125, pl. 14, fig. 85, fig. 86-88; Hornibrook, 1958, pl. 1, figs. 11-13, fig. 14.

Globigerapsis index (Finlay). Bolli, 1957b, p. 165, pl. 36, figs. 14-18.

Globigerinatheka (*Globigerapsis*) *index index* (Finlay). Jenkins, 1971, p. 187-188, pl. 22, figs. 642-645.

Globigerinatheka index index (Finlay). Bolli, 1972, p. 124, pl. 1, figs. 1-4, text-figs. 51-57, 63, and 64.

The FAD of this species is placed within Zone P10 or the *G. subconglobata* Zone (probably Zone P11) (Blow, 1979; Toumarkine and Luterbacher, 1985).

Globigerinatheka mexicana kugleri (Bolli, Loeblich and Tappan)

Globigerapsis kugleri Bolli, Loeblich and Tappan, 1957, p. 34, pl. 6, figs. 6a-c; Postuma, 1971, p. 138-139; Bolli, 1972, p. 128-129, pl. 2, figs. 6-7, text-figs. 12-17.

This species is discriminated from *G. mexicana mexicana* by the more loosely coiled, more globular chambers and a less compact test shape. The two subspecies (*kugleri* and *mexicana*) occur in the *G. subconglobata subconglobata* Zone which is coeval with Zone P11 of Blow (1979). The former subspecies disappeared within Zone P13, whereas the latter survived until Zone P15 or the *Globigerinatheka semiinvoluta* Zone of late Eocene age.

Globigerinatheka mexicana mexicana (Cushman)

Globigerina mexicana Cushman, 1925b, p. 6, pl. 1, figs. 8a-b.

Globigerapsis mexicana (Cushman). Blow and Saito, 1968, text-figs. 1-4.

Globigerinatheka mexicana mexicana (Cushman). Bolli, 1972, p. 129-131, pl. 2, figs. 1-5, pl. 4, figs. 1-6, text-figs. 1-11.

Globigerinatheka subconglobata subconglobata (Shutskaya) (Figures 8-24—26)

Globigerinoides subconglobatus Chalilov var. *subconglobata* Chalilov, Shutskaya, 1958, p. 86-87, pl. 1, figs. 4-11.

Globigerinatheka subconglobata subconglobata (Shutskaya). Bolli, 1972, p. 134, pl. 1, figs. 8-10, 15-16

Although Berggren and Miller (1988) contended that the *G. subconglobata* group, including three subspecies (*subconglobata, euganea* and *curryi*) could not be recognized by the manner proposed by Proto Decima and Bolli (1970), we herein follow the classification of Bolli (1972) because the *G. subconglobata* group can be discriminated from other globigerinathekid groups by its large, globular test, robust wall and occasional presence of bullae. *G. index* has a morphological affinity to *G. subconglobata*, but differs in having a more elongate test outline, loosely coiled test, deeply incised intercameral sutures, and distinct apertures usually not covered by bullae.

"Globigerinoides" higginsi Bolli (Figures 6-1—3)

"Globigerinoides" higginsi Bolli, 1957b, p. 164, pl. 36, figs. 11a-b; Blow, 1979, p. 862-864, pl. 183, figs. 7-9, pl. 184, figs. 1-7.

"Globigerinoides" higginsi is easily identified by its loosely coiled and very high trochospiral test, and moderately to rapidly enlarging chambers in the last and penultimate whorls. A supplementary aperture is not always observed except in the last whorl. The wall structure is microgranular, not cancellate like Neogene *Globigerinoides*. Although its generic position remains questionable, this species commonly occurs in the lower to middle Eocene of the low-latitude area. This species ranges from the base of Zone P9 to P11, but also occurs rarely in the lower part of Zone P12 (Blow, 1979; Toumarkine and Luterbacher, 1985).

Guembelitria columbiana Howe

Gümbelitria columbiana Howe, 1939, p. 62, pl. 8, figs. 12-13.

Beckmann (1957) observed this species

from the *Hantkenina aragonensis* Zone to the *Porticulasphaera* (=*Globigerinatheka*) *mexicana* Zone, referable to Zones P10 to P11 of Blow (1979).

Hantkenina mexicana Cushman

Hantkenina mexicana Cushman, 1925a, p. 3, pl. 2, fig. 2; Brönnimann, 1950, p. 405, 407, pl. 55, figs. 1-6.

The FAD of the earliest member of the genus *Hantkenina, H. nuttalli*, has been used to mark the Early/Middle Eocene boundary in low-latitude regions (Blow, 1969; Berggren, 1969a, b; Stainforth *et al.*, 1975; Toumarkine and Luterbacher, 1985; Berggren and Miller, 1988). Species of *Hantkenina* occur rarely or are entirely absent in the studied sections.

'Hastigerina' cf. *bolivariana* (Petters)

'Hastigerina' cf. *bolivariana* (Petters). Toumarkine and Luterbacher, 1985, p. 127, 7-12 in fig. 27.

Hastigerina bolivariana (Petters) is diagnosed by its globular test which is completely involute on the ventral side and nearly so on the dorsal side, as figured by Petters (1954). '*H.*' cf. *bolivariana* described by Toumarkine and Luterbacher (1985) has a more compact, less planispirally coiled test and a less globular last chamber than Petters' typical form. Although the generic position of this species is questionable, we follow the taxonomy of Toumarkine and Luterbacher (1985) and here use the name *'Hastigerina'* for this species.

Morozovella angulata (White) (Figures 7-21—23)

Globigerina angulata White, 1928, p. 191, pl. 27, figs. 13a-c.

Globorotalia angulata (White). Bolli, 1957a, p. 74, pl. 17, figs. 7-9; Postuma, 1971, p. 170-171.

This is a characteristic species of the middle to late Paleocene interval in tropical to subtropical regions. This species has a low trochospiral, angular-conical test, showing acute to subacute margins in axial view, but lacks a typical peripheral keel. Five chambers in the last whorl are angular in shape and increase gradually in size.

Morozovella bandyi Fleisher

Morozovella bandyi Fleisher, 1974, p. 1030, pl. 14, figs. 3-8.

This species resembles *M. spinulosa*, but is distinguished in possessing a dorsal opening (Fleisher, 1974). This diagnostic feature could not be observed in any specimen obtained from the studied sections. We here consider that *Morozovella bandyi* possesses constantly 4 chambers in the last whorl as compared with 5 in *M. spinulosa* and a more convex spiral side than the latter species. This species ranges from the middle part of Zone P10 to P11 or is confined to the *G. subconglobata* Zone of Bolli (Fleisher, 1974).

Morozovella conicotruncata (Subbotina) (Figures 7-18—20)

Globorotalia conicotruncata Subbotina, 1947, p. 115, pl. 4, figs. 11-13, pl. 9, figs. 9-11.

Acarinina conicotruncata (Subbotina). Subbotina, 1953, p. 220-222, pl. 20, figs. 5-10; 1971, p. 281, p. 284-287, pl. 20, figs. 5a, b, 6-12.

Globorotalia angulata abundocamerata Bolli. 1957a, p. 74, pl. 17, figs. 4-6; Postuma, 1971, p. 166-167.

By the possession of large numbers of chambers (6 to 8) in the last whorl, this species is distinguished from *M. angulata*.

Morozovella lehneri (Cushman and Jarvis) (Figures 8-4—6)

Globorotalia lehneri Cushman and Jarvis, 1929, p. 17, pl. 3, figs. 16a-c; Bolli, 1957b, p. 169, pl. 38, figs. 9-13; Postuma, 1971, p. 198-199.

Globorotalia (*Morozovella*) *lehneri* Cushman and Jarvis. Blow, 1979, p. 1002-1003, pl. 188, figs. 1-10, pl. 251, figs. 3-4.

This species has a low trochospiral biconvex test, which has a strongly lobulated periphery frilled with a spiny keel and 6 to 7 chambers in the last whorl. Chambers are tangentially elongated, and the last and penultimate chambers are nearly equal in size.

Morozovella occlusa acutispira (Bolli and Cita) (Figures 8-13—15)

Globorotalia acutispira Bolli and Cita, 1960, p. 15, pl. 33, figs. 3a-c.

Globorotalia (*Morozovella*) *occlusa acutispira* Bolli

and Cita. Blow, 1979, p. 1009-1011.

Morozovella occlusa differs from *M. velascoensis* in having a thinner lenticular test and small, almost closed umbilicus, and from *M. simulatilis* in its less convex spiral side.

Blow (1979) proposed two subspecies in *M. occlusa* (*occlusa* and *acutispira*). The latter subspecies has of 4 to 4 ½ chambers in the last whorl and displays a lobulated equatorial periphery, whereas, in *M. occlusa occlusa* chambers in the last whorl number more than 5.

Morozovella occlusa occlusa (Loeblich and Tappan) (Figures 8-7—9)

Globorotalia occlusa Loeblich and Tappan, 1957, p. 191, pl. 64, figs. 3a-c. not: pl. 55, figs. 3a-c (=*M. occlusa acutispira*).

Globorotalia (*Morozovella*) *occlusa occlusa* Loeblich and Tappan. Blow, 1979, p. 1007-1009, pl. 90, figs. 9-10, pl. 95, figs. 7-10, pl. 96, figs. 1-3, pl. 103, figs. 4-6, pl. 108, figs. 8-10, pl. 118, figs. 1-7, pl. 213, fig. 6, pl. 214, figs. 1-6, pl. 215, fig. 5.

Blow (1979) showed that this species ranged from the basal part of Zones P4 to P7, and assigned it a middle late Paleocene to early Eocene age.

Morozovella simulatilis (Schwager)

Discorbina simulatilis Schwager, 1883, p. 120, pl. 29, fig. 15.

Globorotalia simulatilis (Schwager). Luterbacher, 1964, p. 665-668, figs. 53-58.

Morozovella spinulosa (Cushman) (Figures 8-1—3)

Globorotalia spinulosa Cushman, 1927, p. 114, pl. 23, figs. 4a-c; Bolli, 1957b, p. 168, pl. 38, figs. 6-7.

Globorotalia (*Morozovella*) *spinulosa spinulosa* Cushman. Blow, 1979, p. 1013-1015, pl. 182, figs. 1-4, pl. 197, figs. 1-6.

This is one of the typical species of late middle Eocene morozovellids and disappeared simultaneously with other hispid species (*Acarinina* and *Truncorotaloides*) at or just above the middle/late Eocene boundary. However, the FAD of this species is unsettled, having been placed at different levels: the base of Zone P10 (Blow, 1979), the middle part of Zone P9 (Toumarkine and Luterbacher, 1985), and the middle part of Zone P8 (Boersma and Premoli-Silva, 1988).

Morozovella velascoensis acuta (Toulmin)

Globorotalia wilcoxensis Cushman and Ponton var. *acuta* Toulmin, 1941, p. 608, pl. 82, figs. 6-8.

Globorotalia acuta Toulmin: Loeblich and Tappan, 1957, p. 185-186, pl. 47, figs. 5a-c, pl. 55, figs. 4-5.

Morozovella velascoensis is characterized by a planoconvex test, well developed keel and thickened and spinose collar as the umbilical shoulder in the last whorl. This species includes three subspecies (*acuta, parva* and *velascoensis). M. velascoensis velascoensis* has a large number of chambers, generally more than 6, in the last whorl, whereas *acuta* and *parva* have fewer such chambers, consistently 5 in the former and 4 to 4 ½ in the latter.

Morozovella velascoensis parva (Rey) (Figures 8-16—18)

Globorotalia velascoensis (Cushman) var. *parva* Rey, 1955, p. 209, pl. 12, figs. 1a-c.

Globorotalia (*Morozovella*) *velascoensis parva* Rey. Blow, 1979, p. 1030-1031, pl. 95, figs. 3-6.

Morozovella velascoensis velascoensis (Cushman) (Figures 8-19—21)

Pulvinulina velascoensis Cushman, 1925c, p. 19, pl. 3, fig. 5.

Globorotalia velascoensis (Cushman). Bolli, 1957a, p. 76, pl. 20, figs. 1-3; Loeblich and Tappan, 1957, pl. 64, figs. 1-2; Postuma, 1971, p. 218-219.

Muricoglobigerina senni (Beckmann)

Sphaeroidinella senni Beckmann, 1953, p. 394-395, pl. 26, figs. 2-4, text-fig. 20

Globigerina senni (Beckmann). Bolli, 1957b, p. 163, pl. 35, figs. 10-12.

This species can easily be identified by its very tightly coiled and highly trochospiral test and muricate wall.

Planorotalites albeari (Cushman and Bermúdez) (Figures 7-15—17)

Globorotalia albeari Cushman and Bermúdez, 1949, p. 33, pl. 6, figs. 13-15; Blow, 1979, p. 883-885, pl. 92, figs. 4, 8-9, pl. 93, figs. 1-4.

Globorotalia pusilla laevigata Bolli, 1957a, p. 78, pl. 20, figs. 5-7.

The genus *Planorotalites* is characterized

by a smaller biconvex lenticular test and its finely perforate, smooth wall surface texture. In this study we follow the taxonomy of Toumarkine and Luterbacher (1985) and recognize four species, *albeari, pseudomenardii, pseudoscitula*, and *pusilla pusilla*, all belonging to the genus *Planorotalites. Planorotalites albeari* has a circular equatorial outline and 6-7 or more chambers in the last whorl.

Planorotalites pseudomenardii (Bolli) (Figures 7-24—26)

Globorotalia pseudomenardii Bolli, 1957a, p. 77, pl. 20, figs. 14-17; Postuma, 1971, p. 204-205.

The axial periphery of the test is acute, with an imperforate keel. Five chambers in the last whorl are strongly compressed and increase rapidly in size.

Planorotalites pseudoscitula (Glaessner) (Figures 8-10—12)

Globorotalia pseudoscitula Glaessner, 1937a, p. 32, text-figs. 3a-c; Subbotina, 1953, p. 261, pl. 17, fig. 1, pl. 16, figs. 17-18; 1971, p. 261-263, pl. 14, figs. 17-18, pl. 17, figs. 1a-c.

Globorotalia renzi Bolli, 1957b, p. 168, pl. 38, figs. 3a-c.

This species has a small, lenticular, thin, biconvex test with a nearly circular periphery. Chambers in the last whorl number from 5 to 7, which increase slowly in size. This species resembles *P. albeari*, but differs in having a thinner lenticular test. *P. pseudoscitula* ranges from Zones P10 to P13, whereas the latter appeared earlier, occurring from Zones P3 to P7.

Planorotalites pusilla pusilla (Bolli)

Globorotalia pusilla pusilla Bolli, 1957a, p. 78, pl. 20, figs. 8-10.

The last whorl comprising about 5 chambers, instead of 6-7 as in *P. albeari*, and its less acute axial periphery are the distinguishing characters of this species.

Pseudohastigerina micra (Cole)

Nonion micrus Cole, 1927, p. 22, pl. 5, fig. 12.

Hastigerina micra (Cole). Bolli, 1957b, p. 161, pl. 35, figs. 1-2.

Pseudohastigerina micra (Cole). Blow and Banner, 1962, p. 704, fig. 2; Saito and Bé, 1964, p. 704, fig. 2.

Pseudohastigerina wilcoxensis (Cushman and Ponton) (Figures 8-22—23)

Nonion wilcoxensis Cushman and Ponton, 1932, p. 64, pl. 8, fig. 11.

Pseudohastigerina wilcoxensis (Cushman and Ponton). Berggren *et al.*, 1967, p. 278-280, figs. 2-6.

This species is regarded as the first planispirally coiled species in the Cenozoic, and the Paleocene/Eocene boundary has been drawn at or just above the FAD of this species (e.g. Berggren, 1969a, 1969b; Aubry *et al.*, 1988).

Subbotina bakeri (Cole)

Globigerina bakeri Cole, 1927, p. 33, pl. 4, figs. 12-13.

Globigerina turgida Finlay: Bolli, 1957b, p. 73, pl. 15, figs. 3-5.

Subbotina bakeri (Cole): Blow, 1979, p. 1255-1256, pl. 160, fig. 5.

The genus *Subbotina* was originally defined in terms of cancellate wall surface with funnellike pore pits. Blow (1979) gave the following diagnostic characters for this genus: 1) a small umbilicus with asymmetrically umbilical-extraumbilical aperture bordered by a porticus, 2) a trochospirally coiled test with inflated chambers, and 3) microgranular wall structure. We used these criteria for the definition of this genus.

This species has been recorded from Zones P8b to P13 (Blow, 1979).

Subbotina eocaena (Gümbel)

Globigerina eocaena Gümbel, 1868, p. 662, pl. II, figs. 109a-b; Subbotina, 1953, pl. 6, figs. 5a-c, pl. 7, figs. 1a-c; 1971, p. 85, p. 88-89, pl. 6, figs. 5a-c, pl. 7, figs. 1a-c; Hang and Lindenberg, 1969, p. 236-245, table I, figs. 1-6.

Subbotina frontosa boweri (Bolli) (Figures 6-4—6)

Globigerina boweri Bolli, 1957b, p. 163, pl. 36, figs. 1a-2b; Postuma, 1971, p. 144-145.

Subbotina frontosa boweri (Bolli). Blow, 1979, p. 1266-1268, pl. 175, figs. 7-9.

Subbotina frontosa, including its two subspecies *boweri* and *frontosa*, has 3 to 3 ½

chambers in the last whorl, in which the final chamber is greatly enlarged. A high-arched primary aperture is located in a slightly extraumbilical position. *S. frontosa boweri* can be discriminated from *S. frontosa frontosa* by its nearly circular aperture with a short lip or rim.

Subbotina frontosa frontosa (Subbotina)

Globigerina frontosa Subbotina, 1953, p. 84, pl. 12, figs. 3a-c. not pl. 12, figs. 4-7c ; 1971, p. 113, p. 116, pl. 7, figs. 3-7.

Subbotina frontosa frontosa (Subbotina) : Blow, 1979, p. 1263-1265, pl. 158, figs. 6-7, pl. 162, figs. 10-11, pl. 175, figs. 4-6.

Subbotina hagni (Gohrbandt)

Globigerina hagni Gohrbandt, 1967, p. 324, 326, pl. 1, figs. 1-9.

This species is mainly diagnosed by its umbilical-extraumbilical slitlike aperture.

Subbotina inaequispira (Subbotina)

Globigerina inaequispira Subbotina, 1953, p. 69, pl. 6, figs. 1-4 ; 1971, p. 84-85, pl. 6, figs. 1-4.

A low trochospiral test with a strongly lobulated equatorial periphery and rapidly increasing globular chambers in the last whorl characterized this species. The range of this species remains unsettled : from Zones P11 to P13 in Blow (1979), from P8 to P12 in Toumarkine and Luterbacher (1985), and from P5 to P10 in Boersma and Premoli-Silva (1988).

Subbotina linaperta (Finlay)

Globigerina linaperta Finlay, 1939a, p. 125, pl. 13, figs. 54-56 ; Hornibrook, 1958, p. 33-34, pl. 1, figs. 19-21.

Globigerina (*Subbotina*) *linaperta* Finlay. Jenkins, 1971, p. 162-163, pl. 18, figs. 551-553.

Subbotina pseudoeocaena (Subbotina)

Globigerina pseudoeocaena Subbotina, 1953, p. 66, pl. 4, figs. 9a-c, pl. 5, figs. 1-2, 6 ; 1971, p. 79-81, pl. 4, figs. 9a-c, pl. 5, figs. 1-2, 6.

Subbotina triangularis (White)

Globigerina triangularis White, 1928, p. 195, pl. 28, figs. 1a-c ; Bolli, 1957a, p. 71, pl. 15, figs. 12-14.

This species is distinguished from *S. triloculinoides* by its somewhat higher trochospiral test and smaller final chamber. It is representative of the Paleocene subbotinids.

Subbotina triloculinoides (Plummer)

Globigerina triloculinoides Plummer, 1926, p. 134, pl. 8, figs. 10a-b ; Bolli, 1957a, p. 70, pl. 15, figs. 18-20 ; Loeblich and Tappan, 1957, p. 183-184, pl. 41, figs. 2a-c, pl. 43, figs. 9a-c, pl. 45, figs. 3a-c.

Globigerina (*Subbotina*) *triloculinoides* Plummer. Jenkins, 1971, p. 163-164, pl. 17, fig. 508.

Subbotina triloculinoides triloculinoides (Plummer). Blow, 1979, p. 1287-1292, pl. 74, fig. 6, pl. 80, fig. 1, pl. 98, fig. 7.

This is the type species of the genus *Subbotina*. The last whorl has 3 to 3 ½ chambers which increase rapidly in size, and its last chamber occupies up to half the size of the entire test.

Subbotina velascoensis (Cushman)

Globigerina velascoensis Cushman, 1925c, p. 19, pl. 3, fig. 6 ; Bolli, 1957a, p. 71, pl. 15, figs. 9-11.

This species is distinguished from other Paleocene subbotinids by its laterally compressed last chamber.

Subbotina yeguaensis (Weinzierl and Applin)

Globigerina yeguaensis Weinzierl and Applin, 1929, p. 408, pl. 43, figs. 1a-c ; Saito and Bé, 1964, p. 702-705, fig. 2.

Truncorotaloides collactea (Finlay)

Globorotalia collactea Finlay, 1939b, p. 327, pl. 29, figs. 164-165.

Truncorotaloides collactea (Finlay). Jenkins, 1965, p. 843-848, figs. 1-27.

Supplementary openings on the spiral side provide an important diagnostic feature for the genus *Truncorotaloides*. Although this feature is not always observable in most of our specimens, this genus can be easily recognized by its angular-rhomboid chambers and distinctly hispid wall surface.

Some workers assign *Truncorotaloides collactea* to the genus *Acarinina* because of the absence of supplementary apertures (Blow, 1979 ; Boersma and Premoli-Silva, 1988). We, however, follow Jenkins (1965), Toumarkine and Luterbacher (1985) and others who

placed it in the genus *Truncorotaloides*.

Truncorotaloides pseudodubia (Bandy)

Globigerinoides pseudodubia Bandy, 1949, p. 123, pl. 24, figs. 1a-c.

Truncorotaloides pseudodubia pseudodubia (Bandy). Blow, 1979, p. 951-953, pl. 171, fig. 4, pl. 194, figs. 5-6.

This species is morphologically close to *T. rohri* and *T. collactea*. It is distinguished from the former by its more compact, slightly higher-trochoid coiling and the uniform size of the chambers in the last whorl, and from the latter in possessing a fairly large test.

Truncorotaloides rohri Brönnimann and Bermúdez (Figures 6-22—24)

Truncorotaloides rohri Brönnimann and Bermúdez, 1953, p. 818-819, pl. 87, figs. 7-9; Bolli, Loeblich and Tappan, 1957, p. 42, pl. 10, figs. 5a-c; Bolli, 1957b, p. 170, pl. 39, figs. 8-12; Postuma, 1971, p. 232-233.

This species has a distinctly hispid test with 5 angular-rhomboid chambers in the last whorl, which increase rapidly in size. A supplementary opening is commonly observed in many specimens. Such subspecies as *guaracaraensis, mayoensis, piparoensis, haynesi* and *libyaensis* are recognized by some workers (Brönnimann and Bermúdez, 1953; Samanta, 1970; El Khoudary, 1977). We also recognized forms assignable to these subspecies in our materials, but the definition of these subspecies needs to be clarified further.

Truncorotaloides topilensis (Cushman) (Figures 6-25—27)

Globigerina topilensis Cushman, 1925b, p. 7, pl. 1, figs. 9a-c.

Truncorotaloides topilensis (Cushman). Bolli, 1957b, p. 170, pl. 39, figs. 13-16a-c; Postuma, 1971, p. 234-235.

This species has consistently 4 chambers in the last whorl, which increase rapidly in size. This is an index species of the late middle Eocene in the studied sections.

Turborotalia cerroazulensis possagnoensis (Toumarkine and Bolli)

Globorotalia cerroazulensis possagnoensis Toumarkine and Bolli, 1970, p. 139-140, pl. 1, figs. 4-9.

Turborotalia cerroazulensis possagnoensis (Toumarkine and Bolli). Toumarkine and Luterbacher, 1985, p. 137, 13-15 in fig. 36.

The presence of 4 to 4 ½ chambers in the last whorl and a relatively high-arched, umbilical to extraumbilical aperture characterize this species.

Turborotalia griffinae Blow

Turborotalia griffinae Blow, 1979, p. 1072-1075, pl. 96, fig. 8.

This species is distinguished from *'Hastigerina'* cf. *bolivariana* by its more lobulated, loosely coiling mode.

Turborotalia wilsoni (Cole)

Globigerina wilsoni Cole, 1927, p. 34, pl. 4, figs. 8-9.

Turborotalia wilsoni (Cole). Toumarkine and Luterbacher, 1985, p. 126, 2-4 in fig. 27.

Toumarkine and Luterbacher (1985) discussed the phylogeny of this species and related forms. This group which has 4 globular chambers in the last whorl and a tendency to involute planispiral coiling contains such forms as *Globigerina wilsoni* Cole, *Globigerina wilsoni bolivariana* Petters, *'Hastigerina'* cf. *bolivariana* (Petters), *Pseudohastigerina globulosa* Hillebrandt, and *Turborotalia griffinae* Blow.

T. wilsoni illustrated by Toumarkine and Luterbacher (1985) has a more compact, less lobulately coiled test with a nearly circular equatorial outline and is slightly less involute on the spiral side than the holotype figures given by Cole (1927). The specimens observed in the studied sections are similar in morphology to illustrations of Toumarkine and Luterbacher (1985).

Zeauvigerina aegyptiaca Said and Kenawy (Figures 8-27—28)

Zeauvigerina aegyptiaca Said and Kenawy, 1956, p. 141, pl. 4, fig. 1; Beckmann, 1957, p. 92, pl. 21, figs. 9a-b, 11.

This species can be easily distinguished from other chiloguembelinids in having a long apertural neck at the terminal end of the last chamber. This species occurs only in the *Planorotalites pseudomenardii* Zone and

Morozovella velascoensis Zone (Beckmann, 1957).

Acknowledgments

The authors wish to express their sincere gratitude to Dr. M.M. Azab and Dr. M.H. El Dawy, of Department of Geology, Faculty of Science, El Minia University, for their assistance in collecting and preparing the examined samples. Our best thanks are extended to Prof. T. Saito of Department of Geoenvironmental Science, Faculty of Science, Tohoku University, and Prof. M.S.M. Ali of Department of Geology, Faculty of Science, El Minia University, for their kind help throughout the course of the present study. This study is largely based on part of the work carried forward by A.M.T. Elewa during his stay at Tohoku University as a visiting scientist, which was supported by a grant from the Egyptian Government (Channel System). The authors are deeply indebted to Mr. Jun Nemoto of Department of Geoenvironmental Science, Faculty of Science,Tohoku University, for printing photographs.

References

Abdel-Kireem, M.R., 1985: Planktonic foraminifera of Mokattam Formation (Eocene) of Gebel Mokattam, Cairo, Egypt. *Rev. Micropaléont.*, vol. 28, no. 2, p. 77-96, pls. 1-3.

——, Blondeau, A., and Shamah, K.M., 1985: Contribution à la stratigraphie du Paléogène de l'Oasis de Kharga (Égypte). l'apparition des premières nummulites en Égypte, leur évolution et leur implication biogéographique. *Rev. Micropaléont.*, vol. 28, no. 2, p. 97-102, pl. 1.

Anan, H.S., and Hamdan, A.R.A., 1993: Paleocene planktonic foraminifera of Jabal Malaqet, east of Al Ain, United Arab Emirates. *N. Jb. Geol. Paläont., Mh.*, vol. 1, p. 27-48, figs. 3-4.

Aubry, M.-P., Berggren, W.A., Kent, D.A., Flynn, J.J., Klitgord, K.D., Obradovich, J.D., and Prothero, D.R., 1988: Paleogene geochronology: An integrated approach. *Paleoceanography*, vol. 3, no. 6, p. 707-742.

Azab, M.M., 1984: *Biostratigraphy of the middle Eocene in Upper Egypt*. Ph. D. Thesis, Ain Shams Univ.

Bandy, O.L., 1949: Eocene and Oligocene foraminifera from Little Stave Creek, Clarke County, Alabama. *Bull. Amer. Paleont.*, vol. 32, no. 131, p. 1-211, pls. 1-27.

Beadnell, H.J., 1905: *The topography and geology of the Fayoum Province of Egypt*. 101 p., Surv. Dept. Egypt.

Beckmann, J.P., 1953: Die Foraminiferen der Oceanic Formation (Eocaen-Oligocaen) von Barbados, Kl. Antillen. *Eclogae geol. Helv.*, vol. 46, p. 301-412, pls. 16-30.

——, 1957: *Chiloguembelina* Loeblich and Tappan and related Foraminifera from the lower Tertiary of Trinidad, B.W.I. *U.S. Natn. Mus. Bull.* 215, p. 83-95, figs. 14-16, pl. 21.

——, El-Heiny, I., Kerdany, M.T., Said, R., and Viotti, C., 1969: Standard planktonic zones in Egypt. *In*, Brönnimann, P. and Renz, H.H. *eds., Proceedings of First International Conference on Planktonic Microfossilt, Geneva, 1967*, vol. 1, p. 92-103.

Benjamini, C., 1980: Planktonic foraminiferal biostratigraphy of the Avedat Group (Eocene) in the northern Negev, Israel. *Jour. Paleont.*, vol. 54, no. 2, p. 325-358, pls. 1-7.

Berggren, W.A. 1969a: Biostratigraphy and planktonic foraminiferal zonation of the Tertiary System of the Sirte Basin of Libya, north Africa. *In*, Brönnimann, P. and Renz, H.H. *eds., Proceedings of First International Conference on Planktonic Microfossils, Geneva, 1967*, vol. 1, p. 104-120.

——, 1969b: Rates of evolution in some Cenozoic planktonic Foraminifera. *Micropaleontology*, vol. 15, no. 3, p. 351-365.

——, 1969c: Cenozoic chronostratigraphy, planktonic foraminiferal zonation and the radiometric time scale. *Nature*, vol. 224, p. 1072-1075.

——, 1977: Atlas of Paleogene planktonic foraminifera, some species of the genera *Subbotina, Planorotalites, Morozovella, Acarinina* and *Truncorotaloides. In*, Ramsey, A.T.S. *ed., Oceanic Micropaleontology*, p. 205-299. Academic Press, London.

——, W.A., Olsson, R.K. and Reyment, R.A., 1967: Origin and development of the foraminiferal genus *Pseudohastigerina* Banner and Blow, 1959. *Micropaleontology*, vol. 13, no. 3, p. 265-288, figs. 1-12, pl. 1.

——, Kent, D.V. and Flynn, J.J. 1985: Paleogene geochronology and chronostratigraphy. *In*, Snelling N.J., *ed., The Chronology of the Geological Record*, p. 141-195. *Geological Society Mem.* 10.

—— and Miller, K.G., 1988: Paleogene tropical

planktonic foraminiferal biostratigraphy and magnetobiochronology. *Micropaleontology*, vol. 34, no. 4, p. 362-380.

Bermúdez, P.J., 1961 : Contribución al estudio de las Globigerinidea de la región Caribe-Antillana (Paleoceno-Reciente). *Bol. Geología (Venezuelana), Spec. Pub.* 3 (Cong. Geol. Venezolano, 3d., Caracas 1959, Mem. 3), p. 1119-1393, pls. 1-20.

Bishay, Y., 1966 : *Studies on the larger Foraminifera of the Eocene of the Nile Valley between Assiut, Cairo and S.W. Sinai*. Ph. D. Thesis, Alexandria Univ.

Blow, W.H., 1969 : Late Middle Eocene to Recent planktonic foraminiferal biostratigraphy. *In*, Brönnimann, P. and Renz, H.H. *eds., Proceedings of First International Conference on Planktonic Microfossils, Geneva, 1967*, vol. 1, p. 199-422, pls. 1-54.

——, 1979 : *The Cainozoic Globigerinida*. 3 vols., 1413 p., 264 pls. E.J. Brill, Leiden.

—— and Banner, F.T. 1962 : The Mid-Tertiary (Upper Eocene to Aquitanian) Globigerinaceae. *In*, Eames, F.E., Banner, F.T., Blow, W.H. and Clarke, W.J., *eds., Fundamentals of Mid-Tertiary Stratigraphical Correlation*, p. 61-151, pls. 8-17. Cambridge Univ. Press.

—— and Saito, T., 1968 : The morphology and taxonomy of *Globigerina mexicana* Cushman, 1925. *Micopaleontology*, vol. 14, no. 3, p. 357-360, figs. 1-4.

Boersma, A. and Premoli Silva, I. and Shackleton, N.J., 1987 : Atlantic Eocene planktonic foraminiferal paleohydrographic indicators and stable isotope paleoceanography. *Paleoceanography*, vol. 2, no. 3, p. 287-331.

Bolli, H.M., 1957a : The genera *Globigerina* and *Globorotalia* in the Paleocene-lower Eocene Lizard Springs Formation of Trinidad ; B.W.I. *U.S. Natn. Mus. Bull.* 215, p. 61-81, pls. 15-20.

——, 1957b : Planktonic Foraminifera from the Eocene Navet and San Fernando Formations of Trinidad, B.W.I. *Ibid.*, p. 155-172, pls. 35-39.

——, 1966 : Zonation of Cretaceous to Pliocene marine sediments based on planktonic Foraminifera. *Asoc. Venezolana Geología, Minería y Petróleo, Bol. Inf.*, vol. 9, p. 3-32.

——, 1972 : The genus *Globigerinatheka* Brönnimann. *Jour. Foram. Res.*, vol. 2, no. 3, p. 109-136, pls. 1-7.

——, Loeblich, A.R. and Tappan, H., 1957 : Planktonic foraminiferal families Hantkeninidae, Orbulinidae, Globorotaliidae, and Globotruncanidae. *U.S. Natn. Mus. Bull.* 215, p. 3-50, pls. 1-11.

—— and Cita, M.B., 1960 : *Globigerine* e *Globirotalie* del Paleocene di Paderno d'Adda (Italia) (1). *Riv. Ital. Paleont.*, vol. 66, no. 3, p. 1-43, pls. 31-33.

—— and Krasheninnikov, V.A. 1977 : Problems in Paleogene and Neogene correlations based on planktonic foraminifera. *Micropaleontology*, vol. 23, no. 4, p. 436-452.

Brönnimann, P., 1950 : The genus *Hantkenina* Cushman in Trinidad and Barbados, B.W.I. *Jour. Paleont.*, vol. 24, no. 4, p. 397-420, pls. 55-56.

——, 1952 : Trinidad Paleocene and lower Eocene Globigerinidae. *Bull. Amer. Paleont.*, vol. 34, no. 143, p. 1-43, pls. 1-3.

—— and Bermúdez, P.J., 1953 : *Truncorotaloides*, a new foraminiferal genus from the Eocene of Trinidad, B.W.I. *Jour. Paleont.*, vol. 27, no. 6, p. 817-820, pl. 87.

Cifelli, R.J., 1972 : The holotypes of *Puluvinulina crassata* var. *densa* Cushman and *Globigerina spinuloinflata* Bandy. *Jour. Foram. Res.*, vol. 2, no. 3, p. 157-159, figs. 1-2.

Cole, W.S., 1927 : A foraminiferal fauna from the Guayabal Formation in Mexico. *Bull. Amer. Paleont.*, vol. 14, no. 51, p. 1-46, pls. 1-5.

——, 1928 : A foraminiferal fauna the Chapapote Formation in Mexico. *Ibid.*, vol. 14, no. 53, p. 1-32, pls. 1-4.

Colom, G., 1954 : Estudio de las biozonas con foraminíferos del Terciario de Alicante. *España Inst. Geol. y Minero, Bol.*, vol. 66, p. 1-279, pls. 1-35.

Cushman, J.A., 1925a : A new genus of Eocene Foraminifera. *U.S. Natn. Mus. Proc.*, vol. 66, no. 2567, p. 1-4, pls. 1-2.

——, 1925b : New Foraminifera from the Upper Eocene of Mexico. *Contr. Cushman Lab. Foram. Res.*, vol. 1, pt. 1, p. 4-8, pl. 1.

——, 1925c : Some new Foraminifera from the Velasco Shale of Mexico. *Ibid.*, vol. 1, pt. 1, p. 18-23, pl. 3.

——, 1925d : An Eocene fauna from the Moctezuma River, Mexico. *Bull. Amer. Assoc. Petrol. Geol.*, vol. 9, p. 298-303, pls. 6-8.

——, 1927 : New and interesting Foraminifera from Mexico and Texas. *Contr. Cushman Lab. Foram. Res.*, vol. 3, pt. 2, p. 111-119, pls. 22-23.

——, 1940 : Midway Foraminifera from Alabama. *Ibid.*, vol. 16, pt. 3, p. 51-73, pls. 9-12.

—— and Bermúdez, P.J., 1949 : Some Cuban species of *Globorotalia*. *Ibid.*, vol. 25, pt. 2, p. 26-45, pls. 5-8.

—— and Jarvis, P.W., 1929 : New Foraminifera from Trinidad. *Ibid.*, vol. 5, pt. 1, p. 6-17, pls. 2-3.

—— and Ponton, G.M., 1932 : An Eocene foraminiferal fauna of Wilcox Age from Alabama. *Ibid.*, vol. 8, pts. 3 & 4, p. 51-72, pls. 7-9.

Elewa, A.M.T. and Ishizaki, K., (1994) : Ostracodes from Eocene rocks of the El Sheikh Fadl-Ras

Gharib stretch, the Eastern Desert, Egypt—Biostratigraphy and paleoenvironments—. *Earth Science* (*Chikyu Kagaku*), vol. 8, no. 1, p. 143-158.

El-Khayal, A.A., 1974: Planktonic foraminiferal biostratigraphy of the Lower Tertiary Hibr Strata of northwest Saudi Arabia. *Fac. Sci. Bull., Riyadh Univ., Saudi Arabia*, vol. 6, p. 174-194.

El Khoudary, R.H., 1977: *Truncorotaloides libyaensis*, a new planktonic foraminifer from Jabal Al Akhdar (Libya). *Rev. Esp. Micropaleont.*, vol. 9, no. 3, p. 327-336, pls. 1-2.

Finlay, H.J., 1939a: New Zealand Foraminifera; key species in stratigraphy, No. 2. *Trans. Roy. Soc. New Zealand*, vol. 69, p. 89-128, pls. 11-14.

——, 1939b: New Zealand Foraminifera; key species in stratigraphy, No. 3. *Ibid.*, vol. 69, p. 309-329, pls. 27-29.

Fleisher, R.L., 1974: Cenozoic planktonic Foraminifera and biostratigraphy, Arabian Sea; Deep Sea Drilling Project, Leg 23A. *In*, Whitmarsh, R.B., *et al., Initial Rept. DSDP*, vol. 23, p. 1001-1072, pls. 1-21. Government Printing Office, Washington.

Glaessner, M.F., 1937a: Planktonforaminiferen aus der Kreide und dem Eozän und ihre stratigraphische Bedeutung. *Pub. Lab. Paleont., Moscow Univ., Studies in Micropaleontology*, vol. 1, p. 27-46, pls. 1-2.

——, 1937b: Studien über Foraminiferen aus der Kreide und dem Tertiär des Kaukasus. *Pub. Lab. Paleont. Moscow Univ., Problems of Paleontology*, vols. 2-3, p. 349-410, pls. 1-5.

Gohrbandt, K.H.A., 1967: Some new planktonic foraminiferal species from the Austrian Eocene. *Micropaleontology*, vol. 13, no. 3, p. 319-326, pl. 1.

Gümbel, C.W., 1868: Beiträge zur Foraminiferenfauna der nordalpinen, älteren Eocängebilde order der Kressenberger Nummulitenschichten. *Bayerische Akad. Wiss. Abh., Math.-Physik. Kl.*, vol. 10, pt. 2, p. 579-730, pls. 1-4.

Haggag, M.A.Y., 1985: Middle Eocene planktonic foraminifera from Fayum area, Egypt. *Rev. Esp. Micropaleont.*, vol. 17, no. 1, p. 27-40, pl. 1.

——, 1986: Middle Eocene planktonic foraminifera from Beni Suef area. *Mid. East Res. Cent., Ain Shams Univ., Sc. Res. Ser.*, vol. 6, p. 59-80, pl. 1.

——, 1989a: Planktonic foraminiferal zonation and evolutionary groups of the middle Eocene in the Nile Valley, Egypt. *N. Jb. Geol. Paläont., Abh.*, vol. 178, p. 109-132, figs. 8-9.

——, 1989b: Evaluation of the planktonic foraminiferal groups around the middle/upper Eocene boundary in Egypt. *Mid. East Res. Cent., Ain Shams Univ., Earth Sc. Ser.*, vol. 3, p. 184-196, pl. 1.

——, 1991: *Globigerina pseudoampliapertura* Zone, a new Late Eocene planktonic foraminiferal zone (Fayoum area, Egypt). *N. Jb. Geol. Paläont., Mh.*, vol. 5, p. 295-307, fig. 5.

—— and Luterbacher, H., 1991: Middle Eocene planktonic foraminiferal groups and biostratigraphy of the Wadi Nukhul section, Sinai, Egypt. *Ibid*, vol. 6, p. 319-334, figs. 7-8.

Hang, H. and Lindenberg, H.G., 1969: Revision der von C.W. *Gümbel 1868 aus dem Eozän des bayerischen Alpenvorlandes beschriebenen planktonischen Foraminiferen. In*, Brönnimann, P. and Renz, H.H. *eds., Proceedings of First International Conference on Planktonic Microfossils, Geneva, 1967.*, vol. 1, p. 229-249, figs. 4-6, pl. 1.

Hillebrandt, A.V., 1976: Los foraminíferos planctonicos, nummulítidos y cocolitofóridos de la zona de *Globorotalia palmerae* del Cuisiense (Eoceno inferior) en el SE de España (Provincias de Murcia y Alicante). *Rev. Esp. Micropaleont.*, vol. 8, no. 3, p. 323-394, pls. 1-9.

Hornibrook, N. de B, 1958: New Zealand Upper Cretaceous and Tertiary foraminiferal zones and some overseas correlations. *Micopaleontology*, vol. 4, no. 1, p. 25-38, pl. 1.

Howe, H.V., 1939: Louisiana Cook Mountain Eocene Foraminifera. *Louisiana Dep. Cons., Geol. Surv. Bull.* 14, p. 1-122, pls. 1-14.

Jenkins, D.G., 1965: A re-examination of *Globorotalia collactea* Finlay, 1939. *N. Z. Jour. Geol. Geophys.*, vol. 8, p. 843-848, figs. 1-27.

——, 1971: New Zealand Cenozoic planktonic Foraminifera. *Geol. Surv. Paleont. Bull.* 42, p. 1-278 p. pls. 1-23.

Khalilov, D.M., 1956: O pelagicheskoi faune foraminifer paleogenovykh otlozhenii Azerbaydzhana. *Akad. Nauk Azerbaydzhan, SSR, Inst. Geol., Trudy*, vol. 17, p. 234-261, pls. 1-5. (*in Russian*)

Khalifa, H. and El-Sayed, G., 1984: Biostratigraphic zonation of the late Cretaceous-early Paleogene succession along El Sheikh Fadl-Ras Gharib road, Eastern Desert, Egypt. *Bull. Fac. Sci., Assiut Univ.*, vol. 13, no. 1, p. 175-190.

LeRoy, L.W., 1953: Biostratigraphy of the Maqfi section, Egypt. *Geol. Soc. Amer., Mem.* 54, p. 1-73, pls. 1-13.

Loeblich, Jr., A.R. and Tappan, H., 1957: Planktonic Foraminifera of Paleocene and early Eocene age from the Gulf and Atlantic coastal plains. *U.S. Natn. Mus. Bull.* 215, p. 173-198, pls. 40-64.

Luterbacher, 1964: Studies in some *Globorotalia* from the Paleocene and Lower Eocene of the central Apennines. *Eclogae geol. Helv.*, vol. 57, p. 631-730, figs. 1-132.

——, 1975: Planktonic foraminifera of the Paleocene and early Eocene, Possagno Section. *Schweizer-*

ische Paläont. Abh., vol. 97, p. 57-67, p. 164-171, pls. 1-4.

Nakkady, S.E., 1950: A new foraminiferal fauna from the Esna Shales and upper Cretaceous Chalk of Egypt. *Jour. Paleont.*, vol. 24, no. 6, p. 675-692, pls. 89-90.

——, 1951: Biostratigraphy of the Um Elghanayem sections, Egypt. *Micropaleontology*, vol. 5, no. 4, p. 453-472, pls. 1-7.

Palmer, D.K., 1934: The foraminiferal genus *Gümbelina* in the Tertiary of Cuba. *Mem. Soc. Cubana Hist. Nat.*, vol. 8, p. 73-76, figs. 1-6.

Petters, V., 1954: Tertiary and Upper Cretaceous foraminifera from Colombia, S.A.. *Contr. Cushman Lab. Foram. Res.*, vol. 5, pt. 1, p. 37-41, pl. 8.

Pijpers, P.J., 1933: Geology and Paleontology of Bonaire (D.W.I.). *Utrecht Univ. Geogr. Geol. Med. Phys.-Geol. Reeks*, no. 8, p. 1-103., pls. 1-2.

Plummer, H.J., 1926: Foraminifera of the Midway Formation in Texas. *Texas Univ. Bur. Econ. Geol. Bull.* 2644, p. 1-206. pls. 1-15.

Postuma, J.A., 1971: *Manual of planktonic Foraminifera*. 420 p. Elsevier Publ. Co., Amsterdam.

Premoli-Silva, I. and Boersma, A., 1988: Atlantic Eocene planktonic foraminiferal historical biogeography and paleohydrographic indices. *Palaeogeogr., Palaeoclimatol., Palaeoecol.*, vol. 67, p. 315-356.

Proto Decima, F. and Bolli, H.M.: 1970, Evolution and Variability of *Orbulinoides beckmanni* (Saito). *Ecologae geol. Helv.*, vol. 63, p. 883-905, figs. 1-51, pls. 1-4.

Rey, M., 1955: Description de quelques espèces nouvelles de foraminifères dans le Nummulitique nord-marocain. *Soc. Géol. France, Bull., ser. 6*, vol. 4, fasc 4-6, p. 209-211, pl. 12.

Said, R., 1960: Planktonic foraminifera from the Thebes Formation, Luxor, Egypt. *Micropaleontology*, vol. 6, no. 3, p. 277-286, pl. 1.

——, 1990: Cenozoic. *In* Said, R., *ed., The Geology of Egypt*, p. 451-486. A.A. Balkema Publishers, Netherlands.

—— and Kenawy, A., 1956: Upper Cretaceous and Lower Tertiary foraminifera from northern Sinai, Egypt. *Micropaleontology*, vol. 2, no. 2, p. 105-173, pls. 1-7.

—— and Kerdany, 1961: The geology and micropaleontology of the Farafra Oasis, Egypt. *Micropaleontology*, vol. 7, no. 3, p. 317-336, pls. 1-2.

—— and Sabry, H., 1964: Planktonic Foraminifera from the type locality of the Esna Shale in Egypt. *Micropaleontology*, vol. 10, no. 3, p. 375-395, pls. 1-3.

Saito, T. and Bé A.W.H., 1964: Planktonic Foraminifera from the American Oligocene. *Science*, vol. 145, no. 3633, p. 702-705, figs. 1-2.

Samanta, B.K., 1970: Middle Eocene planktonic Foraminifera from Lakhpat, Cutch, Western India. *Micropaleontology*, vol. 16, no. 2, p. 185-215, pls. 1-3.

Schwager, C., 1883: Die Foraminiferen aus den Eocaen-Ablagerungen der Lydischen Wüste und Ägyptens. *Palaeontographica*, vol. 30, p. 79-154, pls. 24-29.

Shahin, A., 1992: Contribution to the foraminiferal biostratigraphy and paleobathymetry of the late Cretaceous and early Tertiary in the western central Sinai, Egypt. *Rev. Micropaléont.*, vol. 35, no. 2, p. 157-175, pls. 1-2.

Shutskaya, E.K., 1958: Izmenchivosti nekotorikh nighnepaleogenovikh planktonnikh foraminifer severnogo Kavkaza. *Akad. Nauk SSSR, Voprosy Mikropaleont.*, vol. 2, p. 84-90, pls. 1-3. (*in Russian*)

Stainforth, R.M., Lamb, J.L., Luterbacher, H., Beard, J.H., and Jeffords, R.M., 1975: Cenozoic planktonic foraminiferal zonation and characterisics of index forms. *Univ. Kansas Paleont. Contr.*, Article 62, p. 1-425, figs. 1-213.

Subbotina, N.N., 1947: Foraminifery datskikh i paleogenovikh otlozhenii severnogo Kavkaza. *Vses. Neft. Nauchno-Issled. Geol.-Razved. Inst. (VNIGRI), Trudy*, p. 39-160, pls. 9. (*in Russian*)

——, 1953: *Iskopaemye foraminifery SSSR; Globigerinidae, Hantkeninidae, i Globorotaliidae. Ibid.*, no. 76, p. 1-296, pls. 40. (*in Russian*)

——, 1971: *Fossil foraminifera of the USSR; Globigerinidae, Hantkeninidae and Globorotaliidae*. 321 p., 40 pls. Collet's Ltd., London and Wellingborough. (Tanslated by E. Lees from Russian text of 1953)

Toulmin, L.D., 1941: Eocene smaller Foraminifera from the Salt Mountain Limestone of Alabama. *Jour. Paleont.*, vol. 15, no. 6, p. 567-611, pls. 78-82.

Toumarkine, M. and Bolli, H.M. 1970: Evolution de *Globorotalia cerroazulensis* (Cole) dans l'Eocène moyen et supérieur de Possagno (Italie). *Rev. Micropaleont.*, vol. 13, no. 3, p. 131-145, pls. 1-2.

—— and Luterbacher, H. 1985: Paleocene and Eocene planktonic foraminifera. *In*, Bolli, H.M., Saunders, J.B. and Perch-Nielsen, K., *eds., Plankton stratigraphy*, p. 87-154, figs. 1-42. Cambridge Univ. Press.

Weinzierl, L.L. and Applin, E.R., 1929: The Claiborne Formation on the coastal domes. *Jour. Paleont.*, vol. 3, no. 4, p. 384-410, pls. 42-44.

White, M.P., 1928: Some index Foraminifera of the Tampico Embayment area of Mexico. *Ibid.*, vol. 2, no. 3 and 4, p. 177-215, pls. 27-29 (pt. 1), p. 280-317, pls. 38-42 (pt. 2).

エジプト，イースタン・デザート地域の上部暁新統ー中部始新統浮遊性有孔虫化石層序：イースタン・デザート地域のスエズ湾からナイル川を横断する道路 (EL Sheikh Fadl road) 沿いには，石灰岩，泥灰岩，頁岩・砂岩からなる古第三系の地層群 (Esna, Thebes, Maghagha, Qarara, El Fashn 層) が露出している。これらの地層は浮遊性有孔虫化石を多産し，これらの化石をもとに *Planorotalites pseudomenardii, Acarinina aspensis, Globigerinatheka subconglobata, Morozovella lehneri, Truncorotaloides rohri* の 5 つの化石帯に区分することができる。これらの化石帯は P4 帯 (後期暁新世), P9-10 帯 (後期暁新世から最後期前期始新世), P11 帯下部 (前期中期始新世), P11 帯上部 (前期中期始新世), P12-14 帯 (後期中期始新世) にそれぞれ対比できるものと考えられる。したがって，Esna 層は後期暁新世，Thebes 層は後期暁新世から前期始新世の地質時代を示す。Maghagha 層と Qarara 層は，両者とも中期始新世で，同時異相関係にあることが明らかとなった。

西　弘嗣，A.M.T. Elewa，石崎国熙

Trans. Proc. Palaeont. Soc. Japan, N.S., No. 175, pp. 553-577, 23 Figs., September 30, 1994

975. DESMOSTYLIAN TOOTH REMAINS FROM THE MIOCENE TOKIGAWA GROUP AT KUZUBUKURO, SAITAMA, JAPAN*

KENSHU SHIMADA

Department of Geosciences, Fort Hays State University,
Hays, Kansas 67601, U.S.A.

and

NORIHISA INUZUKA

Department of Anatomy, Faculty of Medicine,
University of Tokyo, Tokyo, 113 Japan

Abstract. Fifteen isolated desmostylian teeth from the Godo Conglomerate Member of the lower part of the Miocene Tokigawa Group at Kuzubukuro, Higashi-Matsuyama City, Saitama Prefecture, are described in detail. The fossils belong to two genera, *Paleoparadoxia* and *Desmostylus*. Twelve teeth belong to *Paleoparadoxia*, of which five are confidently identified as *P. tabatai*. *Paleoparadoxia* teeth include the upper canine, M1, M2, and M3, and lower P3 and M3. Three *Desmostylus* specimens include a milk canine ? and fragments of cheek teeth. The significance of the Kuzubukuro specimens is that both genera occur together in the same stratigraphic unit, although the possibility of one or both being reworked cannot be discarded. Because a number of shark species and some other marine mammals, such as pinnipeds and cetaceans, occur in the Godo Conglomerate as well, the locality is important for reconstructing the paleoecology of the desmostylians.

Key words. *Desmostylus*, Japan, Kuzubukuro, Miocene, *Paleoparadoxia*, teeth, Tokigawa Group.

Introduction

The lower part of the Miocene Tokigawa Group (Koike *et al.*, 1985) at Kuzubukuro in Saitama Prefecture is known for its abundant shark teeth. Horiguchi (1975 *ed.*, 1987 *ed.*) introduced the site in his geological guidebook, in which he encouraged people to collect the numerous shark teeth. Collectors also unearthed marine mammals, such as cetaceans and pinnipeds. However, the site is most significant for the occurrence of desmostylian teeth. Many have been collected by members of the Kuzubukuro Geology Club, a regional group consisting of amateur fossil and mineral enthusiasts. Nearly 20 desmostylian teeth have been recovered from a 16 m × 60 m area. Nowhere else in Japan has such a large number of isolated desmostylian teeth been collected. However, none of the teeth have been formally described (Inuzuka, 1984, table 2). In the summer of 1990, we were given an opportunity to study 15 of the desmostylian teeth from Kuzubukuro. The fossils belong to two genera, *Paleoparadoxia* and *Desmostylus*. The primary purpose of this paper is to describe these

*Received June 16, 1993; revised manuscript accepted May 20, 1994

previously unreported specimens in order to add to the available information on these animals.

Geographical and geological settings

Kuzubukuro lies between the Tokigawa and Oppegawa rivers, two tributaries of the Arakawa River, in the northeast part of the Iwadono Hills of Higashi-Matsuyama City, Saitama Prefecture, central Japan (Figure 1). The Iwadono Hills are located in a structural basin. Here the lower part of the Iwadono Formation of the Miocene Tokigawa Group is exposed. The Iwadono Formation is divided into three fining-upward members: Godo Conglomerate, Negishi Sandstone, and Shogunzawa Siltstone members (Koike *et al.*, 1985) (Figure 2). The fossils described here-

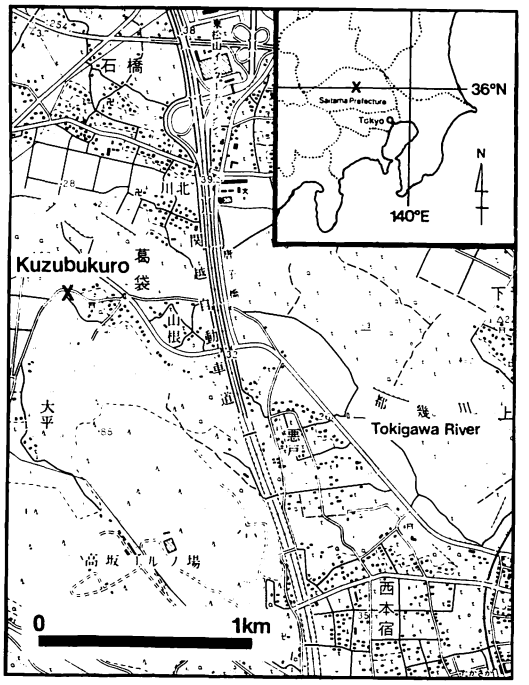

Figure 1. Locality map showing the position of Kuzubukuro (fossil site indicated by X), Higashi-Matsuyama City, Saitama Prefecture, Japan. Modified from the 1 : 25,000 "Higashi-Matsuyama" topographical map issued by the Geographical Survey Institute of Japan.

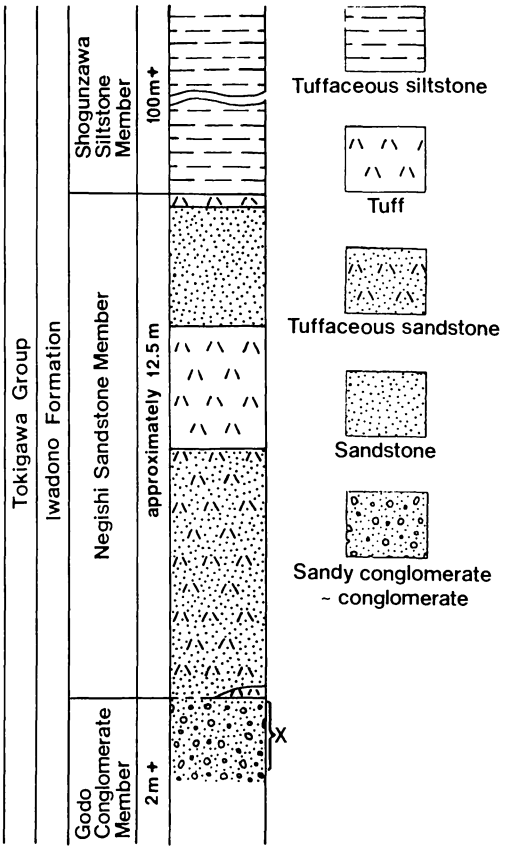

Figure 2. Generalized geologic column of the Tokigawa Group at Kuzubukuro based on Koike and Takei (pers. comm., 1990). The stratigraphic range of the desmostylians described in this paper is shown by X.

in occurred in the Godo Conglomerate. We follow the stratigraphic nomenclature of Koike *et al.* (1985) because of their intensive geological study of the Iwadono Hills. However, other names and combinations have been applied by others who have investigated the area. One scheme is that of Matsumaru and Hayashi (1980) who consider the Kamagata Formation equivalent to the Godo Conglomerate. Majima (1989) lumped the Godo Conglomerate and Negishi Sandstone as the Goudo [=Godo] Formation.

The fossil site is located on land owned by the Nihon Cement Co., Ltd. managed by the

Chichibu Mining Co., Ltd. The mining company has removed the massive tuffaceous siltstone beds of the Shogunzawa Siltstone and part of the underlying Negishi Sandstone. This removal has enabled fossil collectors to reach the Godo Conglomerate. An approximate area of 16 m × 60 m has been quarried in the Godo Conglomerate, to a maximum

Table 1. Supplemental information on desmostylian fossils from Kuzubukuro.

Specimen	Species	Tooth Identification	Measurement (mm)			Number of cusps	ac.c.	tub.	Depth (cm)*	Discovered Date	Discoverer/ Repository
KZD01	*P.t.*	Left upper M2	m-d 26.4	b-l 21.6	c.h. 9.5+	5	3	3	?	Octorber 11, 1981	Minakami, Kazuhiko
KZD02	*P.t.*	Right upper M2	m-d 27.6	b-l 22.2	c.h. 13.9	5	4	2	50	January 8, 1984	Okabe, Isamu
KZD03	*P.t.*	Fragment of a M2 or M3	A-B 20.7+	e-i 11.0+	o-r 16.0+	1+	?	2+	?	February 1984	Honma, Shin-ichi
KZD04	*P.*sp.	Fragmentary column of a cheek tooth	A-B 12.1+	e-i 6.1+	o-r 14.4+	1+	?	?	10	March 1986	Shinkawa, Satoru***
KZD05	*D.*sp.	Fragmentary column of a molar	A-B 15.4+	e-i 9.8+	o-r 24.2+	1+	?	?	?	July 21, 1986	Shinkawa, Satoru***
KZD06	*P.*sp.	Right lower P3	m-d 12.5	b-l 9.0	c.h. 10.6	2	0	0	100	November 1986	Shinkawa, Satoru***
KZD07	*P.t.*?	Right upper M1?	m-d 25.0	b-l 20.4	c.h. 11.3	4	1	3	50	November 16, 1986	Yabe, Hideo
KZD08	*P.*sp.	Column of a cheek tooth	A-B 13.0+	e-i 9.5+	o-r 14.5+	1+	?	?	30	January 15, 1988	Takeda, Shoji
KZD09	*P.t.*?	Right upper canine	m-d 19.9+	b-l 17.0+	o-r 31.4+	1			?	March 12, 1988	Okabe, Isamu
KZD10	*P.t.*?	Left lower M3	m-d 32.9	b-l 22.0	c.h.** 15.5	6	0	1	50	April 10, 1988	Yoshioka, Keisuke
KZD11	*P.t.*	Left upper canine	m-d 13.4+	b-l 11.8+	o-r 18.2+	1			?	August 7, 1988	Yabe, Hideo
KZD12	*D.*sp.	Column of a left lower molar	m-d 18.9+	b-l 18.8+	o-r 49.0+	1+	?	?	30	December 28, 1988	Ohtsu, Shin-ichi
KZD13	*P.t.*	Partial right upper M2	m-d 15.3+	b-l 22.2+	c.h. 9.1	2+	2+	?	30	April? 1989	Nakamura, Toyoki
KZD14	*P.t.*?	Right upper M3	m-d 27.3	b-l 24.3+	c.h. 14.0	4	2	3+	?	September 28, 1989	Ohtsu, Shin-ichi
KZD15	*D.*?	Milk canine?	m-d 7.9+	A-B 8.1	o-r 16.4	1			180	May 5, 1990	Fujii, Koji

* The values represent the depth from the Godo Conglomerate-Negishi Sandstone contact.
** The height of the crown is measured on the buccal side of the column in the second row.
*** Satoru Shinkawa passed away in late February of 1992.

depth of 2 m. The contact between the Godo Conglomerate and the Negishi Sandstone at Kuzubukuro varies from gradational to sharp. The Godo Conglomerate dips between 7 and 10 degrees to the southwest at the site. The member consists of many conglomeratic and sandy-conglomeratic layers that are occasionally bedded. Some small-scale faults are evident, but no detailed lithologic or structural study of the unit has been conducted at Kuzubukuro. The Godo Conglomerate contains well-rounded pebbles of felsic tuff, that range up to 15 cm in diameter, and pebbles of crystalline schist, quartz diorite, gneiss, and hornfels (Koike *et al.*, 1985) that generally range from 1 to 5 cm in size with a wide range in roundness. Koike *et al.* (1985) stated that the Godo Conglomerate had source areas from the west and north, based on the lithology of the clasts. The desmostylian teeth were recovered directly from the conglomerate at levels ranging from about 10 cm below the top to as deep as 180 cm (Table 1 and Figure 2).

The geologic age of the units in the Iwadono Hills is generally determined by biostratigraphic studies of invertebrate fossils. Koike *et al.* (1985) considered the age of the Iwadono Formation as Middle Miocene, although Matsumaru and Hayashi (1980) gave a range from late Early to late Middle Miocene. Matsumaru *et al.* (1982) stated that their Kamagata Formation should be placed in the lowest part of Blow's N9 planktonic foraminiferal zone. Majima (1989) considered his Goudo Formation to be late Early to the earliest Middle Miocene. Koike *et al.* (1985) stated that the Godo Conglomerate and the lower part of the Shogunzawa Siltstone seems to correspond to Blow's zones N9-N13.

The most common fossils in the Godo Conglomerate are shark teeth. Teleostean teeth and mammalian fossils, including teeth and ear bones of cetaceans and teeth of pinnipeds and desmostylians, have also been found. Kohno and Hasegawa (1991) recently described a tooth of an imagotariine pinniped that was found from the basal part of Majima's Goudo Formation near Kuzubukuro. The Godo Conglomerate also contains some foraminifers, but other invertebrates are extremely rare. Most of the fossils are strongly abraded, and the roots of the teeth are generally not preserved, which indicates a high depositional energy.

Materials and methods

A. Materials

Fifteen desmostylian teeth are described herein. Twelve specimens are considered to be *Paleoparadoxia* and three *Desmostylus*. The specimens are numbered as KZD01, KZD02, KZD03, and so on, with KZ representing Kuzubukuro, D the Desmostylia, and the number the chronological order of discovery. Table 1 lists supplemental information on all the teeth.

B. Methods

The neotype of *Paleoparadoxia tabatai* (Tokunaga) was used to determine the species and the tooth class of the samples. The neotype is a nearly complete skeleton found in the Miocene Yamanouchi Formation at Inkyoyama, Izumi-machi, Toki City, Gifu Prefecture. It is often referred to as the Izumi specimen and is housed in the National Science Museum, Tokyo, Japan. The skull and its dentition were studied by Ijiri and Kamei (1961). Clark (1991) recently described a new species, *P. weltoni*, that was discovered from California; however, we think that none of the Kuzubukuro specimens belong to *P. weltoni* as discussed later. Measurements of six paleoparadoxian cheek teeth from Kuzubukuro are compared with described specimens from other localities in Tables 2, 3, and 4.

Inuzuka (1986) proposed the dental formula of *Paleoparadoxia* as 3/3, 1/1, 3/3, 3/3 in which both upper and lower P1s are not present. We follow the convention estab-

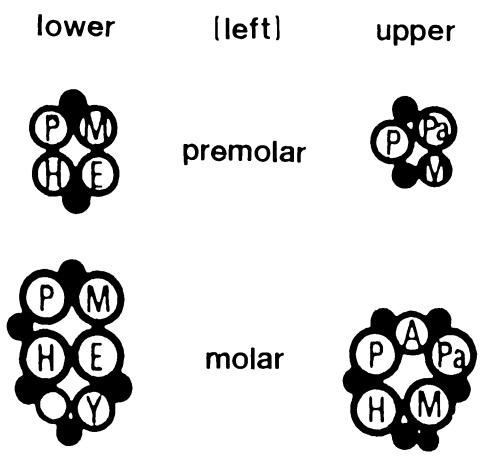

Figure 3. Schematic diagram showing the cusp arrangements of paleoparadoxian cheek teeth in left upper and lower premolars and molars (after Inuzuka, 1987). P, protocone or protoconid; M, metacone or metaconid; Pa, paracone; A, anterior talon; H, hypocone or hypoconid; E, entoconid; Y, posterior talonid. An open circle without identification of cusp represents the generalized position of an accessory cusp. Solid black circles represent generalized positions of tubercles.

lished by Inuzuka (1987) for cusp designations and other purposes to describe paleoparadoxian teeth (Fig. 3). For some specimens (KZD03, KZD04, KZD05, KZD08, and KZD15) in which the tooth class is not securely determined, directional properties of teeth are used.

We describe the specimens in detail, because: 1) only limited information on desmostylian teeth has been published; and 2) each of the specimens described here has unique features. Because many paleoparadoxian cheek teeth are described herein, some general identification keys which we used should be noted. Reinhart (1959, p. 102) reported the characters of the cheek teeth of *Paleoparadoxia* as: having a wide cingulum, that is heavily tuberculated with vertical ridges, completely encircling the cheek teeth that reaches approximately two-thirds up side of crown; cheek teeth of closely appressed cylindrical columns; distinct tendency toward polydonty; a central nipple-like protuberance of enamel moat on the occlusal surface of unworn cheek teeth, with the moat being surrounded by an upraised ring of enamel; and the primary cusps of unworn teeth being higher and of greater diameter than other columns. In order to contrast the cheek teeth of *Paleoparadoxia* from *Desmostylus*, he described the cheek teeth of *Desmostylus* as hypsodont. Reinhart (1959, p. 102) also stated that the paleoparadoxian cheek teeth consist of three transverse rows, two columns per row, but the observation was based only on two specimens of M_3s. Mitchell and Repenning (1963) generalized the paleoparadoxian cheek teeth by stating that the columns "may or may not be appressed, polygonal or circular in cross section, cingulum may be present and may surround entire tooth, enamel base swollen, column height forms about half of crown height." We do not use their character, "enamel base swollen," due to its ambiguity.

Different authors use different criteria to distinguish the tooth features. We define some of the terms below to reduce ambiguities in such criteria.

Cusp: part of crown that forms a polygonal or circular column regardless of height and has a small conical projection on its occlusal surface if unworn or an enamel opening if worn.

Accessory cusp: part of crown that forms an incomplete column or rudimentary cusp and has a projection, depression, or enamel opening on its occlusal surface.

Tubercle: part of crown that forms an incomplete column or rudimentary cusp, with no projection, depression, or enamel opening on its occlusal surface.

Cingulum: an enlargement of enamel on lateral surface of crown.

As Inuzuka and Murai (1980) noted, all of these features are transitional, and often no clear-cut distinction can be made. Thus, we occasionally use some transitional terms, such as tuberclelike accessory cusp and tuberculated cingulum. In addition, we distinguish

between the cervical line and crown base, wherein the former represents an original line, and the latter describes the basalmost part of enamel that shows any kind of damage.

C. Abbreviations

The following abbreviations are used in the tables : *P.t.* = *Paleoparadoxia tabatai* ; *P.t.?* = *Paleoparadoxia ? tabatai* ; *P.w.* = *Paleoparadoxia weltoni* ; *P.* = *Paleoparadoxia* ; *D.* = *Desmostylus* ; m-d = mesiodistal diameter ; b-l = buccolingual diameter ; A-B = A-B direction ; e-i = exterior-interior direction ; o-r = vertical direction ; c.h. = crown height (on the buccal side) ; ac.c. = accessory cusps ; tub. = tubercles ; UCMP = University of California, Museum of Paleontology ; LACM = Natural History Museum of Los Angeles County.

The following abbreviations are used in the figures : m = mesial side ; d = distal side ; b = buccal side ; l = lingual side ; e = exterior side ; i = interior side ; A = side A ; B = side B ; pr = protocone ; me = metacone ; hy = hypocone ; pa = paracone ; ant. ta = anterior talon ; prd = protoconid ; med = metaconid ; hyd = hypoconid ; end = entoconid ; post. tad = posterior talonid.

Systematic paleontology

Domning *et al.* (1986) and Clark (1991) discussed the problems with the family-level taxonomy of the Desmostylia. However, we use the traditional systematics in this paper, because the taxonomy is not our main focus.

Class Mammalia Linnaeus, 1758
Order Desmostylia Reinhart, 1953
Family Paleoparadoxidae Reinhart, 1959
Genus *Paleoparadoxia* Reinhart, 1959
***Paleoparadoxia tabatai* (Tokunaga, 1939)**

Specimen.—KZD11 (Figs. 4, 19-2).

Diagnosis.—KZD11 is half of the crown of an upper canine. The identification is based on the morphological resemblance between

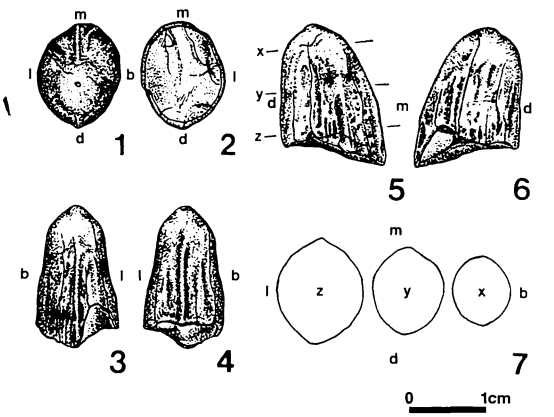

Figure 4. KZD11 : left upper canine of *Paleoparadoxia tabatai*. 1, occlusal surface ; 2, basal surface ; 3, mesial surface ; 4, distal surface ; 5, buccal surface ; 6, lingual surface ; 7, cross-sectional views taken at the position of x, y, and z in 5.

the specimen and the upper canines of the Izumi specimen, particularly the presence of the peculiar crestal pit on the occlusal end of the more or less conical-shaped crown. The side determination is based on the cross-sectional shape of the crown. Because the canine is appressed against the maxilla in the Izumi specimen, the lingual side is flatter than the buccal. Therefore, KZD11 is a left upper canine of *P. tabatai* with the basal half of the crown not preserved.

Description.—The cross sections of KZD11 demonstrate that the rounded mesial and distal margins near the occlusal end of the crown become distinctive toward the basal end. The crestal pit (0.7 mm in diameter and 0.4 mm in depth) is present near the center of the smooth occlusal end of the crown. All other enamel surfaces exhibit a rough texture consisting of many short, shallow grooves, parallel to the long axis of the tooth. A few pits the size of a needle point are distributed throughout the buccal enamel surface. In the buccal and lingual views, the mesial margin gently curves outward, and the distal margin makes a rounded corner near the crest of the crown and extends nearly straight toward the basal end. In mesial and distal

views, both buccal and lingual sides are almost symmetrical, pinching in towards the middle. The enamel at the crown base is 0.7 to 1.0 mm in thickness. The dentine has been rounded due to depositional processes. The pulp cavity is not seen on the dentine surface.

Specimen.—KZD01 (Figures 5, 21-2).

Diagnosis.—KZD01 preserves a nearly complete, unworn(?) crown with no root system. The M^2 and M^3 of the Izumi specimen have a diagnostically enlarged protocone; however, the M^2 and M^3 can be distinguished, because the M^2 has a more distorted oval outline than the M^3 in occlusal view. The location of the protocone, arrangement of other major cusps and tubercles (Figure 3) as well as the shape of the crown in occlusal view indicate that KZD01 is a left M^2. The close resemblance with the Izumi specimen suggests that KZD01 is *P. tabatai*.

Description.—The buccal surface has a tuberculated cingulum, whereas the other lateral surfaces of the crown are smooth and slightly swollen. In occlusal view, the tooth is a distorted oval formed by the rounded lingual and relatively straight buccal sides with a mesiobuccal corner. The protocone is 9.4 mm in height and strongly tilts toward the buccal side. The circular occlusal surface of the protocone, which strongly slants buccally, is 7 mm in diameter, and has a rough surface and a slight central rise with an ambiguous crestal pit. Accessory cusps exist at the mesial and distal base of the protocone. The mesial one (*i.e.*, the lingual anterior talon) has an oval depression on the top; whereas the distal one has a rounded surface with a small crestal pit. The distal end of the intermediate anterior talon fits against the protocone, forming a crescent-shaped outline. The buccal anterior talon is a tubercle, and the paracone is an accessory cusp with a circular depression. The metacone, hypocone, and a distal cusp (probably a well-developed posterior talon), are closely gathered. All three cusps and the intermediate anterior talon range from 6 to 7 mm in diameter and have a nipplelike rise with a crestal pit at their centers. The rise is especially prominent on the metacone. Tubercles alternate with the paracone, metacone, and distal cusp along the buccal side. Because the enamel is partially weathered, evidence of attrition is uncertain. The thickness of the enamel at the crown base ranges from 1 to 2 mm, and it appears to be broken, perhaps due to depositional processes. Dentine is exposed on the basal surface with some depressions corresponding to the positions of the major cusps on the occlusal side. Enamel is exposed near the center of the basal surface representing the contact between protocone, paracone, metacone, and hypocone.

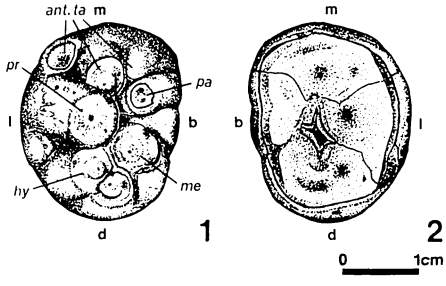

Figure 5. KZD01: left M^2 of *Paleoparadoxia tabatai*. 1, occlusal surface; 2, basal surface.

Specimen.—KZD02 (Figures 6, 21-3).

Diagnosis.—KZD02 preserves a worn crown with a partial root. It is a right M^2 of *P. tabatai*, identified in the same way as KZD01.

Description.—The oval-shaped crown has a lightly protruding mesiobuccal edge in occlusal view. A depression exists at the center of the flatly worn tooth, where the protocone, intermediate anterior talon, paracone, and metacone meet. From this meeting point, the diameter of the protocone is about 10 mm, and that of the intermediate anterior talon and paracone about 8.5 mm. The lingual

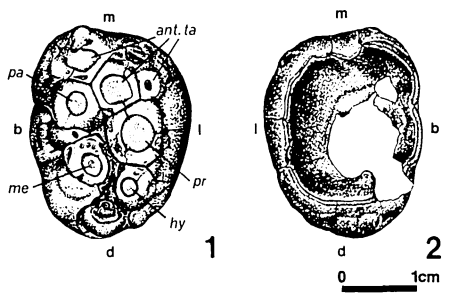

Figure 6. KZD02: right M^2 of *Paleoparadoxia tabatai*. 1, occlusal surface; 2, basal surface. White spaces represent damaged surfaces and portions still covered by sediments and fresh breaks.

anterior talon is a small accessory cusp and the buccal anterior talon is a large accessory cusp; both have dentine exposed at their centers. A small accessory cusp is wedged between the paracone and metacone on the buccal side. The metacone and hypocone are about 6.5 mm in buccolingual diameter. All cusps have a circular or oval exposure of dentine. An unworn, fan-shaped accessory cusp, probably the posterior talon, exists at the slightly swollen distalmost edge of the crown, and it has a conical protuberance with a small crestal pit. A large, flat, worn tubercle sits on the buccodistal corner, and a small worn tubercle is located on the lingual side between the protocone and hypocone. Each major dentine exposure on the occlusal surface shows a faint, flat rise at the center. The width of the enamel surrounding these dentine exposures ranges from 1.9 to 3.3 mm. The crown has a straight mesial side and a swollen distal side in buccal and lingual views. The lingual crown surface shows a gently swollen, wide, smooth cingulum with a small fossa in the middle of the mesial side. Many short, faint grooves run vertically on the basal half of the crown, and the crown forms a tuberculated cingulum on the buccal and distal sides. The cervical line at the center of the crown is horizontal but slopes occlusally at the mesial and basally at the distal ends. A smooth, incomplete root stretches basally. The cervical line outlines a rough square on the basal surface. The incomplete root is smoothly rounded because of abrasion during deposition. The internal root structure is unobservable due to the adhered sediments, but it seems to be single rooted.

Specimen.—KZD13 (Figures 7, 21-4).

Diagnosis.—KZD13 is a distal half of a highly worn crown with no root. Because of the way in which the mesial end of KZD13 is broken, it appears that a large protocone was originally appressed on the mesial side, with perhaps one or more smaller cusps at its side. Assuming that the large missing cusp is a protocone, KZD13 is identified as a partial right M^2 of *P. tabatai*.

Description.—Although the mesial half is missing, the buccal side of the specimen, which forms a cingulum, is slightly better preserved than the lingual side. A tubercle-like accessory cusp is located at the mesiobuccal corner and exhibits a shallow, faint depression. A cingulum occupies the buccodistal corner of the crown. The metacone looks like a distorted pentagon and is about 7.5 mm in both mesiodistal and buccolingual diameters. The hypocone forms a trapezoid about 8.0 mm in mesiodistal diameter and 7.0 mm in buccolingual diameter. Both the metacone and hypocone have a distorted circular patch of dentine exposed at the center. An accessory cusp contacts the distal side of both cusps. The mesiodistal and

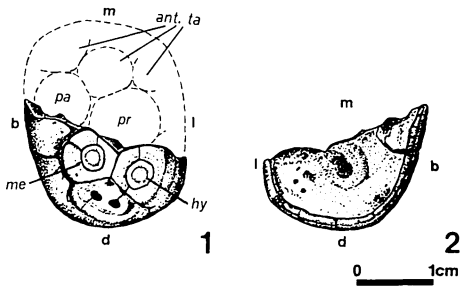

Figure 7. KZD13: partial right M^2 of *Paleoparadoxia tabatai*. 1, occlusal surface; 2, basal surface.

buccolingual diameters of the accessory cusp are about 6 mm and 10 mm, respectively. This accessory cusp seems to be composed of two fused accessory cusps as two small oval enamel openings exist side by side. The broken mesial surface reveals the internal tooth structure of both enamel and dentine in which the basalmost part of the enamel curves in an occlusal direction capping the dentine at the hypocone, metacone, and tuberclelike accessory cusp. The attritional surface declines buccally. A short, lingually declined fissure on the distal surface shows the inclination of the hypocone. The distal crown surface is partly coarse in texture, and a faint groove runs relatively horizontally near the cervical line. Enamel about 1 mm thick surrounds the dentine on the basal surface, except on the broken mesial side. Whether the cervical line has been damaged is not clear. The dentine is apparently polished through depositional processes. A large and a small depression, perhaps pulp cavities, are seen on the dentine surface.

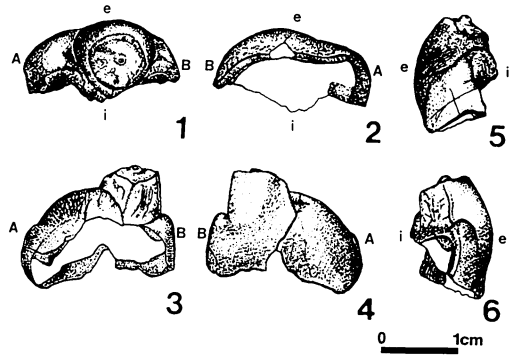

Figure 8. KZD03 : fragment of a M2 or M3 of *Paleoparadoxia tabatai*. 1, occlusal surface ; 2, basal surface ; 3, interior surface ; 4, exterior surface ; 5, side A ; 6, side B. White spaces represent portions still covered by sediments and fresh breaks.

Specimen.—KZD03 (Figure 8).

Diagnosis.—KZD03 is probably a part of either an upper or lower second or third molar of *P. tabatai* when compared to the size of the Izumi molars. The weak cingulum suggests that this specimen may represent the lingual side of a molar, as this tendency is observed in the cheek teeth of the

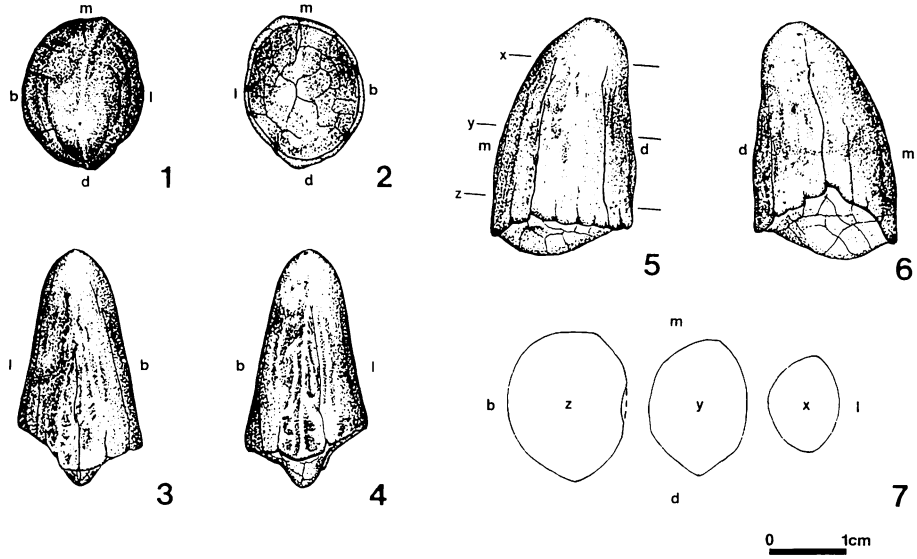

Figure 9. KZD09 : right upper canine of *Paleoparadoxia ?tabatai*. 1, occlusal surface ; 2, basal surface ; 3, mesial surface ; 4, distal surface ; 5, buccal surface ; 6, lingual surface ; 7, cross-sectional views taken at the position of x, y, and z in 5.

Izumi specimen. The declination, relative size, and the arrangement of the cusps indicate that the columnar cusp may be the hypocone of a right upper molar. However, because the columnar cusp is relatively large in height and diameter, it may be the protocone of a left upper molar. Therefore, KZD03 is identified as a fragment of a M2 or M3 of *P. tabatai*.

Description.—KZD03 consists of an unworn cusp, a large tubercle, and a small tubercle. A small nipplelike conical protuberance with a crestal pit exists at the center of a rough, circular occlusal surface on the cusp. The cusp is about 7.5 to 8.0 mm in diameter.

Paleoparadoxia ?tabatai

Specimen.—KZD09 (Figures 9, 19-1).

Diagnosis.—KZD09 is half of the crown of an upper canine, because it more or less resembles the upper canines of the Izumi specimen and KZD11, and has the crestal pit. Although KZD09 is much larger than the Izumi upper canine and KZD11, it is not an incisor, because incisors tend to have a flat, shovellike crown. The size difference between the two specimens may represent sexual dimorphism. KZD09 and KZD11 preserve about the same portion of the canine, but KZD09 is 75 to 80 percent larger than KZD11. A similar ratio was obtained by Hirota (1981) in his study of mandibles of *P. tabatai*. He explained the size differences as sexual dimorphism, with the larger form being male. We tentatively assign KZD09 as *P. ?tabatai*, because the identification is rather tenuous. The cross-sectional shape of the crown suggests that the tooth is a right upper canine.

Description.—The cross sections of KZD09 suggest that the buccal side curves more than the lingual side as the basal end is approached. A smooth, round area surrounds the crestal pit. The pit is 0.3 mm in diameter. The distal margin is somewhat sharper than the mesial margin. The mesial margin forms a gentle arc, whereas the distal margin is rather straight when viewed in the buccolingual direction. The lateral enamel surfaces exhibit many faint ridges and grooves that are parallel to the long axis of the tooth. Two very shallow and wide depressions trend in a mesiodistal direction on the lingual surface. The dentine is rounded due to abrasion during deposition, and no pulp cavity is seen. The thickness of the enamel at the crown base is about 0.7 mm at the buccal and lingual sides, and 1.0 mm and 1.2 mm at the mesial and distal margins, respectively.

Specimen.—KZD07 (Figures 10, 21-1)

Diagnosis.—KZD07 is a nearly complete, moderately worn right M^1 ? identified as *P. ?tabatai*. However, as both M^1s in the Izumi specimen are badly worn and no morphological description of an M^1 has been presented, our identification is made by the process of elimination. KZD07 cannot be a premolar because of its much larger crown size. It is a little small to be a M2 or M3 although the outline of the crown and cusp arrangement in KZD07 closely resembles the right M^2 and M^3 of the Izumi specimen. However, KZD07 has a simpler occlusal pattern than the M^2 but is more complex than P^4 in the Izumi specimen. In addition, KZD07 could not fit into the alveolar space for the M_1 in the Izumi specimen but could fit reasonably into the space of the M^1. However, uncertainty remains in the taxonomic

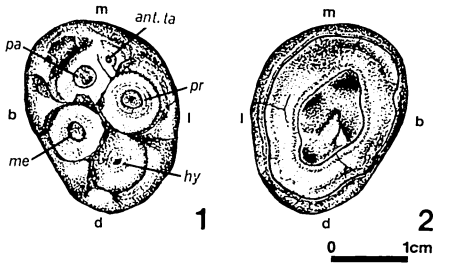

Figure 10. KZD07: right M^1? of *Paleoparadoxia ?tabatai*. 1, occlusal surface; 2, basal surface.

and dental assignments. We also note that a sketch of a cheek tooth (UCMP 45274) identified as *Paleoparadoxia* sp. by Mitchell and Repenning (1963) appears to be similar to KZD07 in size, shape, and arrangement of cusps. Thus, UCMP 45274 may be a right M^1 as well.

Description.—In occlusal view, the tooth has an oval outline in which the mesiobuccal corner protrudes. The columnar protocone is about 9.0 mm in height and 9.0 mm in diameter. The protocone strongly tilts buccally, and its attrition surface slants buccally. The anterior talon is a triangular accessory cusp, and the paracone is a distored oval cusp. Their buccolingual diameters measured on the attrition surface are 3.1 mm and 7.4 mm, respectively. Their mesiodistal diameters, however, are unmeasurable due to the lack of clear mesial margins. The mesiobuccal and buccal sides of the paracone and the mesial side of the anterior talon exhibit a roughly textured, depressed area on the enamel surface. The metacone and hypocone are about 7.5 mm in diameter. All cusps and the anterior talon have an oval-shaped dentine exposure at their centers. There is one tubercle mesial and two tubercles distal to the metacone. The enamel at the crown base is 1.2 mm in thickness. The root shortly extends basally, and a pulp cavity is present. Four depressions that appear to correspond to the positions of the major cusps on the occlusal side are observed within the pulp cavity.

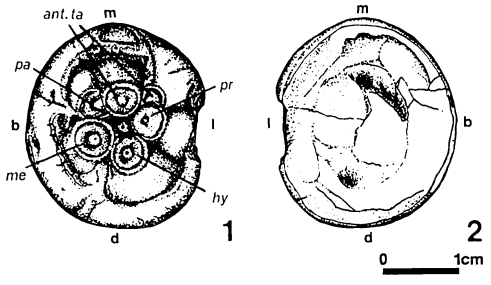

Figure 11. KZD14: right M^3 of *Paleoparadoxia ?tabatai*. 1, occlusal surface; 2, basal surface. White spaces represent portions with fresh breaks.

Specimen.—KZD14 (Figures 11, 22-1).

Diagnosis.—The cingula on the Izumi molars are generally well developed on the buccal side. There is a greater development of the cingulum on one side of KZD14; therefore, we consider this side to be buccal. KZD14 is a right upper molar based on similar lengths of the mesiodistal and buccolingual diameters of the crown and its cusp arrangement (Figure 3). Comparison of the crown size of KZD14 with the right upper molars of the Izumi specimen suggests that KZD14 is either a right M^2 or M^3, and is more likely to be the latter because of its less distorted oval outline in occlusal view. However, since the Izumi M^3s exhibit much taller cusps and less development of the cingulum, KZD14 is considered to be a right M^3 of *P. ?tabatai*.

Description.—The dome-shaped crown consists of four major and two accessory cusps surrounded by a highly developed cingulum. All the tops of the major and accessory cusps are at an equal elevation. Each major and accessory cusp has a conical protuberance, with some exhibiting a crestal pit. The occlusal surfaces of all major and accessory cusps decline toward the center of the crown, forming a gap between them. A conical protuberance with a crestal pit is seen in the gap. The intermediate anterior talon, protocone, metacone, and hypocone have a circular to oval occlusal surface that ranges from about 5 to 6 mm in diameter. All cusps have rounded sides, except for the intermediate anterior talon, which has a flat side. The paracone is appressed to the buccal side of the intermediate anterior talon, giving the paracone a semicircular occlusal surface. The lingual anterior talon is appressed to the lingual side of the intermediate anterior talon and the mesial side of the protocone. The buccal anterior talon is not present. The cingulum rises between the base of the par-

acone and metacone, the metacone and hypocone, and the lingual anterior talon and protocone, forming tubercles. The height of the cingulum on the mesial edge is about 8 mm and gradually increases to about 11 mm toward the distal side. Many faint vertical grooves exist on the surface of the cingulum, and several shallow horizontal grooves occur on the basal half of the cingulum. A shallow fossa exists in the middle of the cingulum basal to the metacone. The middle portion of the lingual surface of the cingulum is depressed. The cingulum directly basal to the intermediate anterior talon has dentine exposed, perhaps representing the mesial facette. The enamel is 0.5 to 1.0 mm thick on the basal surface. The lingual half of the dentine shows a smooth flat surface indicating destruction during deposition, whereas the buccal half exhibits a rough, fresh fracture of dentine damaged at the time of removal from the deposit. The tooth is considered to be single rooted because of a faint circular structure on the dentine surface.

Specimen.—KZD10 (Figures 12, 22-2).

Diagnosis.—KZD10 consists of a well-worn crown of a molar with no root. KZD10 shows the cusp arrangement of the lower molar (Figure 3), which is six appressed cusps arranged in two columns of three transverse rows. This arrangement of cusps is seen in the M_3s of the Izumi specimen, as well as in the Moniwa specimen identified as a left M_3 of *P. tabatai* (Inuzuka and Murai, 1980). Because KZD10 lacks a distinct cingulum, which is found in the Izumi and Moniwa specimens, it is reported here as *P. ?tabatai*. Ijiri and Kamei (1961) noted that the lower cheek teeth in *P. tabatai* tended to be more worn at the buccal and distal sides relative to the mesial and lingual sides. KZD10 is thus identified as a left M_3 of *P. ?tabatai*.

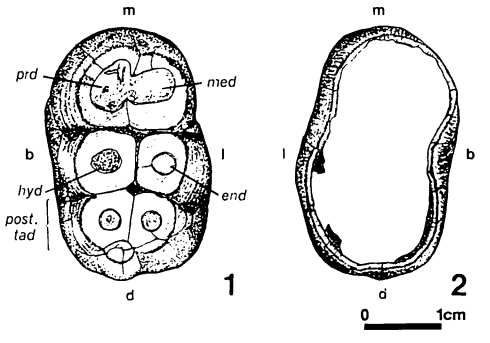

Figure 12. KZD10: left M_3 of *Paleoparadoxia ?tabatai*. 1, occlusal surface; 2, basal surface. White spaces represent portions still covered by sediments.

Description.—The tooth, which is slightly swollen laterally, is in the shape of a stretched oval in occlusal view. The six cusps and the tubercle on the distal edge exhibit a smooth attrition surface that slants buccodistally. In the first row, the protoconid and metaconid are joined, and the dentine of these cusps is exposed as combined distorted ovals. The rounded peak of the metaconid is seen as the highest point of the tooth. The square hypoconid differs from the entoconid and posterior talonids in that it has the largest attrition surface and dentine exposed. The entoconid and two posterior talonids have about equal areas of attrition surface and have a circle of dentine exposed in their centers. The attrition surface of the first and second rows have the same dimension in a buccolingual direction, measuring 15.2 mm, and the third row is slightly narrower, measuring 13.8 mm. The second and third rows have the same dimension on the attrition surface in a mesiodistal direction, measuring about 8 mm, whereas the first row is about 11 mm. Many short, shallow vertical and inclined grooves are distributed on the lower part of the crown forming a rough surface. A shallow, transverse depression runs through the rough basal half of the crown on the distal surface. The enamel along the cervical line is 1 mm thick. The cervical line corresponds to the outline of the tooth, except near the middle where it narrows in a buccolingual direction.

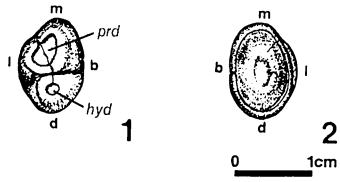

Figure 13. KZD06: right P_3 of *Paleoparadoxia* sp. 1, occlusal surface; 2, basal surface.

Paleoparadoxia sp.

Specimen.—KZD06 (Figures 13, 20).

Diagnosis.—KZD06 is a complete crown of a right P_3 of *Paleoparadoxia* that consists of two complete cusps, protoconid and hypoconid, with a slight extension of a root. This identification is based on a direct comparison with the Izumi specimen. Because KZD06 has a greater mesiodistal diameter than the buccolingual diameter, it probably is a lower cheek tooth. KZD06 cannot be the P_4 or any lower molar as those in the Izumi specimen are much larger in size and structurally more complex (*i.e.*, having a larger number of cusps and accessory cusps); however, the characters of M_1 are speculative due to the poor preservation of this tooth class in the Izumi specimen. Both P_2s in the Izumi specimen have a conical main cusp with a distal tubercle, and P_3s possess three columnar cusps. The protoconid and hypoconid of KZD06 resemble those of the right P_3 in the Izumi specimen. The metaconid appears to be undeveloped in KZD06. The crown height of KZD06 is much lower than the Izumi P_3, but this difference can be explained by the degree of wear. The wear pattern of the hypoconid also differs between the two specimens. KZD06 has a weak buccally declining attrition surface in contrast to the P_3s in the Izumi specimen which exhibit a very steep, distally slanting surface. Because KZD06 morphologically differs from the Izumi P_3s in cusp number, wearing pattern, and size, KZD06 is designated *Paleoparadoxia* sp.

Description.—In occlusal view, the oval-shaped crown, which swells laterally, is slightly concave on its mesiolingual side. The protoconid is located somewhat ligually and measures about 7 mm in a mesiodistal direction, and large amount of dentine is exposed on the attrition surface. The hypoconid, with a mesiodistal diameter of 4.5 mm, comprises the distal 1/3 of the tooth and has a small circle of dentine exposed at the center. The highest point of the tooth is at the junction of the two cusps. The buccal surface of the crown is smoother than the lingual side. A shallow groove, ranging between 0.4 and 0.9 mm in width, surrounds the entire crown running parallel to and about 2.5 mm above

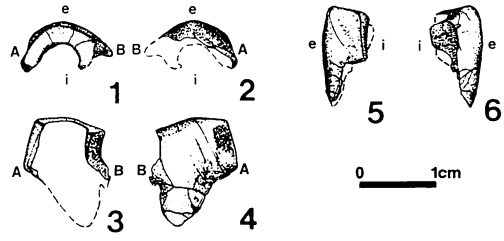

Figure 14. KZD04: fragmentary column of a cheek tooth of *Paleoparadoxia* sp. 1, occlusal surface; 2, basal surface; 3, interior surface; 4, exterior surface; 5, side A; 6, side B. White spaces represent damaged surfaces and portions still covered by sediments.

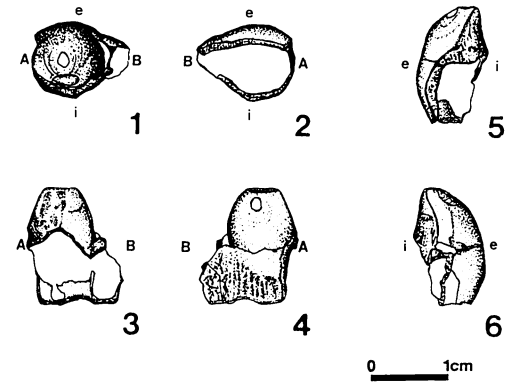

Figure 15. KZD08: column of a cheek tooth of *Paleoparadoxia* sp. 1, occlusal surface; 2, basal surface; 3, interior surface, 4, exterior surface; 5, side A; 6, side B. White spaces represent portions still covered by sediments.

the cervical line. The enamel at the cervical line is about 0.3 mm thick. The short root is highly rounded due to depositional processes. No pulp cavity is recognized, but the tooth is thought to be single rooted.

Specimen.—KZD04 (Figure 14).

Diagnosis.—Estimating the total size of the cusp, we surmise that KZD04 may be a fragmentary column of a cheek tooth of *Paleoparadoxia* ; however, the exact species and tooth class is undetermined.

Description..—KZD04 preserves a small portion of a well-worn cusp. The maximum thickness of the enamel, 2.3 mm, is seen on the occlusal surface.

Specimen.—KZD08 (Figure 15).

Diagnosis.—KZD08 is perhaps a column of a cheek tooth of *Paleoparadoxia*, based on an estimate of the total size of the cusp, but it is too fragmentary to determine the exact species and tooth class.

Description.—KZD08 preserves a relatively complete cusp with a slight extension of enamel. The thickness of the enamel on the basal side is 1.5 mm.

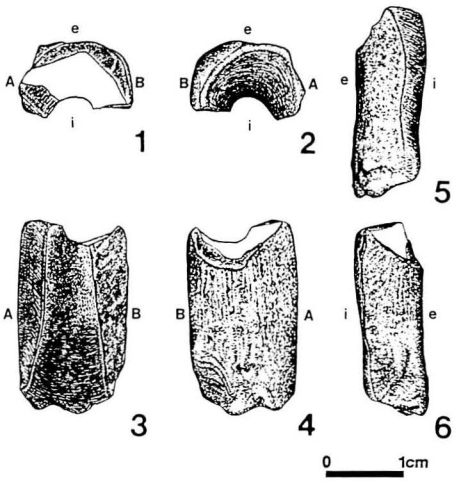

Figure 16. KZD05 : fragmentary column of a molar of *Desmostylus* sp. 1, occlusal surface ; 2, basal surface ; 3, interior surface ; 4, exterior surface ; 5, side A ; 6, side B. White spaces represent portions with fresh breaks.

Family Desmostylidae Osborn, 1905
Genus *Desmostylus* Marsh, 1888
***Desmostylus* sp.**

Specimen.—KZD05 (Figure 16).

Diagnosis.—KZD05 is 1/3 of a well-worn enamel column, and it is thought to be a fragment of a molar of *Desmostylus* due to its

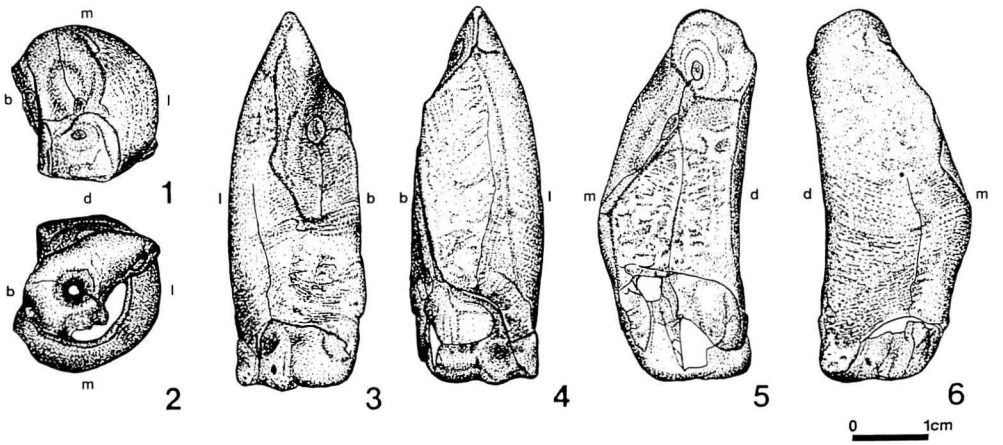

Figure 17. KZD12 : column of a left lower molar of *Desmostylus* sp. 1, occlusal surface ; 2, basal surface ; 3, mesial surface ; 4, distal surface ; 5, buccal surface ; 6, lingual surface. White spaces represent portions still covered by sediments and fresh breaks.

size. The hypsodont crown of KZD05 with no cingulum suggests that it belongs to *Desmostylus*. However, because the fossil is so incomplete, the tooth orientation, tooth class, and species cannot be identified.

Description.—The preserved enamel has a maximum thickness of 7.3 mm. The exterior surface exhibits very coarse texture. Sides A and B on the interior surface show broken surfaces apparently caused by depositional processes. However, the broken surface of side A is well polished and forms a smooth surface; whereas, the broken surface of side B shows an uneven surface, although it is also polished. Numerous parallel enamel prism groups (Vanderhoof, 1937), "Schreger's stripes" (Ijiri, 1939; Reinhart, 1959; Kozawa, 1984), are visible on both broken surfaces but better exhibited on the surface of side A.

Specimen.—KZD12 (Figures 17, 23).

Diagnosis.—KZD12 is considered to be a column of a left lower molar of *Desmostylus* that is characterized by its hypsodont crown with no cingulum. As described below, KZD12 shows two different directions of wear. It also shows two flat lateral sides, which meet at approximately a right angle. Because the columns in upper teeth do not generally form at right angles, the specimen is perhaps a lower molar. Moreover, KZD12 is identified as a metaconid of a left lower molar by considering its size and position (see Inuzuka, 1987, Figure 5). Hence, the wear marks at the mesial and distal sides perhaps represent the mesial facette and the attrition surface, respectively. Its exact tooth class and species are however unknown.

Description.—KZD12 shows two different directions of wear at steep angles. Each worn surface has an enamel opening close to its center exposing the same mass of dentine by penetrating the enamel from two different directions. Two lateral sides are flat, meeting at about a right angle and indicating the attachment of unpreserved columns. These

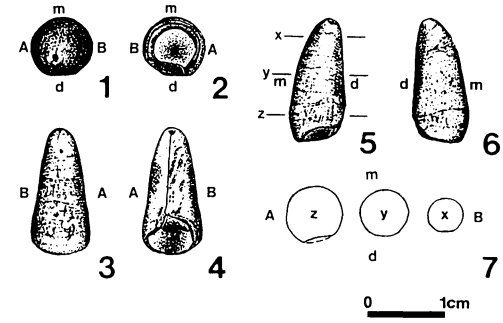

Figure 18. KZD15: milk canine? of *Desmostylus* ?. 1, occlusal surface; 2, basal surface; 3, mesial surface; 4, distal surface; 5, side A; 6, side B; 7, cross-sectional views taken at the position of x, y, and z in 5.

two surfaces are thought to be the buccal and distal sides in which the width of the flat surface is wider on the former than the latter.

Desmostylus ?

Specimen.—KZD15 (Figure 18).

Diagnosis.—KZD15 is tentatively identified as an unworn milk canine? of *Desmostylus*. The identification is based on the presence of the crestal pit suggesting that KZD15 is probably a desmostylian tooth. The specimen is not *P. tabatai*, because it does not have any significant ridge and is not compressed in any direction; therefore, it differs in morphology from any of the Izumi teeth. KZD15 also differs from most teeth of *P. weltoni* in morphology, except for the lower canine that somewhat resembles it; however, KZD15 differs significantly from *P. weltoni* by its small size. By eliminating the possibility of *Paleoparadoxia*, the alternative taxonomic assignment that can be drawn from our current knowledge is *Desmostylus*. Because KZD15 is uniconical in shape, it cannot be the incisor of *Desmostylus* which is characterized by its unicolumnar shape (Hannibal, 1922; Inuzuka, 1988). The only remaining possibility is the canine. Considering the sketch of the canine of *D. hesperus* given by Vanderhoof (1937) and the state-

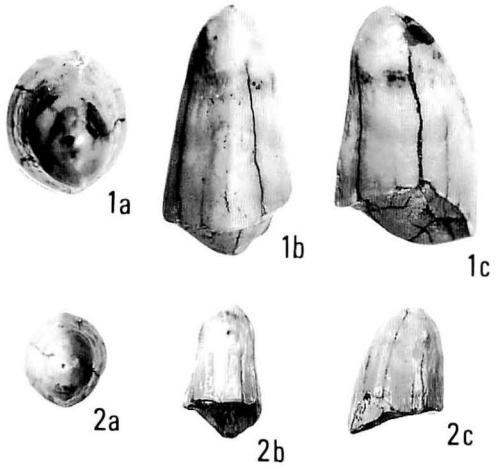

Figure 19. Paleoparadoxian upper canines from Kuzubukuro. 1, right upper canine of *Paleoparadoxia ?tabatai* (KZD09); 2, left upper canine of *Paleoparadoxia tabatai* (KZD11). a, occlusal view; b, distal view; c, lingual view. Approximately natural size.

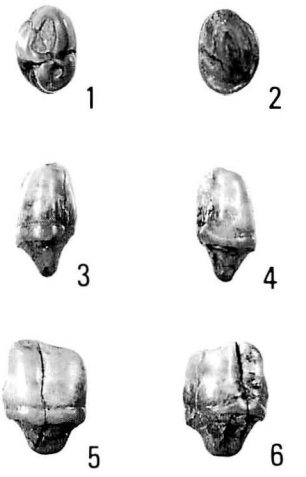

Figure 20. Right P_3 of *Paleoparadoxia* sp. from Kuzubukuro (KZD06). 1, occlusal view; 2, basal view; 3, mesial view; 4, distal view; 5, buccal view; 6, lingual view. Approximately natural size.

ment, "the size of the tusk varies with age," presented by Reinhart (1959), we report KZD15 as a milk canine, although uncertainty still remains. Reinhart (1959) stated that "the tusk" of *Desmostylus* is "oval in cross section and slightly curved," describing the overall view, including both crown and root. The cross section of KZD15 is a nearly complete circle, and therefore the identification of right or left cannot be determined. Whether the tooth is upper or lower is also unknown.

Description.—The crestal pit is 1 mm in diameter and is situated slightly distal of the center of the nearly complete circular outline of the tooth when viewed occlusally. Viewed from sides A and B, the outline of the distal side is straight, whereas the mesial side becomes convex at the occlusal 1/5 and basal 1/4 of the crown. The enamel surface is smooth through the tooth although some slight depressions are present. In mesial and distal views, the overall outline is a symmetrical, acute-angled triangle with a rounded crest and slightly swollen sides near the base. The basal end of the crown on the distal side is rounded due to depositional processes. The thickness of the enamel on the mesial side is about 0.9 mm. The dentine fills in the enamel to a depth of 4.2 mm at the basal side.

Remarks and comparisons

A. *Paleoparadoxia*

a. Canines

Besides this paper, the work of Ijiri and Kamei (1961) is virtually the only report on the upper canine morphology of *Paleoparadoxia*. Because KZD09 and KZD11 consist of half of the crown and the information is limited, a pertinent comparison with even the Izumi specimen can be hardly approached at this stage. Because the only specimen of *P. weltoni* does not provide information about the upper canines (Clark, 1991), we cannot compare it with KZD09 and KZD11. However, potential sexual dimorphism in the size of canines as discussed previously is worth noting.

b. Cheek teeth

Although a number of paleoparadoxian cheek teeth from Japan have been reported, it

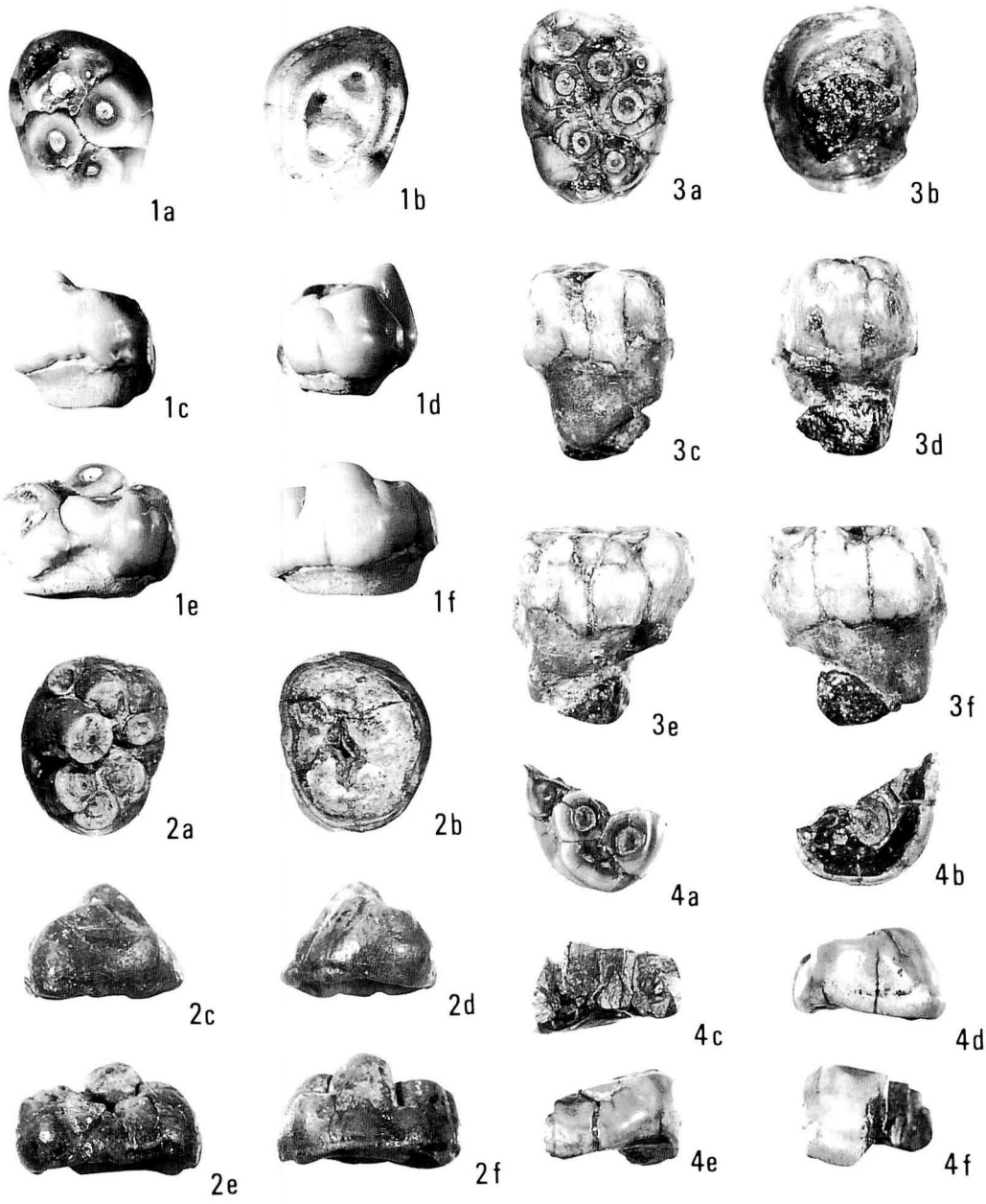

Figure 21. Paleoparadoxian M^1 and M^2s from Kuzubukuro. 1, right M^1? of *Paleoparadoxia ?tabatai* (KZD07); 2, left M^2 of *Paleoparadoxia tabatai* (KZD01); 3, right M^2 of *Paleoparadoxia tabatai* (KZD02); 4, partial right M^2 of *Paleoparadoxia tabatai* (KZD13). a, occlusal view; b, basal view; c, mesial view; d, distal view; e, buccal view; f, lingual view. Approximately natural size.

seems that information on tooth morphology is still limited. Tokunaga (1939) reported two desmostylian teeth from Sado Island, the Sawane specimens, which are now considered to belong to *Paleoparadoxia*. Unfortunately, these teeth were lost by fire during the Second World War; however, another tooth, that was conceivably discovered at the same time, was recently found but has not been studied in detail. In 1944, Takai reported the Hannoura specimen that was determined to be a left P^3 of *D. japonicus*, but it was later re-identified as *Paleoparadoxia* (Inuzuka, 1984); however, the latter identification is still questionable due to morphological differences between the specimen and the Izumi P^3s. A partial set of teeth with a dentary, the Chichibu-Terao specimen, was reported by Arai (1953); however, as the study of the Izumi specimen was still in progress, the report was not able to be comprehensive. Although no specific morphologic trait of the molars of *P. tabatai* was presented, cranial study of the Izumi specimen (Ijiri and Kamei, 1961) made it possible to compare measurements with other specimens. The Akibi specimen, a left P_4? of *P. tabatai* discovered in Toyama Prefecture, was reported by Shikama (1966a). Kamei (1967) reported a right P_1 of *P. tabatai*, the Tomikusa specimen, and microscopic study was later conducted on this tooth by Kobayashi and Kamei (1973). The Wainai specimen, a right M_3 of *P. tabatai*, of uncertain provenance (as it was found in an archeological site in Iwate Prefecture), was described by Inuzuka in 1977. Fujimoto and Sakamoto (1978) briefly reported the discovery of the Chichibu-Ogano specimen, a skeleton of *Paleoparadoxia*, along with pictures of a left P_4? and a right M^2, but the study has not been completed. Tsunoda and Ogano Collaborative Research Group (1978) reported the occurrence of a M1 of *P. tabatai* from the Chichibu basin. They described no morphology but presented a detailed study of the stratigraphic context. Inuzuka and Murai (1980) reported a left M_3 of *P. tabatai*, the Moniwa specimen, which was found in Miyagi Prefecture. Recently, a right P_4 of *P. tabatai* was described by Kaneko and Inuzuka (1992). It was discovered in Toyama Prefecture and was named the Tsuzara specimen. Despite these reports, the morphology of the cheek teeth in *P. tabatai* does not seem to be well established, except for the M_3 due to the study of this particular tooth class by Reinhart (1959).

Technical reports on cheek teeth of *Paleoparadoxia* are even rare in the United States. Reinhart (1959) reported two specimens of *P. tabatai*, UCMP 32076 and UCMP 40862. He described UCMP 32076 as either a right upper or left lower cheek tooth (p. 96), although he also described it as "(left lower) cheek tooth" (p. 144). Recently, this specimen was assigned to a M_3 by Clark (1991); therefore, it is probably a left tooth. UCMP 40862 is a partial right dentary, and the only preserved cheek tooth is identified as a right M_3 (Reinhart, 1959). Four cheek teeth of

Table 2. Measurements of paleoparadoxian P_3s.

Specimen		KZD06 (This report)	Izumi(Ijiri and Kamei, 1961)		UCMP 114285 (Clark, 1991)	
Species		*P.*sp.	*P.t.*		*P.w.*	
Right/Left		Right	Left	Right	Left	Right
Measure-ment(mm)	m-d	12.5	15	16.5	15	15
	b-l	9.0	13	13	11	11

Table 3. Measurements of paleoparadoxian upper molars.

	Tooth Class		M1?		M2		M2		M3	
Kuzubukuro Specimen (This report)	Specimen		KZD07		KZD01		KZD02		KZD14	
	Species		*P.t.*?		*P.t.*		*P.t.*		*P.t.*?	
	Right/Left		Right		Left		Right		Right	
	Measurement (mm)		m-d	b-l	m-d	b-l	m-d	b-l	m-d	b-l
			25.0	20.4	26.4	21.6	27.6	22.2	27.3	24.3+
Izumi (Ijiri and Kamei, 1961)	*P.t.*	Left	20	20	28.5	27	28.5	27	28	25
		Right	16+	21	29	26.5	29	26.5	28	27
UCMP 114285 (Clark, 1991)	*P.w.*	Left	-	-	21*	17*	21*	17*	19	18
		Right	-	-	-	-	-	-	-	-

* Approximate measurement of a damaged tooth.

Table 4. Measurements of paleoparadoxian M_3s.

Specimen		KZD10 (This report)	Izumi (Ijiri and Kamei, 1961)		Wainai (Inuzuka, 1977)	Moniwa (Inuzuka and Murai, 1980)	LACM 4371a (Mitchell, 1963)	UCMP 32076* (Clark, 1991)	UCMP 40862* (Clark, 1991)	UCMP 95944 (Clark, 1991)	UCMP 114285 (Clark, 1991)	
Species		*P.t.*?	*P.t.*		*P.t.*	*P.t.*	*P.*sp.	*P.*sp.	*P.*sp.	*P.*sp.	*P.w.*	
Right/Left		Left	Left	Right	Right	Left	Left	Left	Right	?	Left	Right
Measure-ment(mm)	m-d	32.9	34.5	34.5	24+	34	-	35.2	32.5	34	23	23
	b-l	22.0	25.5	25.5	25	22.5	28.0	25.6	25	29	17	17

* Specimen originally described as *P. tabatai* by Reinhart (1959). The identification of right or left is based on Reinhart (1959).

Paleoparadoxia. sp. were reported in papers by Mitchell (1963) and Mitchell and Repenning (1963): a complete tooth (probably a left M_3) (LACM 4371a), a premolar (LACM 4371b), an incomplete tooth (UCMP 63981), and a complete tooth (UCMP 45274). Recently, Clark (1991) described a new species, *P. weltoni* (UCMP 114285), that has a well-preserved dentition. He also presented measurements of UCMP 95944, a M_3 that belongs to *P.* sp. Besides the specimen of *P. weltoni*, it seems that only UCMP 40862 has been reliably identified by tooth class among the specimens of paleoparadoxian cheek teeth in the United States.

Tables 2, 3, and 4 show the measurements of paleoparadoxian cheek teeth from Kuzubukuro compared to the other known cheek teeth of the genus. Because the attrition phase varies from tooth to tooth, the crown height of all teeth is not treated in these tables. Table 2 shows that KZD06 as a P_3 is much smaller than the corresponding tooth class of the type specimen of *P. tabatai* and *P. weltoni*. Therefore, KZD06 cannot be readily classified into either species although the small size is explained if it is a milk tooth. However, no conclusion can be made only from this isolated tooth. An easily recognized trend seen in Tables 3 and 4 is that the molars of *P. weltoni* are much smaller in size than the Kuzubukuro molars although the M^1s of the former are not preserved. Thus, the Kuzubukuro specimens are not considered to belong to *P. weltoni*. The measurements of M^1s of the Izumi specimen are presented by Ijiri and Kamei (1961); however, the Izumi M^1s are heavily worn preserving only the very basal end of the crown and partially exposed root with a reduced attritional surface area, and are not representative of the unworn teeth. It seems that KZD07 is slightly smaller than the original unworn Izumi M^1s in both mesiodistal and buccolingual directions. If this is true, then all the complete upper molars from Kuzubukuro are smaller in the mesiodistal and buccolingual diameters than the Izumi specimen. A similar result is also seen for M_3 in which KZD10 is smaller than any other reported paleoparadoxian M_3 (with complete measurements) except for UCMP 40862 (*P.* sp.) and UCMP 114285 (*P. weltoni*). In addition, it seems that the buccolingual direction of the complete Kuzubukuro molars are generally proportionally smaller than the Izumi specimen with respect to mesiodistal direction. The presence or absence of cingula on Kuzubukuro molars does not appear to have a bearing on their smaller size, but the major cusps, accessory cusps, and tubercles in the Kuzubukuro specimens are more closely gathered than those in the Izumi specimen. It is curious that Clark (1991) also encountered small size in the molariform teeth of *P. weltoni*, suggesting it could represent either an autapomorphy for *P. weltoni* or a retained primitive condition. However, the reason for the trend for small crowns in the Kuzubukuro teeth is unknown, because they are not in association with a skull.

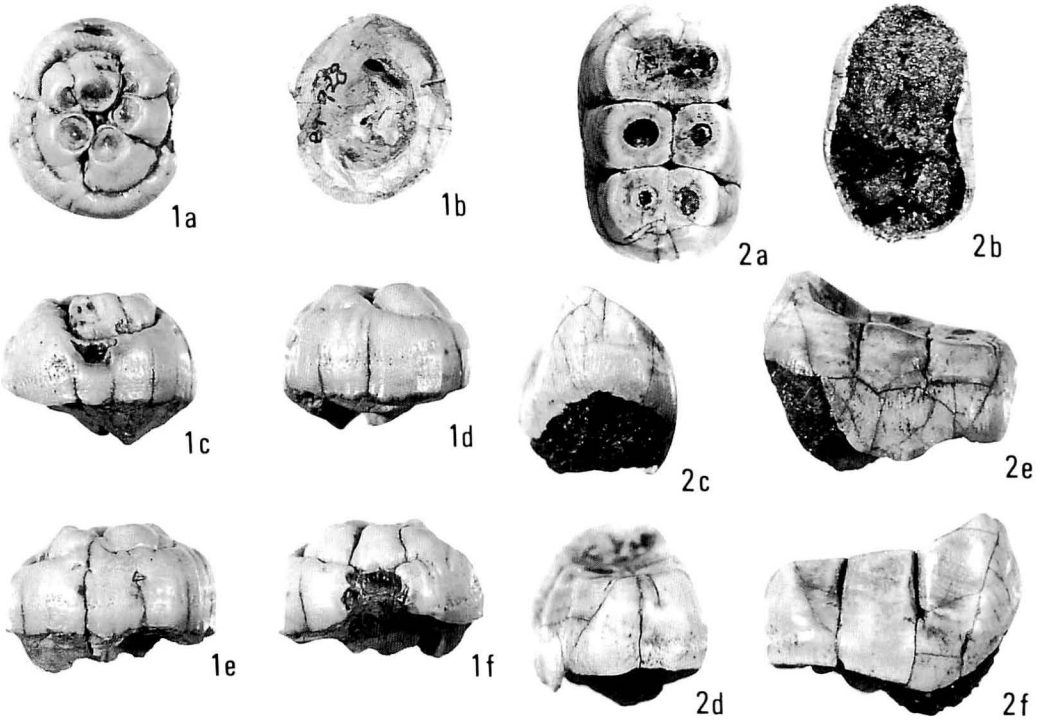

Figure 22. Paleoparadoxian M^3 and M_3 from Kuzubukuro. 1, right M^3 of *Paleoparadoxia ?tabatai* (KZD14) ; 2, left M_3 of *Paleoparadoxia ?tabatai* (KZD10). a, occlusal view ; b, basal view ; c, mesial view ; d, distal view ; e, buccal view ; f, lingual view. Approximately natural size.

B. *Desmostylus*

a. Canine

Although Vanderhoof (1937) and Reinhart (1959) discussed the canines of *Desmostylus*, information about this tooth class is still limited. Therefore, no comparison is made for KZD15.

b. Cheek teeth

The significance of KZD05 and KZD12, which are unambiguously identified as *Desmostylus*, lies in their co-occurrence with *Paleoparadoxia* in a single bed in a limited area, although the teeth may be reworked as discussed later. As Mitchell and Repenning (1963) considered the notes of Yabe (1959), the Izumi skeleton of *P. tabatai* (Ijiri and Kamei, 1961 ; Shikama, 1966b) and the Togari skull of *D. japonicus* (Yoshiwara and Iwasaki, 1902 ; Tokunaga and Iwasaki, 1914) are from two different localities about 3 km apart but from roughly stratigraphically equivalent beds. The co-occurrence of *Paleoparadoxia* (Iwaya specimen) and *Desmostylus* (Nanao specimen) from the same outcrop in the same unit at the Noto Peninsula, central Japan was reported by Inuzuka (1984), Kaseno (1984), and Inuzuka and Karasawa (1986), although the descriptions of the fossils are still unpublished. Therefore, this paper is the second report on the co-occurrence of *Paleoparadoxia* and *Desmostylus* from exactly of the same bed in the same area of Japan. However, no comparisons are made for KZD05 and KZD12, because they are so fragmentary.

Discussion

A. Geological aspects of the fossils

Chinzei (1984) discussed the modes of

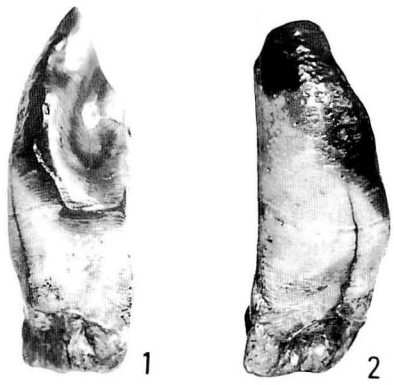

Figure 23. Column of a left lower molar of *Desmostylus* sp. from Kuzubukuro (KZD12). 1, mesial view; 2, lingual view. Approximately natural size.

desmostylian occurrence and roughly divided them into two categories: 1) isolated teeth, and 2) skeletal remains. He stated that many isolated teeth occur in high-energy deposits such as coquinas and conglomerates, and that the majority of these teeth were reworked. He noted that the occurrence of shark teeth with isolated desmostylian teeth could be explained in the same way due to the high resistibility and high fossilization potential of teeth. Although the fossils from the Godo Conglomerate are generally rounded, we have not yet found conclusive evidence that the desmostylians are derived from another horizon. No certain lithologic difference between the enclosing sediments and the sediments still filling depressions and cavities on the teeth has been found. However, we cannot dismiss the possibility that the teeth are reworked. The broken surfaces of sides A and B of KZD05 are polished apparently by depositional processes with distinctively different degrees of polish on the two surfaces. The broken surface of side A is very smooth, whereas side B shows an uneven polished surface. This difference can be interpreted as representing two different depositional stages, with side A exhibiting an older break than side B. Due to taphonomic problems, the taxon range zone of desmostylians cannot be determined with accuracy as commented upon by Chinzei (1984). Although deposition of the lower half of the Iwadono Formation probably took place sometime between the late Early Miocene and middle Middle Miocene (Matsumaru *et al.*, 1982; Koike *et al.*, 1985; Majima, 1989), this does not necessarily represent the true range of the desmostylians.

According to Koike *et al.* (1985), the lithology of the clasts in the Godo Conglomerate suggests that the lands to the north and west were the main sources of supply. Interestingly, about 30 km west of Kuzubukuro is the Chichibu Basin where several occurrences of *Paleoparadoxia* are known (Arai, 1953; Fujimoto and Sakamoto, 1978; Tsunoda and Ogano Collaborative Research Group, 1978; Sakamoto, 1983). All of these fossils are complete or partial skeletons, reducing the likelihood of reworking. Although most of them were found in horizon N9 foraminiferal zone (see Chinzei, 1984), the one discussed by Tsunoda and Ogano Collaborative Research Group (1978) is the oldest known *Paleoparadoxia* in Japan, because it came from horizon N6 (Chinzei, 1984). Unfortunately, because most of these fossils have not been studied well, we could not make any comparison between the Kuzubukuro and Chichibu teeth. However, it would be interesting to compare them in the future.

B. Occurrence of sharks with Desmostylia

The significance of numerous shark teeth found in the Godo Conglomerate should be considered. Because shark systematics are not the focus herein, thus, we follow the nomenclature used in Itoigawa *et al.* (1985). In his report, Inuzuka (1984) showed that desmostylians are known from 59 localities in Japan, and Goto and Kuga (1984) stated that elasmobranchs have been found at 20 of them along with marine mammals, such as pinnipeds, sirenians, and cetaceans. Goto and Kuga (1984) included Kuzubukuro as one of these 20 localities, but they were aware of

only *Isurus hastalis* (Agassiz). Itoigawa *et al.* (1985) reported that the most abundant shark species from Kuzubukuro are *Odontaspis cuspidata* Agassiz and *Isurus desori* (Agassiz). This observation seems to be correct, but some other important factors should be added. Although *I. desori* is the most abundant species of the genus *Isurus, I. hastalis* is also commonly found. We can confirm the occurrence of *I. planus* (Agassiz) at the site, first tentatively recognized by Itoigawa *et al.* (1985). The taxon range zone of *I. planus* is the Middle to Late Miocene of the circum-Pacific region, the United States (California) and Japan (Kuga, 1985; Itoigawa *et al.*, 1985; Karasawa, 1989). Kuga (1985) noted that the species occurred in the Moniwa Formation in Miyagi Prefecture, the Iwaya Calcareous Sandstone Bed in Ishikawa Prefecture, and the Fujina Formation in Shimane Prefecture, where isolated desmostylian bones and teeth are also known (Inuzuka, 1984). Although the data are still limited, there seems to be both stratigraphic and geographic significance in their co-occurrence. Several other species of *Isurus* are recognized as well, and the whole genus appears to be the predominant shark group at Kuzubukuro. Based on the work of the Kuzubukuro Geology Club, one of the authors (Shimada) is convinced that at least 20 shark species, and perhaps as many as 25 to 30 species, are represented in the Godo Conglomerate Member, including *Carcharodon megalodon* Agassiz, *Isurus benedeni* (Le Hon), and *Dalatias licha* (Bonnaterre).

The *Odontaspis-Isurus* assemblage and the other shark species from Kuzubukuro appear to be similar to the fossils from the Miocene formations of the Noto Peninsula in central Japan, as reported by Karasawa (1983, 1989). The Miocene units of the Noto district are known as one of the richest areas for desmostylians, including the Iwaya and Nanao specimens (Takai, 1944; Kaseno, 1964, 1984; Shikama, 1966a; Inuzuka and Karasawa, 1986). Kaseno (1984) noted that desmostylian remains are found in shallow marine strata of the early Middle Miocene (ca. 14–13 Ma). However, Chinzei (1984) indicated the possibility of the desmostylian material from the Noto Peninsula being reworked, because most specimens are found as isolated teeth or bone from coarse-grained deposits, although some of the desmostylians from the Noto Peninsula less likely to be reworked (Inuzuka and Karasawa, 1986). Even if the fossils from Kuzubukuro and Noto Peninsula are allochthonous, the fact that there are similarities in the vertebrate fauna from these two distant areas is noteworthy.

Desmostylians in association with shark fossils have been documented in the United States as well (*e.g.*, Merriam, 1906; Anderson, 1911; Mitchell and Lipps, 1965; and Zuidema, 1970). Vanderhoof (1937) pointed out that the teeth of *Carcharodon* and *Isurus* constantly occur with *Desmostylus*. Repenning and Packard (1990) recently discussed the probable predation on *Paleoparadoxia* by sharks. They noted the nearly complete but undescribed Stanford specimen discovered in California and its association with 24 shark teeth comprising many *Isurus* and some *Galeocerdo* teeth.

Due to taphonomic considerations, it is difficult to say whether the sharks and desmostylians of the Godo Conglomerate coexisted or are just co-occurring. It seems also unlikely that the Kuzubukuro fossils will yield evidence that would reveal their true paleoecological relationship. However, as Goto and Kuga (1984) stated, it is natural to think that sharks and desmostylians coexisted during the Miocene by their frequent associations in the fossil record. Moreover, as Kuga (Inuzuka, 1984 *ed.*) mentioned, we believe that sharks were likely predators and scavengers on desmostylians during the Miocene.

Acknowledgment

We especially thank Dr. Tadao Kamei, professor emeritus of Kyoto University who

provided this research opportunity. We gratefully acknowledge Dr. Richard J. Zakrzewski, Fort Hays State University, for improving this paper; Dr. Michael E. Nelson, formerly of Fort Hays State University, for allowing the use of university facilities; Dr. Yukimitsu Tomida, National Science Museum in Tokyo, for allowing access to the Izumi specimen; and Isamu Baba, a secretary of Kuzubukuro Geology Club, for supporting the overall project. Mitsuko Koike of Oi Senior High School and Kensaku Takei of Kosei Gakuen Senior High School provided very useful information about the geology of Kuzubukuro. We are greatly indebted to all of the individuals who discovered the described fossils and provided access to them. We also thank Gregory A. Liggett, Cameron L. Liggett, Larry A. Codington, Takashi Oe, Takefumi Murai, Teruo Naito, Kiyohiko Ogai, Kiyoshi Nomura, Yuji Takakuwa, Lemin Huang, Eiko Shimada, and many other people who have supported and encouraged our work in various ways.

References

Anderson, F.M., 1911: The Neocene deposits of Kern River, California, and the Temblor Basin. *Proc. Calif. Acad. Sci., ser. 4*, vol. 3, 101 p.

Arai, J., 1953: New discovery of Desmostylid (*Cornwallius ?* sp.) in the Chichibu Basin. *Bull. Chichibu Mus. Nat. Hist.*, no. 3, p. 65-86.**

Chinzei, K., 1984: Modes of occurrence, geologic range and geographic distribution of desmostylians. *In*, Inuzuka, N., Takayasu, K., Chinzei, K., and Yoshida, K., *eds.*, *Desmostylians and Their Paleoenvironment. Assoc. Geol. Collabor. Japan., Monogr.* 28, p. 13-23.**

Clark, J.M., 1991: A new early Miocene species of *Paleoparadoxia* (Mammalia: Desmostylia) from California. *Jour. Vert. Paleont.*, vol. 11, no. 4, p. 490-508.

Domning, D.P., Ray. C.E., and McKenna, M.C., 1986: Two new Oligocene desmostylians and a discussion of tethytherian systematics. *Smithsonian Contr. Paleobio.*, no. 59, 56 p.

Fujimoto, H. and Sakamoto, O., 1978: A preliminary report on *Paleoparadoxia* sp. discovered from the Tertiary system of the Chichibu basin, central Japan. *Chichibu Mus. Nat. Hist.*, no. 18, p. 1-10.**

Goto, M. and Kuga, N., 1984: Fossil elasmobranchs occurred with desmostylians in Japan. *In*, Inuzuka, N., Takayasu, K., Chinzei, K., and Yoshida, K., *eds.*, *Desmostylians and Their Paleoenvironment. Assoc. Geol. Collabor. Japan., Monogr.* 28, p. 45-49.**

Hannibal, H., 1922: Notes on Tertiary sirenians of the genus *Desmostylus. Jour. Mammal.*, vol. 3, p. 238-240.

Hirota, K., 1981: Problems on paleoparadoxian mandible (*Paleoparadoxia tabatai*). *Fossil Club Bull.*, vol. 14, p. 9-15.**

Horiguchi, M., 1975 *ed.*: [Exploring the geology in Saitama Prefecture, *Geology Guidebook*] (Nichiyo no Chigaku), vol. 1, 258 p. Tsukiji Shokan, Tokyo.*

——, 1987 ed.: [Exploring the natural history in Saitama Prefecture, *Geology Guidebook*] (Nichiyo no Chigaku), vol. 1, 2nd ed., 273 p. Tsukiji Shokan, Tokyo.*

Ijiri [Iziri], S., 1939: Microscopic structure of a tooth of *Desmostylus. Proc. Imp. Acad. Tokyo*, vol. 15, no. 5, p. 135-138.

—— and Kamei, T., 1961: On the skulls of *Desmostylus mirabilis* NAGAO from South Sakhalin and of *Paleoparadoxia tabatai* (TOKUNAGA) from Gifu Prefecture, Japan. *Earth Science* (*Chikyu Kagaku*), vol. 53, p. 1-27.**

Inuzuka, N., 1977: On a right third inferior molar of *Paleoparadoxia tabatai* (TOKUNAGA) from "Wainai" remains, Iwate Prefecture. *Earth Science* (*Chikyu Kagaku*), vol. 31, no. 4, p. 165-166.*

——, 1984: Studies and problems on the order Desmostylia. *In*, Inuzuka, N., Takayasu, K., Chinzei, K., and Yoshida, K., *eds.*, *Desmostylians and Their Paleoenvironment. Assoc. Geol. Collabor. Japan., Monogr.* 28, p. 1-12.**

——, 1984 *ed.*: Discussion on the desmostylians and their paleoenvironment, *In*, Inuzuka, N., Takayasu, K., Chinzei, K., and Yoshida, K., *eds.*, *Desmostylians and Their Paleoenvironment. Assoc. Geol. Collabor. Japan., Monogr.* 28, p. 129-138.**

——, 1986: Hyracoidea; Proboscidea; Desmostylia; Sirenia. *In*, Goto, M., and Ohtaishi, N., *eds.*, *Comparative Odontology*, p. 177-187. Ishiyaku-shuppan, Tokyo.*

——, 1987: Primitive desmostylians, *Behemotops* and the evolutionary pattern of the Order Desmostylia. *Reprinted from Prof. M. Matsui. Mem. vol.*, Sapporo, Japan, p. 13-25.*

——, 1988: The skeleton of *Desmostylus* from Utanobori, Hokkaido, I. Cranium. *Bull. Geol. Surv. Japan*, vol. 39, no. 3, p. 139-190.**

—— and Karasawa, H., 1986: Some fossils of

Paleoparadoxia from Miocene Calcareous Sandstone on the Noto Peninsula, Central Japan, *Earth Science* (*Chikyu Kagaku*), vol. 40, no. 4, p. 294-300.*

—— and Murai, T., 1980: On a left third inferior molar of *Paleoparadoxia tabatai* from the Moniwa Formation, Miyagi Prefecture. *Earth Science* (*Chikyu Kagaku*), vol. 34, no. 2, p. 105-108.*

Itoigawa, J., Nishimoto, H., Karasawa, H., Okumura, Y., 1985: Miocene fossils of the Mizunami Group, central Japan, 3. Elasmobranchs. *Mizunami Fossil Mus., Monogr.* 5, 89 p.*

Kamei, T., 1967: A note on a fossil premolar of *Paleoparadoxia. In, Fossils of Anan-cho*, Committee of Education, Anan-cho, Nagano Pref., p. 129-130.*

Kaneko, K. and Inuzuka, N., 1992: Desmostylian fossils from the Yatsuo Group in Toyama Prefecture, Central Japan and their paleoenvironments. *Earth Science* (*Chikyu Kagaku*), vol. 46, no. 2, p. 153-164.**

Karasawa, H., 1983: Fossil elasmobranch teeth from the Miocene formations in Noto Peninsula, central Japan. *Bull. Mizunami Fossil Mus.*, no. 10, p. 185-192.*

——, 1989: Late Cenozoic elasmobranchs from the Hokuriku district, central Japan. *Sci. Rep., Kanazawa Univ.*, vol. 34, no. 1, p. 1-57.

Kaseno, Y., 1964: A tooth of *Desmostylus* found at Shiratori, southern Noto, Japan. *Ann. Rep. Noto Mar. Lab., Kanazawa Univ.*, vol. 4, p. 59-64.

——, 1984: Occurrence and stratigraphical horizon of the desmostylian fossils from Noto, Japan. *In*, Inuzuka, N., Takayasu, K., Chinzei, K., and Yoshida, K., *eds.*, *Desmostylians and Their Paleoenvironment. Assoc. Geol. Collabor. Japan., Monogr.* 28, p. 69-72**

Kobayashi, I. and Kamei, T., 1973: A histological study on a tooth of *Paleoparadoxia. Mem. Fac. Sci., Kyoto Univ., Ser. Geol. and Min.*, vol. 40, no. 1, p.13-25.

Kohno, N. and Hasegawa, Y., 1991: A new occurrence of imagotariine pinniped from the Middle Miocene Goudo Formation in Higashimatsuyama City, Saitama, Japan. *Trans. Proc. Palaeont, Soc. Japan., N.S.*, no. 162, p. 801-805.

Koike, M., Takei, K., Shimono, T., Machida, J., Akimoto, K., Hashiya, I., Yoshino, H., and Hirakoso, S., 1985: Miocene formations of Iwadono Hills. *Jour. Geol. Soc. Japan*, vol. 91, no. 10, p. 665-677.**

Kozawa, Y., 1984: On the teeth structure of the food habitude of desmostylids. *In*, Inuzuka, N., Takayasu, K., Chinzei, K., and Yoshida, K. *eds.*, *Desmostylians and Their Paleoenvironment. Assoc. Geol. Collabor. Japan., Monogr.* 28, p. 119-128.**

Kuga, N., 1985: Revision of Neogene mackerel shark of the genus *Isurus* from Japan. *Mem. Fac. Sci., Kyoto Univ., Ser. Geol. and Min.*, vol. 51, no. 1 & 2, p. 1-18.

Majima, R., 1989: Neogene stratigraphy along the Arakawa River near Yorii, and of the Ogawa Basin, Hiki Hills, and Iwadono Hills, central Saitama Prefecture, central Japan. *Geosci. Repts., Shizuoka Univ.*, vol. 15, p. 1-24.**

Matsumaru, K. and Hayashi, A., 1980: Neogene stratigraphy of the eastern marginal areas of Kanto Mountains, central Japan. *Jour. Geol. Soc. Japan*, vol. 86, no. 4, p. 225-242.**

——, Matsuo, Y., and Kishi, R., 1982: Miocene foraminifera from the Chichibu Basin and the south Hiki Hill, Saitama Prefecture, Japan. *Jour. Saitama Univ., Fac. Educ.* [Math. and Nat. Sci.], vol. 31, p. 39-63.

Merriam, J.C., 1906: On the occurrence of *Desmostylus* MARSH. *Science, N.S.*, vol. 24, p. 151-152.

Mitchell, E.D., 1963: Brachydont desmostylian from Miocene of San Clemente Island, California. *Bull. Southern Calif. Acad. Sci.*, vol. 62, pt. 4, p. 192-201.

—— and Lipps, J.H., 1965: Fossil collecting on San Clemente Island. *Pacific Discovery*, vol. 18, no. 3, p. 2-8.

—— and Repenning, C.A., 1963: The chronologic and geographic range of desmostylians. *Contr. Sci., Los Angeles County Mus.*, no. 78, p. 1-20.

Reinhart, R.H., 1959: A review of the Sirenia and Desmostylia. *Univ. Calif. Pub. Geol. Sci.*, vol. 36, no. 1, p. 1-146.

Repenning, C.A. and Packard, E.L., 1990: Locomotion of a desmostylian and evidence of ancient shark predation. *In*, Boucot, A.J., *ed.*, *Evolutionary paleobiology of behavior and coevolution*, p. 199-203.

Sakamoto, O., 1983: On the occurrence of the skeletons of *Paleoparadoxia tabatai* (TOKUNAGA) from Chichibu Basin, Central Japan. *Bull. Saitama Mus. Nat. Hist.*, no. 1, p. 17-26.**

Shikama, T., 1966a: On some desmostylian teeth in Japan, with stratigraphical remarks on the Keton and Izumi Desmostylids. *Bull. Natn. Sci. Mus., Tokyo*, vol. 9, no. 2, p. 119-170.

——, 1966b: Postcranial skeletons of Japanese Desmostylia. *Palaeont. Soc. Japan, Spec. Papers*, no. 12, p. 1-202.

Takai, F., 1944: [On the occurrence of *Desmostylus* from the phosphate deposit in Noto Peninsula, Japan]. [*Bull. Resource Sci. Res. Inst., Japan*], no. 5, p. 59-62.*

Tokunaga, S., 1939: A new fossil mammal belonging to Desmostylidae. *Jub. Pub. Comm. Prof. H.*

Yabe's 60th Birth., p. 289-299.
—— and Iwasaki, J., 1914: Notes on *Desmostylus japonicus. Jour. Geol. Soc. Tokyo*, vol. 21, p. 33.
Tsunoda, F. and Ogano Collaborative Research Group, 1978: Lithological features and stratigraphic succession of the basal part of the Miocene groups—the members bearing on *Paleoparadoxia tabatai*—developed in the Chichibu Basin. *Jour. Coll. Lib. Arts, Saitama Univ.*, vol. 14, p. 129-138.**
Vanderhoof, V.L., 1937: A study of the Miocene sirenian *Desmostylus. Bull. Dep. Geol. Univ. Calif.*, vol. 24, no. 8, p. 169-262.
Yabe, H., 1959: A problem on the geological range and geographical distribution of Desmostylids. *Trans. Proc. Palaeont. Soc. Japan, N.S.*, no. 33, p. 44-51.
Yoshiwara, S. and Iwasaki, J., 1902: Notes on a new fossil mammal. *Jour. Coll. Sci., Imp. Univ., Tokyo, Japan*, vol. 16, art. 6, p. 1-13.
Zuidema, H.P., 1970: Fossil sea mammal. *Sea Frontiers*, vol. 16, no. 1, p. 20-24.

* *in Japanese*
** *in Japanese with English abstract*

Godo 神戸, Higashi-Matsuyama 東松山, Iwadono 岩殿, Kamagata 鎌形, Kamikarako 上唐子, Kuzubukuro 葛袋, Negishi 根岸, Oppegawa 越辺川, Shogunzawa 将軍沢, Tokigawa 都幾川.

埼玉県葛袋の中新統都幾川層群産の束柱目歯化石：埼玉県東松山市葛袋に分布する中新統都幾川層群下部の神戸礫岩部層から産出した束柱目の単離歯15点を詳細に記載した。これらには *Paleoparadoxia* と *Desmostylus* の両属が含まれる。このうち12点は *Paleoparadoxia* 属で，さらにそのうち5点が *P. tabatai* に同定できる。歯種は上顎の犬歯，第1，第2，第3大臼歯，下顎の第3小臼歯と第3大臼歯が同定できた。*Desmostylus* 属は臼歯の咬柱片から同定した。葛袋標本は *Paleoparadoxia* と *Desmostylus* が同じ産地の同一層準から産した点に意義がある。しかし，これらが二次化石である可能性も否定できない。同じ産地からは鰭脚類，鯨類といった海生哺乳類や各種のサメ化石を産し，束柱目の古生態を復元するうえで重要である。
島田賢舟・犬塚則久

Trans. Proc. Palaeont. Soc. Japan, N.S., No. 175, pp. 578-586, 5 Figs., September 30, 1994

976. DISCOVERY OF MICROCODIUM TEXTURE FROM THE AKIYOSHI LIMESTONE IN THE AKIYOSHI TERRANE, SOUTHWEST JAPAN*

HIDEAKI MACHIYAMA

Department of Earth and Planetary Sciences, Graduate School of Science, Hokkaido University, Sapporo, 060

Abstract. Microcodium texture was discovered from a blackish-brown sparry calcite zone distributed to the south of Mt. Wakatakeyama area, situated in the eastern part of the Akiyoshi Limestone outcrop. This sparry calcite zone is biostratigraphically situated in the upper part of the *Quasifusulinoides* sp. A zone, which is overlain by the *Montiparus* sp. A zone, and is middle Kasimovian (early Late Carboniferous) in age. According to the formation process of "*Microcodium*", which is formed secondarily within a meteoric environment, the author proposes to call it microcodium texture, because "*Microcodium*" is not a taxonomic unit. From the presence of microcodium texture, it is considered that the blackish-brown sparry calcite zone was formed in a meteoric environment under an exposure surface developed during the sea-level fall. This suggests that an unconformity (sequence boundary) is present just above the blackish-brown sparry calcite zone.

Key words. Akiyoshi Limestone, Akiyoshi Terrane, Kasimovian, *Microcodium*, unconformity, Upper Carboniferous.

Introduction

The Lower Carboniferous to Middle Permian Akiyoshi Limestone, which was deposited on a seamount and accreted in Late Permian time, is distributed in the westward of the Akiyoshi Terrane, Southwest Japan. With regard to the formation of the Akiyoshi Limestone, Ota (1968) has already made it clear that this limestone is an organic reef complex. He concluded that the Akiyoshi Limestone took the form of an atoll reef in Middle Carboniferous time. However, there are few sedimentological studies compared to many biostratigraphical studies on the limestone using foraminifers and corals. Sedimentological and paleoecological studies within the reef have been done by Nagai (1985) and Sugiyama and Nagai (1990). Details of the Upper Carboniferous to Permian sequence are, however, still unknown, because these studies mainly dealt with the Lower Carboniferous when the reef was conspicuously developed.

The Akiyoshi Limestone ranges in age from Early Carboniferous (middle Tournaisian) to Middle Permian (Midian) (Haikawa, 1988; Ozawa and Kobayashi, 1990). Although this limestone deposition spans approximately 100 million years, no unconformity has yet been recognized by sedimentological aspects. Within samples from the dark brown limestone facies (blackish-brown sparry calcite zone) distributed to the south of the Mt. Wakatakeyama area, "*Microcodium*" is proved to be present. Based on the occurrence of "*Microcodium*" in the Akiyoshi Limestone, it is formed secondarily in origin within a mete-

*Received November 19, 1993; revised manuscript accepted June 8, 1994

oric environment, as has been stated by Klappa (1978). Thus, "*Microcodium*" is better called microcodium texture, because it is not a taxonomic unit, but is a biogenic structure. This paper presents the first report on the occurrence of microcodium texture from Japan, and examines the formation of the blackish-brown sparry calcite zone.

Previous work of blackish brown sparry calcite zone

The dark brown limestone facies within the generally white-gray Akiyoshi Limestone was firstly reported as Mg-rich limestone developing over the unconformity at the base of the *Triticites simplex* zone by Hasegawa (1963). Later, he called this limestone facies the blackish-brown sparry calcite zone (BBSC zone), and discussed its stratigraphic significance (Hasegawa, 1988). He considered that the BBSC zone might indicate the presence of an unconformity or an important geologic event, such as a catastrophic biological event. In the study of Late Carboniferous to Early Permian fusulinacean biostratigraphy by Ozawa *et al.* (1991), the BBSC zone (=dolomitized limestone or dolostone reported by Ozawa *et al.*, 1991, Fig. 1) was recognized in the following five horizons: 1) the upper part of *Pseudofusulinella hidaensis* zone, 2) the lower part of *Protriticites subschwagerinoides* zone, 3) the upper part of *Montiparus montiparus-Quasifusulinoides ohtanii* zone, 4) *Montiparus matsumotoi* zone, and 5) the upper part of *Triticites* (*Rauserites*) *stuckenbergi* zone. With regard to the formation of BBSC zone, Ozawa suggested that lime-muddy limestone was secondarily replaced irregularly by BBSC including organic matter, and its formation might take place immediately after deposition (T. Ozawa, pers. comm., 1992). It has also been considered that the BBSC is not dolomite and is formed under fresh-water conditions (M. Musashino, pers. comm., 1992). In the study of the western part of the Akiyoshi Limestone by Sano and Kanmera (1991a, 1991b), they also indicated that the BBSC (=brown-colored calcite of Sano and Kanmera, 1991a, 1991b) occurred as the replacement of the Kasimovian (lower Upper Carboniferous) to Asselian (lower Lower Permian) parent rocks, and was formed synchronously with or immediately after the deposition of the Kasimovian to Asselian parent rocks.

Locality and stratigraphy

The examined samples were collected at the southern part of Mt. Wakatakeyama (Figure 1), when a joint field survery was carried out in October of 1990 as a part of joint research on "The Carboniferous-Permian Boundary in Japan" led by Prof. M. Kato of Hokkaido University (1990-1993), sponsored by the Japanese Ministry of Education.

According to the fusulinacean biostratigraphy by Ota and Ota (1993), the strata along the Mt. Wakatakeyama route are divided into the following eight zones in ascending order (Figure 2):

1) *Pseudofusulinella hidaensis* Zone,
2) *Protriticites matsumotoi* Zone (s.s.),
3) *Quasifusulinoides* sp. A Zone,
4) *Montiparus* sp. A Zone,
5) *Schwagerina* sp. A Zone,
6) *Triticites simplex* Zone (s.s.),
7) *Pseudoschwagerina muongthensis* Zone, and
8) *Pseudofusulina vulgaris* Zone.

In this route, the BBSC zone is distributed in the *Quasifusulinoides* sp. A zone (Ota and Ota, 1993) and is a few meters thick (Figure 2). Thus, it is considered that the horizon of this BBSC zone is middle Kasimovian (early Late Carboniferous) in age. The parent rocks of BBSC zone including microcodium texture (="*Microcodium*") consist of oncoid-bioclastic wackestone, and are interpreted as low-energy deposits. This lithofacies is underlain by phylloid algal-bioclastic grainstone/packstone, and overlain by well-sorted peloid grainstone (Figure 2).

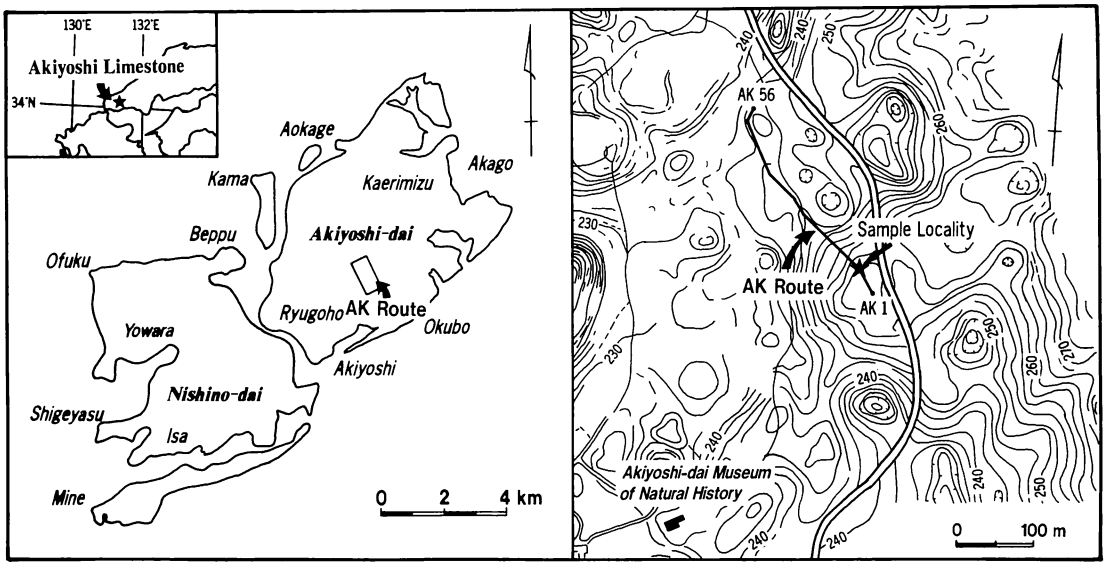

Figure 1. Map showing the measured route (AK Route) and locality of microcodium texture. Contour interval in the right figure is 2.5 meters. Modified from Ota and Ota (1993).

Description of microcodium texture

Diagnosis.—A cob-shaped subcylindrical form with a central, thin, cylindrical tube (a micritized cavity) surrounded by brown-colored peripheral radial calcite plates. Each calcite plate takes the form of a "corn-grain" (Mamet, 1991), and the stacked plates show a "corn cob" (Mamet, 1991) form. The schematic reconstruction of microcodium texture is shown by Figure 3. The corn-grain plates corrode the surrounding limestones.

Description.—In hand specimens, the BBSC is abundantly present as irregular spots in the parent rocks. Under the microscope, microcodium texture which corrodes the surrounding parent rocks (oncoid-bioclastic wackestone) is frequently recognized (Figure 4A), and often occupies more than 80% in volume of the samples. The microcodium texture has a cylindrical form, and some of them are undulate. They are 1.0 to 1.2 mm in diameter, and central cylindrical cavities are about 0.1 mm in diameter. The calcite plates like "corn-grain" are 0.4 to 0.6 mm in radius, and 0.06 to 0.12 mm thick (Figures 4B, 4C, 4D).

Classification and origin of microcodium texture.—"*Microcodium*" was firstly described in the marine Miocene strata of Baden (southern Germany) by Glück (1912). From their shape and arrangement of calcite crystals, he established a new species *Microcodium elegans*, and placed it in the family Codiaceae of the Chlorophyta. However, because of the peculiar shape of "*Microcodium*", various origins, such as bacterial, plant roots, or inorganic, have been put forth by many workers. In general, "*Microcodium*" occurs frequently in calcrete (*e.g.*, Esteban, 1974). Klappa (1978) has discovered recent "*Microcodium*" under the present-day surface in a rubbly calcareous soil in southeastern Spain. He has studied its origin in detail, and has made comparison between ancient and recent "*Microcodium*". As a result of his detailed study, Klappa (1978) has concluded that "*Microcodium*" is the result of calcification of mycorrhizae, a symbiotic association of fungi and the cortical cells of roots. He has also stated that "*Microcodium*" is a pedological feature and a

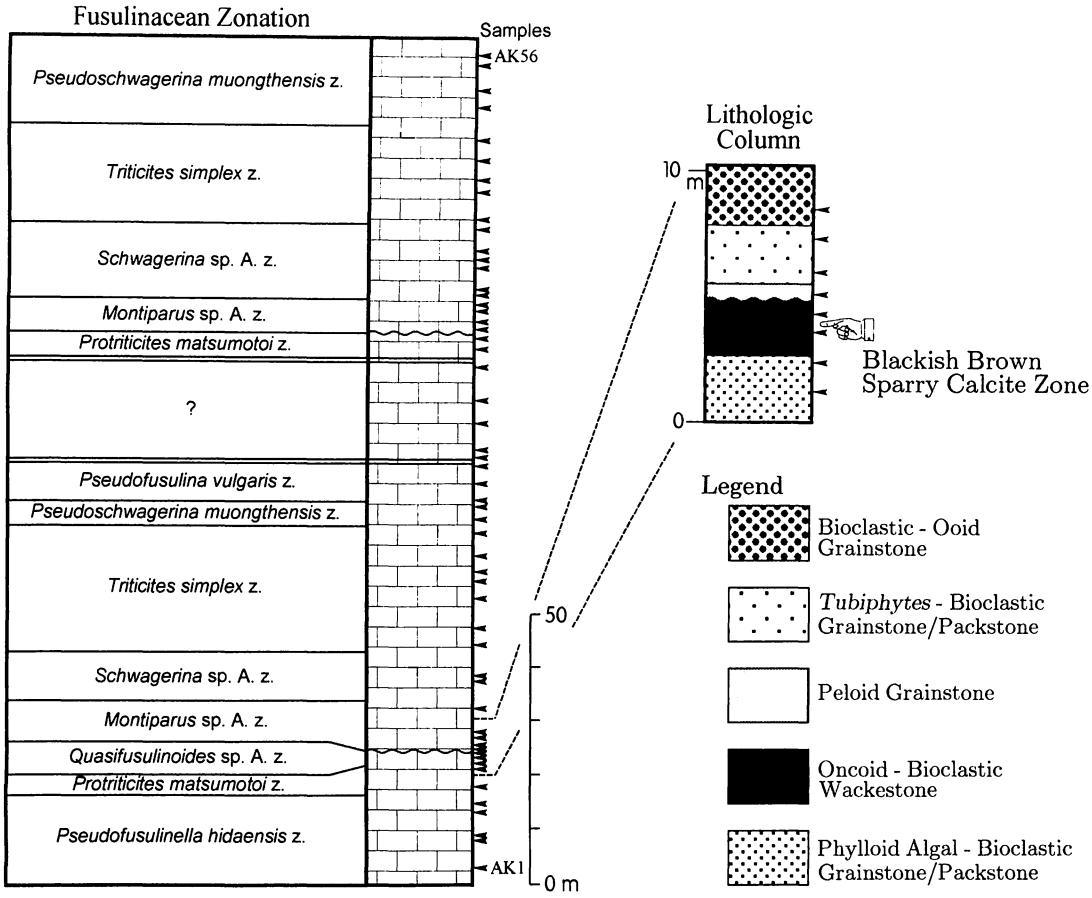

Figure 2. The Upper Carboniferous to Lower Permian limestone columnar section and sampling horizons of AK Route, and lithologic column around the blackish-brown sparry calcite zone. Note the fusulinacean zone between the two double lines is undefined, and fusulinacean zones repeat themselves (Ota and Ota, 1993). A wavy line shows an unconformity. Hand mark indicates the horizon of the blackish-brown sparry calcite zone.

valuable criterion for the recognition of the existence of a paleosol. This conclusion is in accordance with the opinion of Bodergat (1974), who has demonstrated that the carbon within the calcite is organic in origin, and has been metabolized by "*Microcodium*" in a meteoric environment. Mamet and Roux (1982) recognized "*Microcodium*" in the Carboniferous to Permian of the Canadian Arctic region (Yukon Territory, Axel Heiberg and Ellesmere Islands). Contrary to these opinions, they have emphasized that "*Microcodium*" has an algal affinity. Later, Mamet *et al.* (1987) described "*Microcodium*" as being questionably a member of the family Microcodiaceae (Maslov, 1956) of codiacean algae or *incertae sedis*. However, Mamet and Roux (1982) interpreted the grains of "*Microcodium*" in the grainstones as reworked grains, such as intraclasts, from older deposits. This interpretation suggests that "*Microcodium*" was formed prior to the deposition of the grainstones. Thus, the formation process of ancient "*Microcodium*" seems to be similar to that of recent "*Microcodium*" proposed by Klappa (1978). In this way, it is considered that "*Microcodium*" originates secondarily within a meteoric envi-

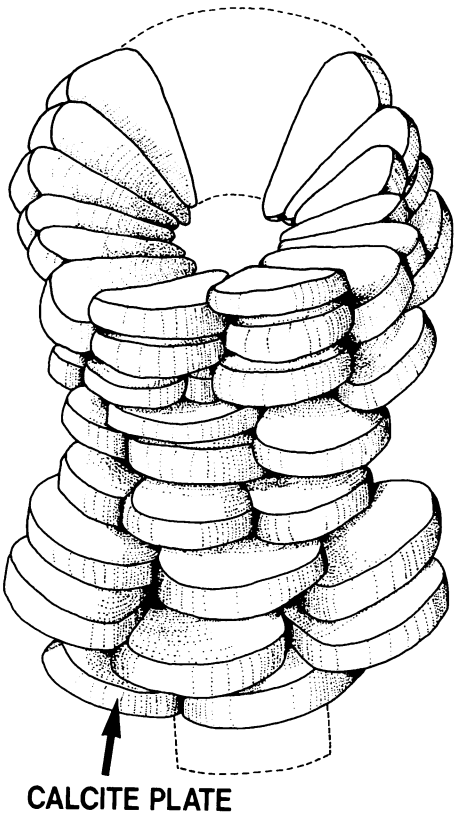

Figure 3. Schematic reconstruction of microcodium texture. Calcite plates are 0.4 to 0.6 mm in radius, and 0.06 to 0.12 mm thick. After Mamet *et al.* (1987).

ronment, as has been stated by Bodergat (1974) and Klappa (1978).

As mentioned above, "*Microcodium*" is not a taxonomic unit such as a calcareous alga, but a structure related to fungi. That is to say, "*Microcodium*" is a biogenic structure like stromatolites and oncoids. Thus, the generic name "*Microcodium*" must not be given to this structure. Toomey *et al.* (1989) have made a re-examination of the Pennsylvanian to Permian oncoids described previously as *Osagia*. They have shown that *Osagia* consists primarily of tubules of the cyanobacteria *Girvanella*, or its diagenetically altered end-product ("algal dust" or "algal paste"), intimately associated with various encrusting foraminifers. They concluded that *Osagia* is not a genus but a biogenic structure, and coined the term osagid grains. In the same way, though Klappa (1978) preferred *Microcodium* grain to "*Microcodium*", the author suggests that the name "*Microcodium*" be given up, with the structure now in question being better called microcodium texture, because "*Microcodium*" is a texture rather than a grain.

Formation of blackish brown sparry calcite zone

As mentioned before, microcodium texture (="*Microcodium*") is recognized in the BBSC zone of the Mt. Wakatakeyama route. As shown in Figures 5A and 5B, the microcodium texture together with the parent rocks is penetrated by dikelets called broken limestone, which represent the phenomena of mechanical destruction and the injection of pulverized particles (Sano and Kanmera, 1991a, 1991b). Since the formation of broken limestone has been interpreted as related to the accretionary processes, the above-stated observation suggests that the microcodium texture was formed after the deposition of the parent rocks (oncoid-bioclastic wackestone) and prior to the process of broken limestone (Sano and Kanmera, 1991b). Thus, the structure cannot be of modern origin.

From the viewpoint of carbon and oxygen isotopes, the $\delta^{13}C$ value of microcodium-texture-bearing sample is lower, about 2 per mil or less value in $\delta^{13}C_{PDB}$ (analysts are M. Musashino, M. Kusakabe, and S. Shin, unpublished data), than samples from the overlying limestones. They compared the result with the studies of recent carbonates in Barbados by Allan and Matthews (1977) and the Mississippian Newman Limestone in North America by Allan and Matthews (1982). The $\delta^{13}C$ and $\delta^{18}O$ values of the vadose zone in Barbados and of the strata, a few meters in thickness, under the horizon of a developed paleosol and weathering surface in the New-

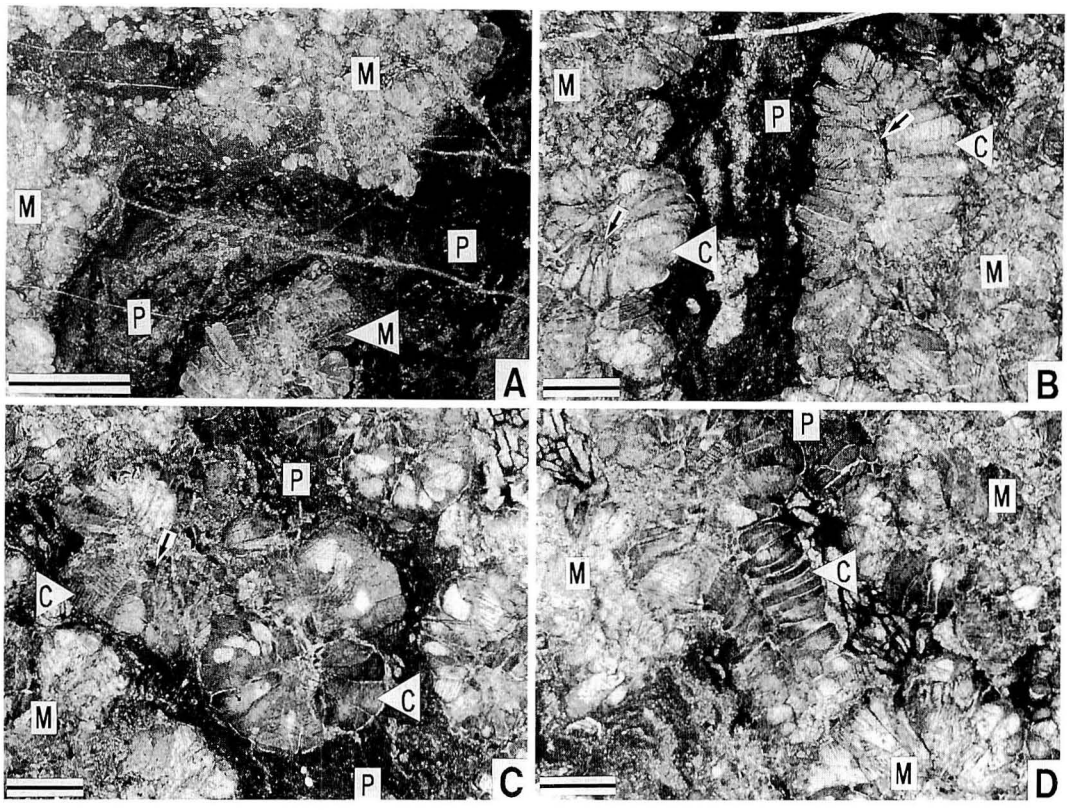

Figure 4. Thin-section photomicrographs of microcodium texture from AK Route. A. Microcodium texture (corn-grain calcite plates : M) corrodes the surrounding parent rock (oncoid-bioclastic wackestone : P). Scale bar is 2 millimeters in length. B. Slightly obliquely cut transverse section (left) and longitudinal section (right) of microcodium texture (M). Note corn-grain calcite plates (C) and a central thin micritized cavity (arrows). Scale bar is 0.5 millimeters in length. C. Slightly obliquely cut transverse sections of microcodium texture (M) are present as irregularly distributed spots in the parent rock (P). Note peripheral radial calcite plates (C) and a central thin cylindrical tube (arrow). Scale bar is 0.5 millimeters in length. D. Oblique sections of microcodium texture (M). Note "corn cob" form stacked by calcite plates (C). Scale bar is 0.5 millimeters in length.

man Limestone are lower than those of the overlying and underlying strata. In general, it is known that $\delta^{13}C$ and $\delta^{18}O$ values are low in a meteoric environment (*e.g.*, Scoffin, 1987). Thus, as has been pointed out by Musashino *et al.* (unpublished data), it is considered that the appearance of a meteoric environment developed during a sea-level fall was the cause of formation of the BBSC zone. This is in accordance with the origin of microcodium texture reported by Klappa (1978). In addition, the presence of microcodium texture was one of the diagnostic features of caliche (calcrete) facies (Esteban and Klappa, 1983). From the above, it is considered that the BBSC zone within the *Quasifusulinoides* sp. A zone and below the *Montiparus* sp. A zone was formed by the formation of microcodium texture together with possible calcrete genesis. That is to say, a hiatus with an exposure surface may be present. This suggestion is in agreement with the result of the fusulinacean biostratigraphy by Ota and Ota (1993), who supposed the presence of a stratigraphical gap between the *Quasifusulinoides* sp. A zone and the

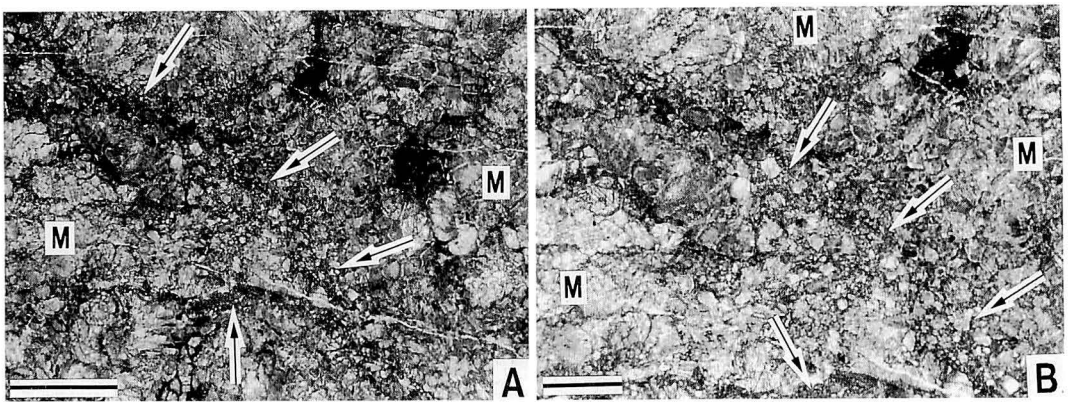

Figure 5. Thin-section photomicrographs of microcodium texture and its destruction. A. Microcodium texture (M) is penetrated by complexly anastomosing comminution zones (arrows). Scale bar is 1 millimeter in length. B. Close-up of A. Scale bar is 0.5 millimeters in length.

Montiparus sp. A zone. This supposition supports Hasegawa's opinion (Hasegawa, 1988), though Ota and Ota (1993) have pointed out that no catastrophic biological event occurred at the time. The author has not been able to clearly recognize other features of calcrete facies around the BBSC zone. In the future, it will be necessary to study the successions of BBSC zone in detail, and to recognize an exposure surface.

Conclusion

As a result of the study of samples from the BBSC zone in the *Quasifusulinoides* sp. A zone of Ota and Ota (1993), situated to the south of Mt. Wakatakeyama area in the eastern part of the Akiyoshi Limestone, the BBSC zone proves to contain "*Microcodium*." According to the formation process of "*Microcodium*" by Klappa (1978), who has demonstrated that "*Microcodium*" is the products of calcification of mycorrhizae, a symbiotic association between fungi and root cortical cells, the author suggests calling "*Microcodium*" microcodium texture, because "*Microcodium*" can not be a taxonomic unit. From the genesis of microcodium texture, the isotope study, and the fusulinacean biostratigraphy, it is thus inferred that the BBSC zone was formed in a meteoric environment possibly under an exposure surface developed during a sea-level fall. This suggests that an unconformity is present in the BBSC zone.

As mentioned before, Ozawa *et al.* (1991) have recognized five horizons of the BBSC zone around the Carboniferous-Permian boundary. Sano and Kanmera (1991a, 1991b) have also reported BBSC zones (their brown-colored calcite) in the Kasimovian to Asselian parent rocks of western part of the Akiyoshi Limestone. Their brown-colored calcite is clearly interpreted as microcodium texture (Sano and Kanmera, 1991b : Pl. VI, Figs. 1-5). From these facts, microcodium texture possibly exists in many horizons. Hereafter, these may provide good marker horizons showing a sequence boundary for sequence stratigraphy studies, because they are interpreted as being formed in a meteoric environment appearing with a sea-level fall. The BBSC zone is also known in the Omi Limestone (Y. Hasegawa, pers. comm., 1993), and this zone is in almost the same horizon with the Akiyoshi Limestone (the horizon between the *Fusulina-Fusulinella* zone and the *Triticites* zone by his zonation scheme). Thus, there is a possibility that this particular horizon indicates the tract of a global sea-level change. As detailed foraminiferal

zonation schemes are proposed (*e.g.*, Ozawa and Kobayashi, 1990), it is expected that more details pertaining to global sea-level changes will be compiled if system tracts should be recognized by studies of limestone petrography, stable isotopes, and diagenetic sequence stratigraphy (Kano, 1992).

Acknowledgments

The author is grateful to Professor Makoto Kato of Hokkaido University for valuable suggestion during the course of this work, and Dr. Makoto Kawamura of Hokkaido University for critical reading of the manuscript. The author wishes to thank Professor Yoshiyuki Hasegawa of Niigata University and Professor Tomowo Ozawa of Nagoya University for permitting me to quote their unpublished data on the blackish-brown sparry calcite zone. The author also wishes to thank Professor Makoto Musashino of Kyoto University of Education for permitting me to quote his unpublished geochemical data. The author wishes to acknowledge Associate Professor Toshio Kawamura of Miyagi University of Education and Mr. Takehiko Haikawa of Akiyoshi-dai Museum of Natural History for help in the field. Thanks are also due to Messrs. Toshiaki Kuwajima and Hidehiko Nomura, Technical Staffs of Hokkaido University, who helped me to make thin sections.

A part of this work was supported by a Grant-in-Aid for Scientific Research from the Japanese Ministry of Education.

References cited

Allan, J.R. and Matthews, R.K., 1977 : Carbon and oxygen isotopes as diagenetic and stratigraphic tools : data from surface and subsurface of Barbados, West Indies. *Geology*, vol, 5, p. 16-20.

Allan, J.R. and Matthews, R.K., 1982 : Isotope signatures associated with early meteoric diagenesis. *Sedimentology*, vol. 29, p. 797-817.

Bodergat, A.M., 1974 : Les microcodiums, milieux et modes de développement. *Docum. Lab. Géol. Fac. Sci. Lyons*, vol. 62, p. 137-235.

Esteban, M., 1974 : Caliche textures and *Microcodium*. *Boll. Soc. geol. ital.*, vol. 92, *Suppl.* 1973, p. 105-125.

———. and Klappa, C.F., 1983 : Subaerial exposure, p. 1-54, *In*, Scholle, P.A., Bebout, D.G. and Moore, C.H. *eds., Carbonate depositional environments*. AAPG, Mem., no. 13.

Glück, H., 1912 : Eine neues teinbildende Siphonee (Codiacee) aus dem marinen Tertiär von Süddeutschland. *Mitt. bad. geol. Landesanst. Bd.*, vol. 7, p. 3-24.

Haikawa, T., 1988, The basement complex and conodonts biostratigraphy of the lowest parts in the Akiyoshi Limestone Group, Southwest Japan. *Bull. Akiyoshi-dai Mus. Nat. Hist.*, no. 23, p. 13-37, pls. 4-7. (*in Japanese with English abstract*)

Hasegawa, Y., 1963 : New find of fossils in the reddish tuffaceous shale in the Akiyoshi province. *Earth Sci.* (*Chikyu Kagaku*), no. 64, p. 32-37.

———., 1988 : Stratigraphy and paleontological evolution around the Carboniferous-Permian boundary in the Inner Zone of Southwest Japan. *Reports on Grant-in-Aid for Scientific Research* (*C*), p. 1-14, figs. 1-3, pls. 1-3, Niigata Univ. (*in Japanese*)

Kano, A., 1992 : Diagenetic sequence stratigraphy : a new method for the carbonate basin analysis (abstract). *29th Internat. Geol. Cong.*, Abst. vol. 2, p. 327, Kyoto, Japan.

Klappa, C.F., 1978 : Biolithogenesis of *Microcodium* : elucidation. *Sedimentology*, vol. 25, p. 489-522.

Mamet, B.L., 1991 : Carboniferous calcareous algae, p. 370-451, *In*, Riding, R. *ed., Calcareous algae and stromatolites*. Springer, Berlin.

Mamet, B.L. and Roux, A., 1987 : Sur la présence de *Microcodium* (Algue ?, *Incertae sedis* ?) *dans le Paléozoïqu supérieur de l'Arctique canadien. Can. J. Earth Sci.*, vol. 19, p. 357-363.

Mamet, B.L., Roux, A. and Nassichuk, W.W., 1987 : Algues carbonifères et permiennes de l'Arctique canadien. *Geol. Surv. Canada, Bull.*, no. 342, p. 1-143.

Maslov, V.P., 1956 : Fossil calcareous algae of the USSR. *Trans. Acad. Sci. USSR Geol. Inst.*, no. 160, p. 1-301. (*in Russian*)

Nagai, K., 1985 : Reef-forming algal chaeteted boundstone found in the Akiyoshi Limestone Group, Southwest Japan (Reconstruction of the "Akiyoshi organic reef"-I). *Bull. Akiyoshi-dai Mus. Nat. Hist.*, no. 20, p. 1-15, pls. 1-6.

Ota, M., 1968 : The Akiyoshi Limestone Group : A geosynclinal organic reef complex. *Bull. Akiyoshi-dai Mus. Nat. Hist.*, no. 5, p. 1-44, pls. 1-31. (*in Japanese with English abstract*)

Ota, Y. and Ota, M., 1993: Faunal change of the Upper Carboniferous to Lower Permian fusulinaceans from the Akiyoshi Limestone Group, Southwest Japan: On materials along the AK Route, adjacent to the Akiyoshi-dai Museum of Natural History. *Bull. Akiyoshi-dai Mus. Nat. Hist.*, no. 28, p. 1-57, pls. 1-3. (*in Japanese with English abstract*)

Ozawa, T. and Kobayashi, F., 1990: Carboniferous to Permian Akiyoshi Limestone Group. *In*, Organizing Committee Benthos '90 *ed., Fossil and recent benthic foraminifera in some selected regions of Japan. Guide book for field trips, 4th International Symposium on Benthic Foraminifera, Sendai*, 1990, p. E1-E31, pls. 1-13.

————., Kobayashi, F. and Watanabe, K., 1991: Biostratigraphic zonation of Late Carboniferous to Early Permian sequence of Akiyoshi Limestone Group, Japan and its correlation with reference sections in the Tethyan Region. *Saito Ho-on Kai, Spec. Pub.*, no. 3, p. 327-341.

Sano, H. and Kanmera, K., 1991a: Collapse of ancient oceanic reef complex-What happened during collision of Akiyoshi reef complex?-Geologic setting and age of Akiyoshi terrane rocks on western Akiyoshi-dai plateau. *Jour. Geol. Soc. Japan*, vol. 97, p. 113-133.

———— and Kanmera, K., 1991b: Collapse of ancient oceanic reef complex-What happened during collision of Akiyoshi reef complex?-Broken limestone as collapse products. *Jour. Geol. Soc. Japan*, vol. 97, p. 217-229.

Scoffin, T.P., 1987: *An introduction to carbonate sediments and rocks*. 274 p., Blackie, Glasgow and London.

Sugiyama, T. and Nagai, K., 1990: Growth forms of auloporidid corals in the Akiyoshi Limestone Group, Southwest Japan: Paleoecological studies of reef-building organisms in the Akiyoshi organic reef complex I. *Bull. Akiyoshi-dai Mus. Nat. Hist.*, no. 25, p. 7-25, pls. 3-5. (*in Japanese with English abstract*)

Toomey, D.F., Lowenstein, T.K. and Mitchell, R.W., 1989: Re-examination of laminated osagid grains from a Lower Permian Midcontinent limestone. *Palaios*, vol. 4, p. 51-62.

Akiyoshi 秋吉, omi 青海, Wakatakeyama 若竹山.

秋吉石灰岩からの microcodium 組織の発見: 秋吉石灰岩東部の若竹山南方に分布する黒褐色 sparry calcite 帯から microcodium 組織を見いだした。この黒褐色 sparry calcite 帯は紡錘虫分帯から *Quasifusulinoides* sp. A 帯と *Montiparus* sp. A 帯の間に位置しており，時代的には後期石炭紀 (Kasimovian 中期) に形成されたものととらえられる。"*Microcodium*" は植物の根の皮層細胞と菌類との共生による mycorrhizae の石灰化の産物であり生物種とは認められないので，これを "microcodium 組織" と呼称する事を提案する。microcodium 組織の存在や黒褐色 sparry calcite 帯の炭素・酸素同位体値が周囲のものより低いことから，この黒褐色 sparry calcite 帯は海水準低下時に地表に露出した際の淡水影響下で形成されたものと考えられる。したがって黒褐色 sparry calcite 帯は不整合 (シークエンス境界) を示す良いマーカーとなると思われる。 町山栄章

PROCEEDINGS OF THE PALAEONTOLOGICAL SOCIETY OF JAPAN

日本古生物学会　第143回例会

日本古生物学会第143回例会が，6月25-26日に熊本大学理学部で開催された（参加者135名）.

シンポジウム

「白亜紀の陸と海の生物の多様性の解析と国際対比(IGCP 350)—白亜紀のイベント解析に向けて—」
……世話人：岡田博有・岩崎泰顕・田代正之・平野弘道・松川正樹

東アジアの白亜紀環境変化の解明へ向けた古生物学への期待……岡田博有

本邦の上部白亜系の大型化石と微化石の化石層序の精度：古地磁気層序との対比に基づいて
……利光誠一・松本達郎・野田雅之・米谷盛寿郎

放散虫化石による白亜紀の国際対比と古環境の変遷：北西太平洋縁辺域の古海洋変遷試案
……竹谷陽二郎・岡村　真

海洋無酸素事変に関する大型化石と微化石の対比の貢献：北海道の上部白亜系を例として
……平野弘道・長谷川卓

東アジアの非海生二枚貝層序の問題点
……田村　実・西田範行・池上直樹・木下和弥

非海生二枚貝類の生息環境とchronological indexとしての評価：日本の下部白亜系を例として
……松川正樹・伊藤　慎

関門層群の淡水魚類化石相の多様性……藪本美孝

手取層群における恐竜相の多様性とその意義：アジア大陸の恐竜相と比較して
……東　洋一・濱田隆士・阿部信一

東アジアの白亜紀後期の被子植物花粉の多様化
……高橋　清

細胞組織からみた植物群の解析と古環境：手取型と領石型の植物群を例として……大花民子・木村達明

中国東北部の下部白亜系の海成層と非海成層の対比と古生物地理学的意義……二上政夫・松川正樹・陳　丕基

テクトニクス解釈の道具としての二枚貝類：西南日本の下部白亜系を例として……田代正之

微化石からみた東アジアの白亜系—石油探査に関連して—……米谷盛寿郎・秋葉文雄・栗田裕司

個人講演

黒瀬川構造帯からのシルル紀新世・デボン紀新世放散虫化石……梅田真樹

四国秩父帯のリン酸塩ノジュールから産出した放散虫化石の年代……竹村厚司・来見田桂子・山北　聡

ペルム紀後期Albaillellariaの骨格構造
……竹村厚司・来見田桂子・山北　聡

Lithomelissa sphaerocephalus (Nassellaria亜目)の内部骨格構造について……舟川　哲

Magnetobiostratigraphic correlatiton of the Upper Cretaceous system of Japan……Kodama, K., Takeuchi, T., Nishibayashi, M., and Tashiro, M.

炭素同位体比層序による白亜系の国際対比—蝦夷層群の微化石層序によるクロスチェック—……長谷川卓

浮遊性有孔虫群集からみた西赤道—北太平洋の過去15万年間の海洋環境変動……木元克典・尾田太良

AMS法による南極リュツォ・ホルム湾東岸域の隆起海成堆積物の^{14}C年代の再検討
……五十嵐厚夫・沼波秀樹・土屋泰孝・福地光男・斎藤常正

南極リュツォ・ホルム湾東部における海氷中の浮遊性有孔虫分布の季節変化
……五十嵐厚夫・沼波秀樹・土屋泰孝・福地光男・斎藤常正

東北日本太平洋沿海域に於ける現生石灰質ナノプランクトン群集……萩野恭子・松岡裕美

九州の三宝山帯の後期三畳紀層産の三角貝の新属新種の記載と日本の後期三畳紀三角貝…田村　実・西村英一

南部北上山地稲井層群のアンモナイト—1：大沢層（下部三畳系）……石橋　毅・長谷川清史・佐藤喜男・鎌田耕太郎・村田正文

南部北上山地稲井層群のアンモナイト—2：伊里前層(中部三畳系)……長谷川清史・石橋　毅・佐藤喜男・鎌田耕太郎・村田正文

Gaudryceratidae科のアンモナイトの2・3について—III
……松本達郎

*Polyptychoceras haradanum*の共存化石とその化石層序学的意義……早川浩司

テチス浅海域に於ける白亜紀—古第三紀境界付近の*Colpospira* (*Acutospira*)種群の古動物地理区

ポスターセッション

Palaeontological Society of Japan (PSJ) Council Actions

During its meeting on June 24, 1994, the PSJ Council enacted the following changes to PSJ membership.

New members elected :

Yutaka Hara, Seiiti Kamada, Yoshio Kataoka,
Shogo Konishi, Miwa Maruyama, Taisuke Murata,
Yoshito Nakashima, Takashi Nishimura, Hiroshi Oda,
Takenori Sasaki, Kenji Shimizu, Katue Yamane,
Hajime Yokoi.

Resigned members :

(Fellow)

Seiichi Mabuchi, Shunji Watari.

(Ordinary member)

Yutaka Tsubaki, Kyoji Takasaki.

Deceased members :

(Fellow)

Hiroshi Ozaki.

(Ordinary member)

Jost P. Wiedmann, Regionald Wright Barker.

行事予定

◎学会創立60周年にあたる1995年の年会・総会は，1995年2月2日～4日に名古屋大学理学部で開催されます。講演申込（予稿集原稿送付）は12月5日（必着）締切です。講演申込の方法や予稿集原稿の書き方については，「化石」48号または54号をご覧下さい。1995年年会総会では，シンポジウム「哺乳類の系統進化研究の現状と将来展望」（世話人：瀬戸口烈司，冨田幸光，小澤智生）が予定されています。このほか，夜間小集会やワークショップなどの企画を歓迎しますので，希望される方は早めに行事係までご連絡下さい。

◎1995年例会（第144回例会）は，横須賀市自然博物館で6月後半に開催の予定です。シンポジウムを計画されている方は，1994年12月末までにその既要（開催の趣旨，講演者と題目）を行事係までお知らせ下さい。

学会講演（含ポスターセッション）申込先：
〒113　東京都文京区本郷7-3-1　東京大学大学院理学系研究科地質学教室
☎03（3812）2111（内線4519）　Fax. 03（3815）9490　棚部一成　（行事係）

本誌の発行に要する費用は，会員の会費以外に，文部省科学研究費補助金ならびに賛助会員からの会費が当てられています。現在の賛助会員は下記の通りです。

インドネシア石油株式会社
北九州市立自然史博物館
帝国石油株式会社
三井石油開発株式会社
関東天然ガス株式会社
石油資源開発株式会社
兵庫県立人と自然の博物館
（アイウエオ順）
奇石博物館
ダイヤコンサルタント
日鉱石油開発㈱探査部

○文部省科学研究費補助金（研究成果公開促進費）による。

1994年9月27日　印刷
1994年9月30日　発行

ISSN　0031-0204
日本古生物学会報告・紀事
新篇　175号
2,500円

発行者　日本古生物学会
〒113 東京都文京区本駒込5-16-9
日本学会事務センター内
電話 03－5814－5801
編集者　斎藤常正・森　啓
編集幹事　島本昌憲
印刷者　仙台市若林区六丁の目西町8-45
笹氣出版印刷株式会社　笹氣幸緒
本社022-288-5555 東京03-3455-4415

Transactions and Proceedings of the Palaeontological Society of Japan

New Series No. 175 September 30, 1994

CONTENTS